Physics – Uspekhi **46** (4) 335 – 371 (2003)

REVIEWS OF TOPICAL PROBLEMS

PACS numbers: **04.70.–s**, 97.60.Lf, 98.35.Jk

Search for black holes

A M Cherepashchuk

DOI: 10.1070/PU2003v046n04ABEH001282

Contents

Abstract. **Methods and results of searching for stellar mass black holes in binary systems and for supermassive black holes in galactic nuclei of different types are described. As of now (June 2002), a total of 100 black hole candidates are known. All the necessary conditions Einstein's General Relativity imposes on the observational properties of black holes are satisfied for candidate objects available, thus further assuring the existence of black holes in the Universe. Prospects for obtaining sufficient criteria for reliably distinguishing candidate black holes from real black holes are discussed.**

1. Introduction

Black holes (BHs) are predicted by A Einstein's General Relativity (GR). In 1968, J A Wheeler [1] was the first to coin the term 'black hole'. First let us refresh our memories concerning the main properties of BHs which are important for astronomical observations [2 – 4].

By definition (see, for example, Ref. [5]), a BH in an asymptotically flat space-time is a region from which no causally connected signal can escape to the light-like future infinity. In other words [6], a BH represents a region which can not reciprocally communicate with the external Universe since the escape velocity for it is equal to the speed of light in vacuum c. The boundary of this region is called the event horizon.

The characteristic BH size is determined by the gravitational (Schwarzschild) radius $r_g = 2GM/c^2$, where M is the mass and G is Newton's gravity constant. Numerically, for $M = 10M_\odot$ ($\odot$ is the sign of the Sun) the value of the gravitational radius is $r_g = 30$ km and for $M = 10^9 M_\odot$ it is equal to 20 astronomical units (AU), i.e., half the Solar system size (1 AU $= 1.5 \times 10^{13}$ cm is the mean distance from the Earth to the Sun). The event horizon radius is $r_h = r_g$ for a non-rotating (Schwarzschild) BH and $r_h < r_g$ for a rotating BH (for the maximally rotating Kerr BH with angular momentum $r_h = 0.5 r_g$).

It is important to note that for a BH forming at our time the event horizon has not yet been formed due to the relativistic time retardation near the horizon for the remote observer. So the surfaces of 'modern' BHs lie very close to the event horizon and approach it for an infinitely long time from the viewpoint of the remote observer. For such an observer, all processes near these surfaces are infinitely stretched in time and hence unobservable. For the 'modern' BH the term collapsing objects [7] is widely used; for astronomers, these are 'almost' black holes.

It is important to emphasize that the event horizon is just a coordinate peculiarity in space-time. It can be removed by choosing the appropriate reference frame. For example, an observer freely falling into a BH does not feel the event horizon, he/she can penetrate into the BH and see the central

A M Cherepashchuk P K Sternberg State Astronomical Institute, Universitetskiĭ prosp. 13, 119992 Moscow, Russian Federation
Tel. (7-095) 939 28 58. Fax (7-095) 932 88 41
E-mail: cher@sai.msu.ru

Received 11 July 2002
Uspekhi Fizicheskikh Nauk **173** (4) 345 – 384 (2003)
Translated by K A Postnov; edited by S M Apenko

singularity but can not transfer any information to the external observer.

A unique peculiarity of the event horizon and the internal region of a BH is that they 'accept' information from the external space-time future [4, 8]. In particular, the evolution of the event horizon at any time depends not on what has occurred in the past, but on what will occur in the future (see the resent review by I D Novikov and V P Frolov [4]).

In view of such unusual properties of BHs, the possibility of their existence in the Universe has been actively discussed over the last several decades. The ultimate answer to this question should come from astronomical observations. In 1964, Ya B Zel'dovich [9] and E E Salpeter [10] first pointed to the possibility of astronomical observations of BHs. They predicted a powerful energy release during non-spherical accretion of matter onto a BH. Papers [11, 12] noted good prospects of studies of binary systems for searches for BHs (see also Ref. [13]). The theory of disk accretion onto neutron stars (NS) and BHs, elaborated in papers [14–17], allowed the rapid unveiling of the nature of compact X-ray sources discovered by the 'UHURU' satellite [18] as accreting NSs and BHs in binary systems. By the present time, many hundreds of X-ray binary systems have been discovered in our and nearby galaxies. Optical studies of X-ray binary systems [19–23] have enabled reliable mass determination of NSs and BHs in close binary systems [24]. Three-dimensional gas-dynamic models of gas flows in close binary systems (CBS) have elucidated formation mechanisms of accretion disks [25–30]. Models of advection-dominated disks around BHs, which allow one to explain an anomalously low luminosity of accreting BHs in many galactic nuclei and low mass X-ray binary systems, have been proposed in the last years (see, for example, Refs [31–36]). See [37–40] for a review and criticism of these models. Along with successful searches for stellar mass BHs, an important breakthrough has occurred recently in studies of supermassive BHs in galactic nuclei. Although quasars and active galactic nuclei have been the primary candidates [7, 10, 41–45], the most compelling case for the presence of supermassive compact objects have recently been obtained from studies of relatively 'quiet' galactic nuclei (see, for example, proceedings of recent symposia [46–48]).

In this review we summarize the results of searches for black holes. Various aspects of this problem are also discussed in recent reviews [4, 49–53].

2. Methods of searching for black holes

Three types of BHs are known:

(1) stellar mass BH $M = (3-50)M_{\odot}$ forming at late stages of massive stellar evolution. Stellar evolution ends up with the formation of a white dwarf [if the mass of the evolved stellar core is $M_{\rm c} \leqslant (1.2-1.4)M_{\odot}$], a neutron star (if $M_{\rm c} < 3M_{\odot}$), and a BH (if $M_{\rm c} \geqslant 3M_{\odot}$). In the case of the so-called soft equation of state of neutron star matter, when its maximal mass is about 1.5 solar masses, a comparatively low mass BH with $M \gtrsim 1.5M_{\odot}$ could exist [54];

(2) supermassive BH in galactic nuclei [$M = (10^6-10^{10})M_{\odot}$];

(3) primordial BH formed at the early stages of the Universe. Only sufficiently massive primordial BHs with $M > 10^{15}$ g could survive to the present time because of quantum evaporation of BH proposed by Hawking [55]. From the observational point of view, little is known about the primordial BH (see review [4]).

Recently, the existence of intermediate mass BHs with $M = (10^2-10^4)M_{\odot}$ located in circumnuclear regions in galaxies (at a mean distance of ~ 390 pc from the nucleus) has been discussed [56]. Masses of these objects are evaluated from their X-ray luminosity and spectrum [$L_{\rm x}(0.2-2.4\ {\rm keV}) = (10^{37}-10^{40})$ erg s^{-1}]. The intermediate mass BHs are assumed [57] to possibly originate from continuous coalescence of compact objects formed from hundreds of massive stars in a cluster several parsecs in size. The characteristic time of such a merging process is $\sim 10^9$ years [57]. In connection with the coalescence models, binary supermassive black holes in galactic nuclei could exist in principle. Scenarios of the BH coalescence are theoretically examined in Refs [58, 59]. The possibility of these bright sources being microquasars with relativistic jets directed toward the observer is also considered [60, 61]. In that case the masses of relativistic objects are of the order of several $M_{\odot}$. The recent optical identification of one such object [61] lends credence to this hypothesis. At the same time, recent measurements of the velocity dispersion of stars in the central parts of globular cluster M15 suggest an intermediate mass central BH with $\sim 2500M_{\odot}$ [62].

From the astronomical point of view, to detect a BH it is necessary:

(1) to measure the mass of the object;

(2) to show that its radius does not exceed $r_{\rm g}$;

(3) to obtain observational evidence that the object has no observed hard surface but virtually the event horizon.

Masses of BHs are reliably measured using the motion of nearby gas and stars. As in most cases the characteristic distances are large ($r \gg r_{\rm g}$), it is sufficient to use Newtonian gravity law. Recently, the possibility of measuring solitary BH masses using the gravity microlensing effect has appeared [63, 64] (the duration of the brightness variation of a remote star is proportional to the square root of the mass of the gravitational lens).

It is very hard to measure BH radii. So far only relatively crude [$r < (10-100)r_{\rm g}$] indirect estimates have been employed, such as studies of the powerful X-ray luminosity and spectrum during accretion of matter onto the BH, analysis of rapid X-ray time variability, studies of X-ray line profiles, etc.

The main signatures of an accreting BH of stellar mass (see, for example, Refs [4, 49]) include a large mass of the object and a powerful X-ray emission with no steady X-ray pulsations or type I X-ray bursts typical for accreting NSs which have solid surfaces and rapidly rotate. Note that some accreting NSs also do not exhibit X-ray pulsations and type I X-ray bursts, i.e., these criteria are only necessary but not sufficient conditions for reliable identification of massive compact objects as BHs.

Thus far no sufficient observational selection conditions for BHs have been found, but it should be stressed that all necessary criteria based on GR are fulfilled for known BH candidates.

Observational studies of BHs are carried out in two directions:

(1) searches for massive compact objects — BH candidates. Up to the present time, great progress has been made: the number of known BH candidates (in X-ray binary systems or galactic nuclei) is approaching 100;

(2) searches for sufficient criteria allowing for the unique identification of the discovered BH candidate as a real BH. There are a lot of difficulties here, but there is some progress and much hope is placed on future space X-ray, interferometric, and gravitational wave experiments.

We specially mention what sense astronomers observers put in the term 'black hole'. Although BHs have 'virtually' been discovered, the final proofs of their existence in the Universe have not yet been obtained. Nevertheless, astronomers observers, of course with some forced interpretation, apply the term 'black hole' to those massive and compact objects for which all presently known observational appearances agree with GR predictions for BHs. Here the principal observational benchmarks for BHs, as noted above, are as follows:

(a) stellar mass BH, accreting objects in X-ray binaries — a large mass ($m_x > 3M_\odot$), a powerful ($L_x \cong 10^{36} - 10^{39}$ erg s^{-1}) X-ray emission with an absence of steady X-ray pulsations and type I X-ray bursts, as well as a small radius [$r < (10-100)r_g$] derived, as a rule, from the rapid hard X-ray variability on timescales $10^{-2} - 10^{-3}$ s;

(b) supermassive BH in galactic nuclei — a large mass [$\sim (10^6 - 10^9)M_\odot$], a high mass to luminosity ratio ($M/L > 10-1000$) for nuclei of quiet galaxies, or a total luminosity close to the Eddington limit for active galactic nuclei, as well as a small radius [$r < (10-100)r_g$] as estimated from rapid variability or from direct measurements of the nuclear size by high angular resolution methods.

Moving ahead, we note that modern observations accounting for observational selection effects suggest that in our Galaxy, comprising about 10^{11} stars, there are $\sim 10^{10}$ white dwarfs, $\sim 10^8$ neutron stars, and $\sim 10^7$ black holes.

3. Methods of determining black hole mass

3.1 Nuclei of galaxies

There are two principal means for determining the mass of active galactic nuclei (see, for example, Dibai [44, 65, 66]).

1. Motion of gas and stars near the nucleus is assumed to be controlled by its gravity field (Woltjer [67]). In this case, the virial relation $v^2 \sim r^{-1}$ should exist between the velocities v of stars or gaseous clouds surrounding the nucleus and the distance r to the nucleus. Hence the estimate of the mass of the nucleus m_x can be obtained:

$$m_x = \frac{\eta v^2 r}{G}\,, \tag{1}$$

where $\eta = 1-3$ depending on the assumed kinematic model for motion of test bodies around the galactic nucleus.

Modern observational facilities (the Hubble Space Telescope, the largest ground-based new generation telescopes equipped with compensation systems for atmospheric distortions, intercontinental radio interferometers for observation of cosmic megamasers, etc.) in many cases allow us to see directly the gas (and in the case of our Galaxy center — individual stars, too) moving near the nucleus (Fig. 1). So the mass of the galactic nucleus is uniquely found by directly applying the Newton's gravity law and from a relation like Eqn (1).

If the circumnuclear gas-dust disk is unavailable for direct imaging and studies, another method is used based on statistical examination of stellar kinematics in central parts of the galaxy, which is mainly determined by gravitational

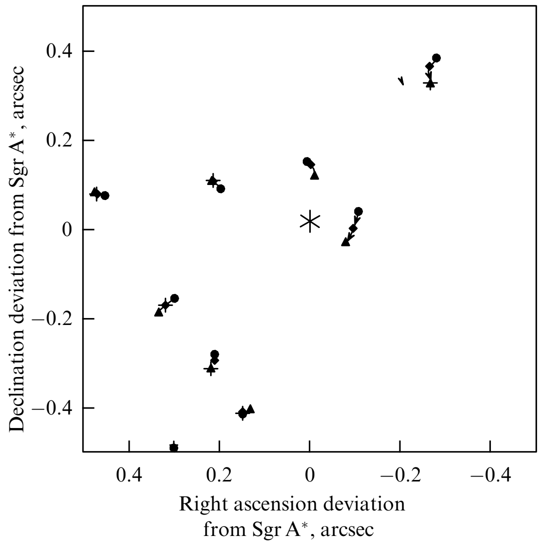

Figure 1. Observed stellar motions in the sky plane in the vicinity of the nucleus of our Galaxy controlled by gravitational attraction of the central BH with mass $\sim 2.6 \times 10^6 M_\odot$ [68]: ● — observations in 1995, ◆ — in 1996, ▲ — in 1997.

interaction with the nucleus. By observing the brightness distribution $I(r)$, rotational velocities $V(r)$, and velocity dispersion along the galactic diameter (near its nucleus) and making use of the expression for the mass distribution $M(r)$ which is derived from Boltzmann's equation with account for collisionless stellar interactions [50, 69], we can evaluate the mass $M(r)$ comprised within the volume of radius r:

$$M(r) = \frac{V^2 r}{G} + \frac{\sigma_r^2 r}{G}\left[-\frac{\mathrm{d}\ln v(r)}{\mathrm{d}\ln r} - \frac{\mathrm{d}\ln\sigma_r^2}{\mathrm{d}\ln r} - \left(1 - \frac{\sigma_\theta^2}{\sigma_r^2}\right) - \left(1 - \frac{\sigma_\varphi^2}{\sigma_r^2}\right)\right]. \tag{2}$$

Here σ_r, σ_θ, and σ_φ are the radial and two azimuthal components of the velocity dispersion of stars, $v(r)$ is the stellar density, which in the first approximation can be set proportional to the brightness $I(r)$ (see Refs [50, 69] for more detail).

In active galactic nuclei, where powerful broad emission lines are observed, the mass of the nucleus can be estimated using Eqn (1). Velocities v of gas clouds forming the broad emission line component are derived from the half-width of this broad component. The formation mechanisms of high velocity clouds near the central BH in active galactic nuclei are described, for example, in Ref. [70]. The distance r from the gas clouds to the nucleus center can be estimated by two means: from the photoionization model of the circumnuclear region [71–73, 44, 65, 66], or by the time delay Δt between the rapid variability of the broad emission line component relative to that of the continuum spectrum, $r \cong c\Delta t$ (the so-called 'reverberation mapping method' [74–76]). The retardation of rapid variability in lines relative to continuum in nuclei of Seyfert galaxies was discovered by Lyutyi and Cherepashchuk in 1971 [77–81] (Fig. 2). At present, this effect is widely used to obtain the most reliable estimations of the BH masses in active galactic nuclei (see, for example, Refs [82–89]).

2. The second method of estimation of the active galactic nucleus mass is based on the hypothesis that the bolometric

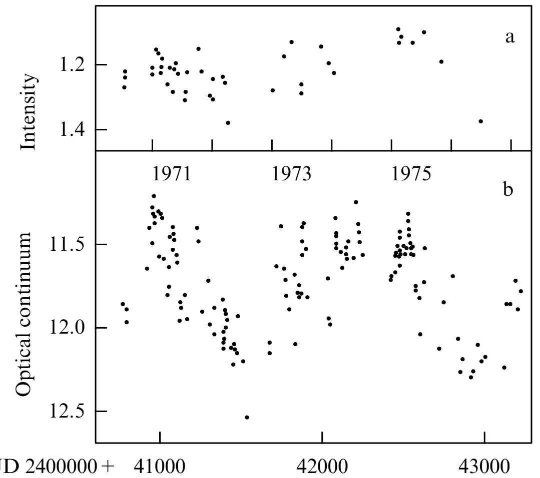

Figure 2. The $H_\alpha + [NII]$ emission line (a) and optical continuum variability (the U band of the UBV system) (b) in the Seyfert I galactic nucleus NGC 4151 (observations by Lyutyi and Cherepashchuk [81]). The change in the $H_\alpha + [NII]$ line intensity is delayed relative to the continuum. This allows estimation of the distance of gaseous clouds from the central supermassive BH and determination of the BH mass.

luminosity of the nucleus is close to the Eddington limit L_E where radiation pressure balances gravity attraction (Zel'dovich and Novikov [41]):

$$L_E = 1.3 \times 10^{38} \mu \frac{m_x}{M_\odot} , \qquad (3)$$

where μ is the number of nucleons per electron in accreting plasma and m_x is the mass of the nucleus. Among galactic nuclei, quasars display the highest luminosity, up to 10^{47}–10^{48} erg s^{-1} (the luminosity of the nucleus of our Galaxy is $\leqslant 10^{35}$ erg s^{-1} or $\leqslant 10^{-9}$ of the Eddington value). So the lower mass limit derived from Eddington luminosity is most relevant for quasars [41]. The condition

$$L_{QSO} \leqslant L_E$$

implies masses $m_x \geqslant 10^9 M_\odot$.

The mass of a galactic nucleus can be estimated also by indirect methods, such as from the form and width of the iron K_α emission line, from the maximum pulsation frequency of emission from accretion disk, from the dependence of the active galactic nucleus luminosity on the central BH mass, from the absorption band intensity near K-edges of the nucleus X-ray spectrum [90], etc. These methods will be considered below when analyzing individual objects.

3.2 X-ray binary systems

The components of an X-ray binary system are not seen separately. Only the radial velocity curve and light curve of the binary are measured (Fig. 3). Assuming a point-like mass of the optical star and making use of the Newtonian gravity law, the mass function of the optical star is inferred from the radial velocity curve (see, for example, Ref. [49]):

$$f_v(m) = \frac{m_x^3 \sin^3 i}{(m_x + m_v)^2} = 1.038 \times 10^{-7} K_v^3 P (1 - e^2)^{3/2} , \qquad (4)$$

where m_x and m_v are masses of the relativistic object and the optical star (in solar units), respectively, i is the orbital inclination (the angle the line of sight makes with the orbital normal), K_v is the observed radial velocity semi-amplitude of the optical star (in km s^{-1}), P is the orbital period (in days), and e is the orbital eccentricity (derived from the deviation of the radial velocity curve shape from pure sine-like form). The mass function $f_v(m)$ is the observed quantity and provides the absolute lower limit on the mass of the relativistic object

$$m_x > f_v(m) .$$

The optical star in an X-ray binary system is not a point-like object. It is tidally distorted and illuminated by X-ray radiation from the accreting relativistic object. So the observed radial velocity curve does not perfectly reflect the orbital motion of the optical star. It is necessary to investigate the effect this deviation from the point-like form has on the system's mass function measurement.

As shown in Refs [92, 49], the effect of the optical star being not point-like, its pear-like shape and X-ray illumination on the mass function is small for the large mass ratio of

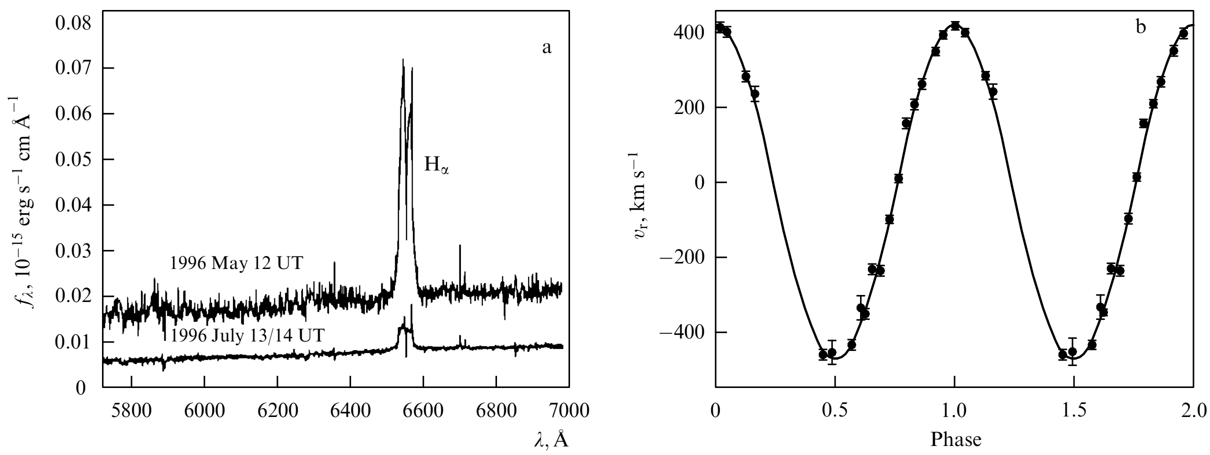

Figure 3. (a) Optical spectra of X-ray nova, a binary system with a BH, Nova Oph 1977 (H1705–250) in the quiescent state, obtained by Filippenko et al. [91] on May 12 and June 13–14 1996. Multiple absorption lines in the spectrum of the companion star K5 V are visible. Doppler shifts of these lines are utilized to construct the radial velocity curve. A powerful broad two-humped emission hydrogen line H_α is also seen, which is formed in the accretion disk around the BH. (b) Radial velocity curve [91].

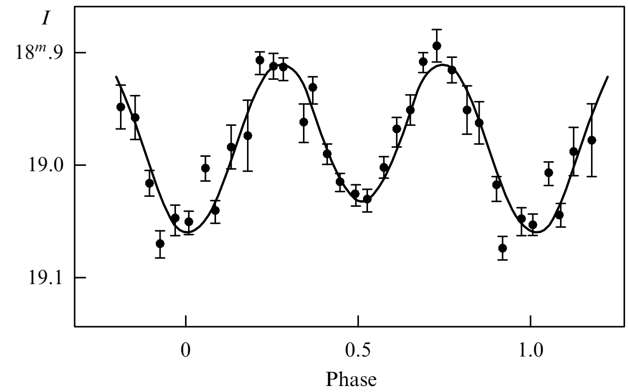

Figure 4. The observed infrared (⫯) and theoretical (—) light curves of the X-ray nova binary system with BH XN Musc (GRS 1124–68) in the quiescent state. The curves are mainly shaped by the ellipsoidal effect of the optical K2 V star. The inclination angle of the orbit to the sky plane is estimated to be $i = 41°$ (from Remillard et al. [94] and Antokhina and Cherepashchuk [95]).

the components $q = m_x/m_v > 5$ (the case of X-ray novae among which most BH candidates were discovered). For quasi-persistent X-ray binaries with massive O–B components, where $q < 1$ the mass function $f_v(m)$ should be corrected for the non-zero size of the optical star since the center of mass of the binary system lies inside the optical star body [49, 92, 93]. The corresponding correction of mass m_x for known systems is usually less than 10%.

The BH mass is determined from Eqn (4):

$$m_x = f_v(m)\left(1 + \frac{1}{q}\right)^2 \frac{1}{\sin^3 i} . \tag{5}$$

As X-ray binary components can not be seen separately, there are two free parameters, q and i, which must be determined from additional conditions. These conditions are as follows [49].

3.2.1 Optical or infrared light curve of the binary system. The light curve $l(t)$ determines the binary inclination angle i:

$$l(t) = l(t, q, \mu, i, r_d, L_d) . \tag{6}$$

Here μ is the degree of the optical star filling its Roche lobe (for X-ray novae $\mu = 1$ because in the quiescent state the accretion disk and gaseous stream from the optical star are observed), and r_d and L_d are the radius and luminosity of the accretion disk, respectively. In the case of X-ray novae in the quiescent state and massive X-ray binaries with O–B components, the light curve $l(t)$ is mainly defined by the optical star ellipticity and for $q > 1$ most strongly depends on the parameter i (Fig. 4). The ellipticity effect is due to tidal deformation of the optical star figure in the gravity field of the relativistic object. The orbital revolution of the system causes periodic optical variability. The disk luminosity L_d can be found from spectrophotometric observations. The method of determination of i from the light curve $l(t)$, primarily shaped by the ellipticity effect, was first proposed by Lyutyĭ, Sunyaev, and Cherepashchuk in 1973 [22, 23] and is widely used to determine BH masses in X-ray binary systems (see Refs [96–101], as well as reviews [49, 51]). As noted in some modern reviews on observational studies of BHs (for example, [51, 102]), so far this is the only reliable method to evaluate i.

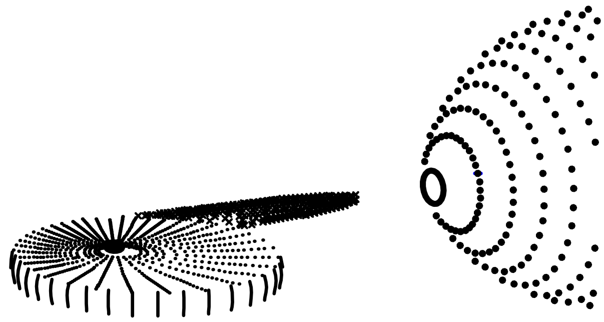

Figure 5. A mathematical model of an X-ray binary system based on three-dimensional gas-dynamic calculations by Boyarchuk's group [25–27] for the orbital period phase $\varphi = 0.35$.

3.2.2 Rotational absorption line broadening in the optical star spectrum. The star is not a point-like object and fills or almost fills its Roche lobe whose relative size depends on the component mass ratio q (Fig. 5). So observing the optical star spectrum with high resolution (Fig. 6) and determining the value $V_{\rm rot} \sin i$ from rotational broadening of absorption lines one can find q from the equation (see, for example, Refs [104, 105]):

$$V_{\rm rot} \sin i = 0.462 K_v \frac{1}{q^{1/3}} \left(1 + \frac{1}{q}\right)^{2/3} . \tag{7}$$

In Eqn (7) the assumption was made that axial and orbital rotation of the optical star are synchronized, which takes place for most BH X-ray binaries, in particular, for X-ray novae, in which, as we noted above, optical A–M stars with convective envelops fill their Roche lobes.

3.2.3 Distance to the system. Knowing the distance to the system d allows the absolute mean radius of the star R_v to be determined from the visual stellar magnitude of the optical star and its spectral class if the interstellar reddening is known. Then, assuming the optical star form to be described by the Roche equipotential of the binary system (whose size depends on q), we arrive at the equation relating the parameters q, μ, and i [106, 24]:

$$\sin i = \frac{0.38\mu}{R_v} \sqrt[3]{\frac{GP^2 f_v(m)}{4\pi^2}} \frac{1+q}{q^{1.208}} . \tag{8}$$

For persistent X-ray binaries with massive O–B companions, optical stars can underfill their Roche lobes; then the use of Eqn (8) enables us to evaluate the optical star Roche lobe filling factor μ.

3.2.4 X-ray eclipses. If the X-ray source in an X-ray binary system is eclipsed by the optical star over the time interval D (in the case where i is close to 90°), there is an independent equation relating parameters q, μ, and i:

$$D = D(q, \mu, i) . \tag{9}$$

Tables of the eclipse durations $D(q, \mu, i)$ are calculated for the Roche model both for circular and elliptical orbits (see,

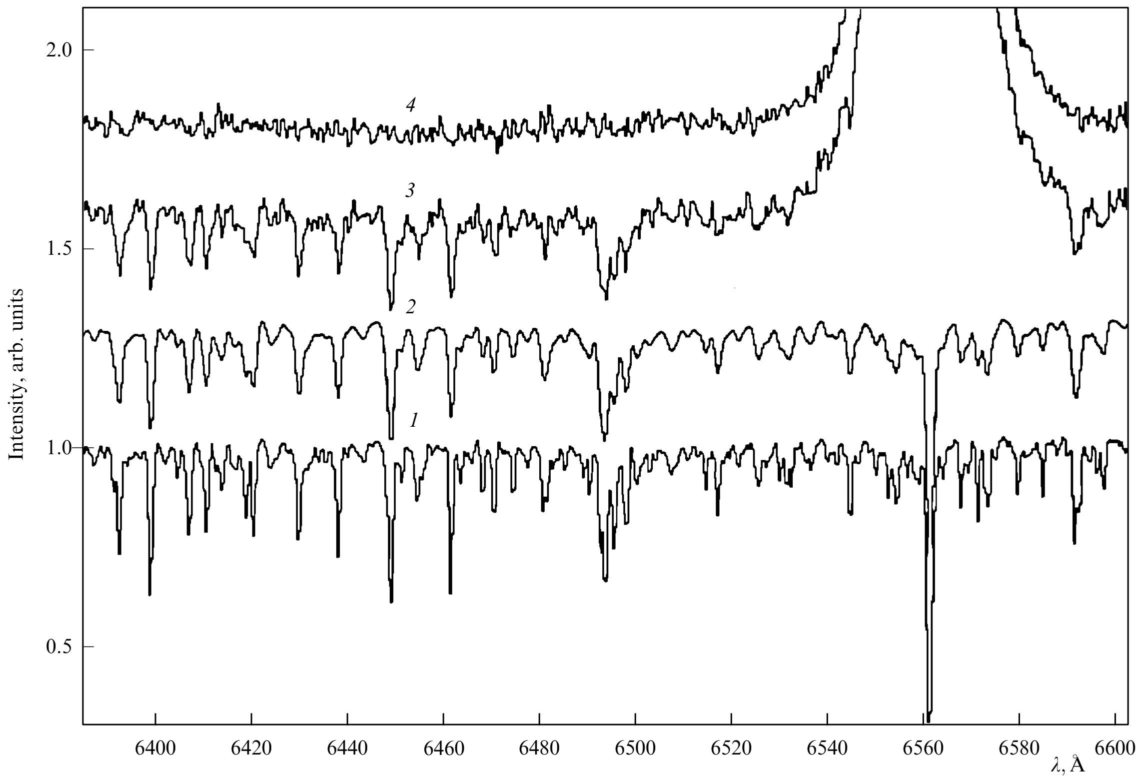

Figure 6. The effect of the rotational broadening of absorption lines in the spectrum of the optical K0 IV star in the BH X-ray nova binary system V404 Cyg (from Casares and Charles [103]): *1* — the spectrum of the comparison star HR 8857 with narrow lines; *2* — the spectrum of the comparison star HR 8857 artificially broadened by the rotation ($V_{\rm rot} \sin i = 39.1$ km s^{-1}); *3* — the average observed spectrum of V404 Cyg; *4* — the residual spectrum after the rotationally broadened spectrum of the comparison star HR 8857 has been subtracted from the spectrum of V404 Cyg.

for example, Ref. [107]). Unfortunately, so far no X-ray eclipses have been observed from known X-ray binaries with BHs because of the relatively small size of the optical star (in X-ray novae). The fact of this absence of X-ray eclipses can be used to evaluate the upper limit on the binary inclination angle *i*.

3.2.5 Spectroscopic estimate of the optical star mass $m_{\rm v}$. The knowledge of the precise spectral class and luminosity class of the optical star allow its mass $m_{\rm v}$ to be evaluated and for known *i* to find $m_{\rm x}$ from Eqn (4) [108, 287]. This estimate of mass $m_{\rm v}$ can be done only to within a factor of ~ 2 [109], so the BH mass $m_{\rm x}$ obtained by this method is approximate. Additional constraints on the X-ray binary parameters can be obtained from analysis of the variability of linear polarization of its optical radiation [110].

3.2.6 Variability of absorption line profiles in the optical star spectrum. Antokhina and Cherepashchuk [111] and Shabhaz [112] proposed a new method of determination of the X-ray binary parameters based on studies of the variability of absorption line profiles in the optical star spectrum with the orbital period phase. This variability is due to the pear-like shape of the optical star in the X-ray binary system and temperature distribution inhomogeneity over its surface, caused by gravitational limb darkening and X-ray heating. The amplitude of the effect attains 10% of the line profile width and significantly depends on the parameters *q* and *i*. It is important that this method provides an estimate of the parameter *i* independent on the accretion disk luminosity. In paper [113], the joint influence of the ellipsoidal effect and X-ray illumination on the absorption line profile in the spectrum of the optical star in an X-ray binary system is calculated (Fig. 7).

Thus, the mass function $f_{\rm v}(m)$ enables the BH mass $m_{\rm x}$ to be uniquely determined from Eqn (5) provided that *q* and *i* are known from Eqns (6) and (7). Other additional conditions can be used to check the obtained value of $m_{\rm x}$. That the

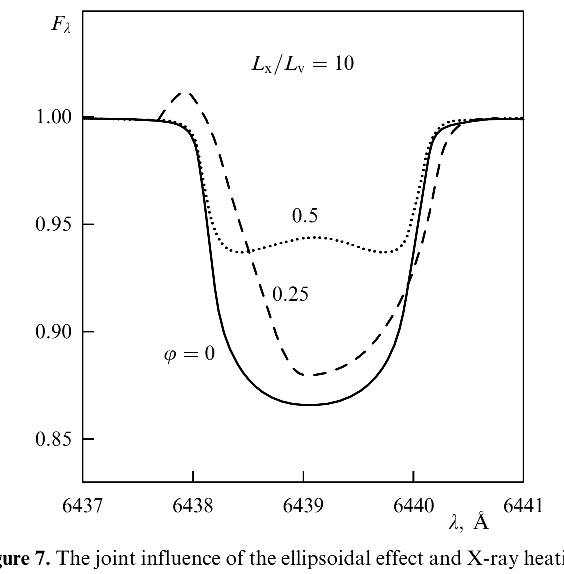

Figure 7. The joint influence of the ellipsoidal effect and X-ray heating on an absorption line profile in the spectrum of the optical companion of an X-ray binary system (from Antokhina et al. [91]). Three profiles for different orbital period phases are shown.

number of additional conditions exceeds the number of unknown parameters increases the reliability of the BH mass determination.

Lately, new indirect estimates of the BH masses in X-ray binaries have appeared based on modeling of X-ray quasi-periodic oscillations from accreting BHs [114]. These estimates are based on studying global oscillations of the inner edge of the accretion disk in the normal direction. The BH masses found by this method are in accordance with values obtained by the classical method.

4. About black hole radii determination

4.1 Nuclei of galaxies

Having huge masses, BHs in the nuclei of nearby galaxies have appreciable angular sizes (more than 10^{-6} arcseconds), which makes it promising to design corresponding space radio interferometers to directly measure the BH radii or, at least, the radii of the last marginally stable orbit ($3r_g$ in the case of a Schwarzschild BH) (see, for example, Ref. [115]). In particular, the gravitational radius of the BH in our Galactic center ($m_x = 2.6 \times 10^6 M_\odot$) is 8×10^6 km ($11R_\odot$), or ~ 0.05 AU. The corresponding angular size for the distance to the Galactic center ~ 8 kpc is $\sim 7.1 \times 10^{-6}$ arcseconds. The angular size of the gravitational radius of the BH in the center of M31 (the Andromeda galaxy) with a BH mass of $m_x = 7.5 \times 10^7 M_\odot$ is 2.4×10^{-6} arcseconds. These values could well be measured by the next generation space interferometers. For example, the proposed angular resolution of the X-ray space interferometer will attain 10^{-7} arcseconds [115], the angular resolution of the 'Radioastron' interferometer will be of the order of 10^{-6} arcseconds in radio band [116]. The use of such powerful facilities in future galactic nuclei studies will open up the principal possibility to watch physical processes close to the event horizon (or at least near the last marginally stable orbit) of a supermassive BH. Modern methods of intercontinental radio interferometry made it possible to study the formation process of the collimated jet in M87 at a distance of $\sim 30-100$ gravitational radii [117] (Fig. 8).

Application of modern high angular resolution methods, including intercontinental radio astronomical observations of megamasers, has yielded thus far only crude upper limits on the radii of massive dark bodies in the galactic nuclei: $r < (10^3 - 10^4) r_g$.

Strong, but unfortunately indirect, constraints on BH radii have been obtained from the iron K_α emission line profile at an energy ~ 6.4 keV in spectra of active galactic nuclei observed by X-ray observatories ASCA, CHANDRA, and XMM with a high spectral resolution (see, for example, Refs [118–120]). This line emerges due to fluorescence excited by X-ray continuum quanta in the inner, very dense ($n \sim 10^{15}$ cm^{-3}), partially ionized parts of the accretion disk [119]. Relativistic effects near the BH horizon are responsible for the line redshift, a specific asymmetry of the line profile, and its huge width (up to 100 000 km s^{-1}). This gives us the possibility to obtain important clues as to the presence of BHs in galactic nuclei and to put constraints on the radius of the relativistic object (Fig. 9). Observations of spectra of some galaxies (for example, M51) by the CHANDRA satellite [121] revealed the presence of only a narrow (the total width ~ 0.02 keV) iron line at an energy 6.45 keV with a large equivalent width (~ 2 keV). This line appears due to

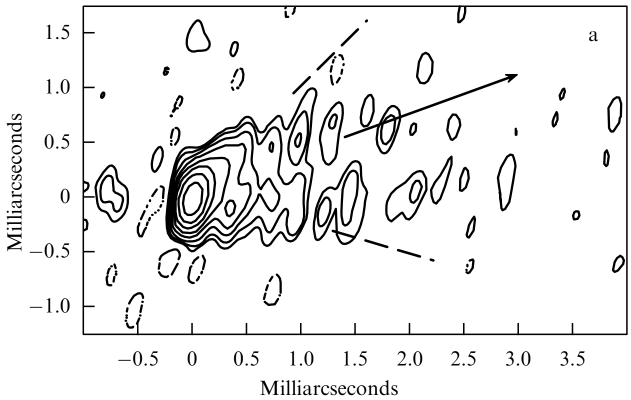

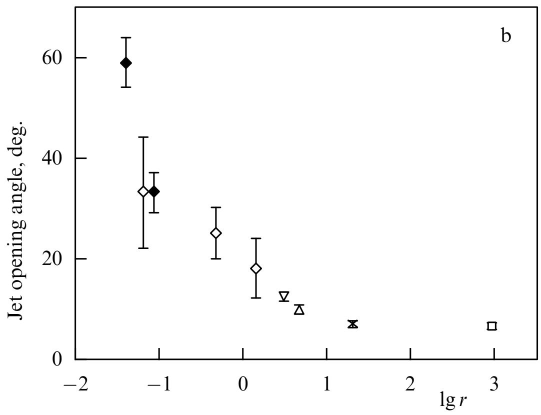

Figure 8. (a) The image of M87 galaxy nucleus at the 7 mm wavelength obtained by the global radio interferometry method with an angular resolution of 0.33×0.12 milliarcsecond (from Junor et al. [117]). The arrow indicates the direction of the large-scale jet a few kiloparsecs in length. The jet opening angle near the galactic nucleus is 60°, then at the scale $30-100\,r_g$ and beyond until $1000\,r_g$ ($r_g = 2GM/c^2 = 0.0003$ pc) the jet collimation occurs up to the standard opening angle of several degrees (1 milliarcsecond for M87 corresponds to 0.071 pc or $\sim 240\,r_g$). (b) The dependence of the jet's full opening angle on the distance to the central BH in the M87 nucleus (from Junor et al. [117]). These data suggest that the jet could be formed in the accretion disk around the BH by magneto-gasdynamic processes [117].

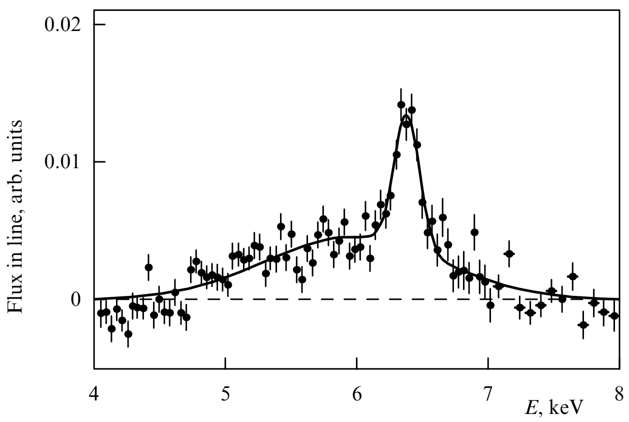

Figure 9. The mean profile of the iron K_α line at 6.4 keV in spectra of Seyfert galactic nuclei (from Nandra et al. [119]). The narrow component is centered to the laboratory frame energy 6.4 keV (accounting for the redshift of the galaxies) and has a width of ~ 0.1 keV. The broad component is strongly red-shifted with a central energy of ~ 6.1 keV and has a width of ~ 0.7 keV; its contribution is $\sim 75\%$ of the total line emission energy.

fluorescence of comparatively cold matter near the galactic nucleus illuminated by the hard X-ray emission with a power-law spectra from the central source [121]. It is possible to assume that in such cases the central relativistically rotating parts of the accretion disk are screened by the edge of a gas-dust torus, which presumably exists in the vicinity of active galactic nuclei [122, 123] (see, however, [124]). Paper [125] shows that the emission iron K_α line in the nucleus of Seyfert I galaxy NGC 5548 measured by the CHANDRA satellite is narrow (the width FWHM = 4515 km s^{-1}), while the same line was measured by ASCA four years before in 1996 as having much broader width. The unique and very rapid (on timescale $\sim 10^4$ s) variability of the iron K_α emission line profile was detected by ASCA from Seyfert I galaxy NGC 4151 [126]. As in the case of X-ray binary systems, the important estimate of the radius of the galactic nucleus is obtained from studies of its rapid variability (especially in the X-ray band). For example, a rapid (on timescales of about 10 minutes) strong (by 5 times) X-ray (2 – 10 keV) variability has recently been detected by CHANDRA from our Galaxy nucleus [127]. The high angular resolution $\sim 0''.5$ allowed the authors of Ref. [127] to argue that this rapid variability is indeed related to the source Sgr A residing in the center of our Galaxy and not to an X-ray binary system occasionally projected on the Galaxy center (Fig. 10). Besides, this rapid X-ray variability was accompanied by an enhanced radio luminosity from the Galaxy nucleus [127], which strongly supports the genetic relation of the rapidly varying X-ray component to the Galaxy nucleus. In that case $r \leqslant ct_{\min}$ is just 20 gravitational radii, which is a strong limitation on the size of the nucleus of our Galaxy.

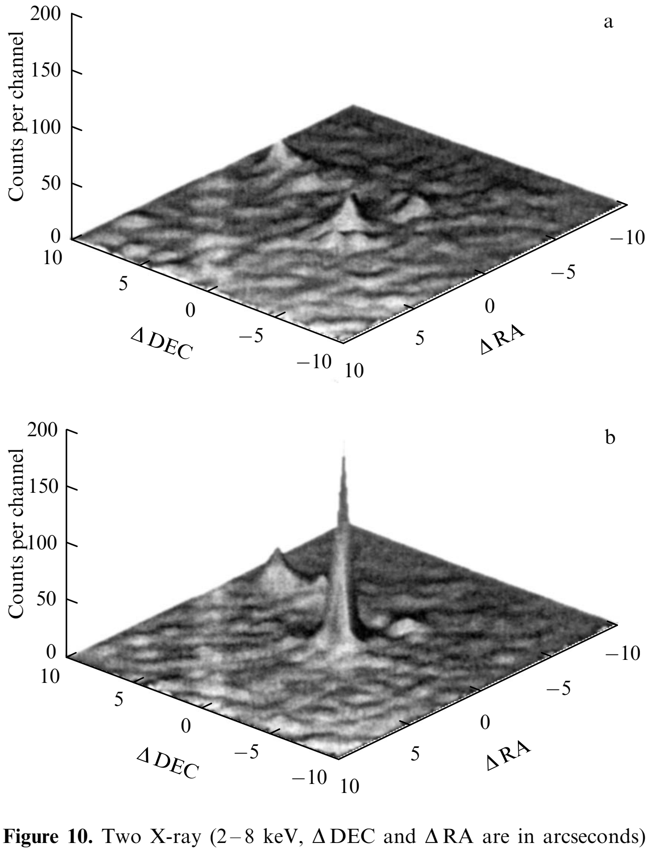

Figure 10. Two X-ray (2 – 8 keV, Δ DEC and Δ RA are in arcseconds) images of the Galactic center showing a strong and rapid variability of the X-ray emission from the Galactic nucleus. This evidences its small size ($\leqslant 20\,r_g$). The images were taken by the CHANDRA X-ray observatory on 21.09.1999 (a) and on 26 – 27.10.2000 (b) with an angular resolution of $\sim 0''.5$ corresponding to 0.02 pc (from Baganoff et al. [127]).

Similar rapid X-ray variability is observed in some active galactic nuclei. For example, ROSAT and RXTE observations of Seyfert I galaxy Mkn 478 (PG 1440+356) revealed strong (up to 50%) short X-ray outbursts on timescales as short as 500 – 800 s [128]. Then the nucleus size is $r < ct_{\min} = 1.5 \times 10^{13}$ cm (for $t_{\min} = 500$ s). Since the BH mass in this galaxy as determined by the photoionization method is $6 \times 10^7 M_\odot$ [128], the corresponding gravitational radius is 1.8×10^{13} cm. From here the authors conclude that a Kerr BH with the horizon radius $0.5 r_g = 0.9 \times 10^{13}$ cm resides in this galactic nucleus. It is also possible that the superfast X-ray variability here is due to the relativistic beaming effect in X-ray emission from plasma moving with relativistic velocities in the observer's direction.

Another possible evaluation of the BH radius is associated with studies of rare X-ray transient phenomena in nuclei of quiet galaxies (see, for example, Refs [129 – 136]). In total, 5 transient galactic nuclei are known at present [134]. Among them is galaxy NGC 5905, from which an X-ray outburst with an amplitude up to 170 times that of the quiescent state was observed on a timescale of several years. This outburst was not accompanied by the corresponding optical outburst in the continuum, and only weak changes in emission lines related to the X-ray outburst effect on gas clouds surrounding the nucleus were seen. The most relevant scenario to explain such X-ray transients is the tidal disruption of stars in the vicinity of a BH in the galactic nucleus predicted by M J Rees [137, 138]. When a star flies near a supermassive BH, the following events occur consecutively: tidal deformation of the star, its disruption, the fall of stellar matter onto the BH, its capture, and gravitational energy release (see, for example, Refs [139, 140]). The rate of tidal disruption of stars near a supermassive BH in the average galactic nucleus is estimated to be 1 star per 10^4 years. Since the temperature of the corresponding transient accretion disk at $3r_g$ is $\sim 3 \times 10^5$ K, the main energy release occurs in the hard ultraviolet and soft X-ray bands. The amount of accreting matter in fly-by of one star is $\leqslant 1 M_\odot$ [134]. Those stars near the supermassive BH that have not been totally disrupted due to huge tidal perturbations could be stars with rapid axial rotation, strong mixing, and intensive mass loss, which causes their anomalous observational characteristics [141].

4.2 X-ray binary systems

Direct measurement of the gravitational radii of stellar mass BHs will hardly be possible even in future space experiments since the angular size of a $10 M_\odot$ BH at a distance of 1 kpc is minuscule, $\sim 2 \times 10^{-10}$ arcseconds. In addition, due to the high density of matter in the inner parts of the accretion disk, the surroundings of a stellar mass BH could be unobservable in principle. So indirect methods are applied to evaluate the radii of stellar mass BHs.

The most simple and reliable method of the BH radius estimation is based on the determination of the minimal variability time of X-ray luminosity. For example, in Cyg X-1 the minimal X-ray variability time in the low state of the system with a hard power-law X-ray spectrum is $t_{\min} \cong 10^{-3}$ s [142]. Then the characteristic size of the source is

$$r < ct_{\min} = 300 \text{ km} = 10\, r_g\,.$$

The importance of rapid variability of accreting BHs was first noted in papers by Shwartzman [143] and Sunyaev [144].

The X-ray luminosity and spectrum of an accreting object provide the principally important information on the compactness of the object. The theory of disk accretion [14–17] suggests that in the case of an accreting BH huge power is released in the X-ray band

$$L_{\mathrm{x}} = 0.057\dot{M}c^2 = 3\times10^{36}\,\frac{\dot{M}}{10^{-9}M_{\odot}/\mathrm{yr}}\ \mathrm{erg\ s^{-1}}\quad \text{for a Schwarzschild BH}\,,$$

$$L_{\mathrm{x}} = 0.42\dot{M}c^2 = 3\times10^{37}\,\frac{\dot{M}}{10^{-9}M_{\odot}/\mathrm{yr}}\ \mathrm{erg\ s^{-1}}\quad \text{for a Kerr BH}\,.$$

The emerging X-ray spectrum has a power-law shape with exponential cutoff at high energies.

Unfortunately, it is impossible to distinguish an accreting BH from a NS by X-ray luminosity because the accretion rate $\dot{M}$ onto the relativistic object is never known precisely. In addition, in the theory of advection-dominated flows (ADAF) [35, 36], the overwhelming fraction of the accretion energy released is stored in hot ions that have no time to pass the energy to electrons and bring thermal energy under the BH horizon. Observation of the X-ray iron line at energy 6.4 keV in Cyg X-1 by the ASCA satellite with an energy resolution of $\Delta E/E \approx 2\%$ [145] demonstrated that this line is present in all phases of the orbital period of the X-ray binary system, and has a small total width (< 0.2 keV) and an equivalent width of $\sim 10-30$ eV. Apparently, this line originates in the outer parts of the accretion disk where FeXI ions are present [145]. So it seems impossible to significantly constrain the BH radius using this line.

To conclude we remind that accreting BHs should exhibit neither X-ray pulsar nor type I X-ray burster phenomena since, according to GR, they have no observable solid surfaces.

5. Supermassive black holes in galactic nuclei

In most cases galaxies have compact condensations of stars and gas in their central parts which are commonly called nuclei (see, for example, Refs [146, 147]). As a rule, nuclei are clearly distinguished in spiral galaxies and almost indiscernible in irregular galaxies. A comparatively small fraction of galaxies ($\sim 1\%$ of the total number) has active nuclei. These galactic nuclei demonstrate powerful non-stationary activity with high luminosity in X-ray, UV, and radio bands. Although active galactic nuclei are rather rare, their studies are of principal importance to understand the nature of galactic nuclei.

Galaxies with active nuclei are usually subdivided into four main types: Seyfert galaxies, radio galaxies, BL Lac objects (blazars), and quasars. Seyfert galaxies in most cases are spiral galaxies with bright nuclei that radiate in continuum and in strong broad emission lines of hydrogen, helium, and other elements [44, 65, 66, 73]. Type I Seyfert galaxies demonstrate broad permitted and narrow forbidden emission lines, while in spectra of type II Seyfert galaxies both permitted and forbidden lines are narrow (< 1000 km s^{-1}). Most radio galaxies are elliptical galaxies with a powerful radio emission exceeding their optical luminosity. BL Lac objects, named after the famous BL Lacertae, are characterized by the absence of lines in the spectrum, a strong optical variability with amplitude up to five stellar magnitudes (i.e., change in the luminosity 100 times), a variable moderate radio emission, and a significant polarization of the emission. Quasars are also very active galactic nuclei of very remote giant (with a size of up to 50 kpc) galaxies at redshifts from $z = 0.04$ to $z = 4-6$. The redshift of the famous quasar 3C 273, a radio source, is $z = 0.158$ (the corresponding distance is 630 Mpc or about 2 billion light years). Quasars are the most powerful stationary emitting objects in the Universe. The total luminosity of quasars, including radio, IR, X-ray, and gamma-ray bands, attains $10^{47}-10^{48}$ erg s^{-1}, which by 3 orders of magnitude exceeds the luminosity of the host galaxy. Finally, the so-called liners close the luminosity range of active galactic nuclei from the low end. These are galaxies showing narrow (a few hundred km s^{-1}) emission lines in their spectra, very similar to HII zones. The nuclear luminosity of liners is $\sim 10^{41}-10^{39}$ erg s^{-1} and possibly less. Recently, CHANDRA observations of many liners revealed the presence of point-like X-ray sources in circumnuclear regions with a luminosity from 10^{38} to 10^{41} erg s^{-1} [148].

All galaxies with active nuclei demonstrate optical variability on timescales from several days to many years [149–153]. The minimal variability timescale $t_{\min}$ is used to place upper limits on the emitting region size $r \leqslant ct_{\min}$, which lies in the range $(3\times10^{15}-10^{17})$ cm, i.e., below 0.1 pc. In view of such a small volume wherein a giant energy is released, special mechanism of energy liberation are required. One such mechanism is the accretion of matter from stars and gas onto a supermassive BH located in the galactic center (see, for example, Refs [41–43, 45]). Since the efficiency of the accretion energy release is two orders of magnitude higher than in nuclear reactions, the mechanism of accretion onto supermassive BHs is most frequently used to explain the giant luminosity of quasars and active galactic nuclei (see, for example, Refs [43, 154, 122, 155]). Strongly collimated jets of matter moving with relativistic velocities are observed from many active galactic nuclei [156]. The jet sizes attain tens of kiloparsecs, much larger than the galactic sizes. The origin of the jets is thought to be related to magnetohydrodynamical processes in the internal parts of accretion disk around supermassive black hole or to rapid rotation of the black hole itself (see, for example, Refs [43, 157–162]).

5.1 Masses of supermassive black holes in active galactic nuclei

The first estimates of the masses of supermassive BHs ($m_{\mathrm{x}} > 10^8 M_{\odot}$) in the nuclei of most active galaxies (quasars) were done by Zel'dovich and Novikov [41] using the formula for the Eddington limit (3). Later on, masses of nuclei of Seyfert galaxies were evaluated from emission line intensities and profiles using the photoionization model of the nuclear region (Dibai [44, 65, 66]). Now it is recognized (see, for example, Refs [82, 88, 163]) that the most reliable and model-independent supermassive BH mass estimates are obtained from emission line spectrum and emission line variability time delay with respect to continuum variability. The latter effect was discovered in Ref. [79].

Almost simultaneously with the discovery of variability of Seyfert galactic nuclei continuum emission [149–151], emission line variability was reported in the spectrum of Seyfert galactic nucleus NGC 3516 (Andrillat and Souffrin [164]): the H_{β} hydrogen line almost completely disappeared over a 25 year interval. Three years before this study, emission lines in spectra of some quasars were reported to vary [165, 166]; in particular, the resonance line MgII in the 3C 345 quasar

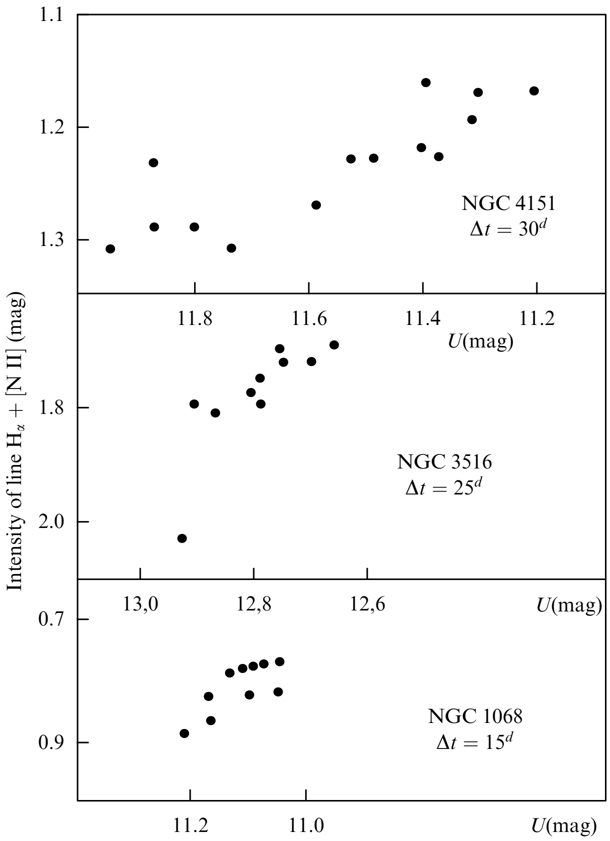

Figure 11. The correlation between the H_α + [NII] emission line and the continuum intensity in the Seyfert galactic nuclei NGC 4151, 3516, 1068 accounting for the time delay Δt of the line emission variability with respect to the continuum (from Lyutyi and Cherepashchuk [79]).

spectrum significantly changed over the time interval of one year (Dibai and Esipov [165]). Brightness variability of 3C 273 and 3C 48 was first reported in 1963 [167, 168].

In August 1970, using the 125-cm reflector of the Crimean Laboratory of Sternberg Astronomical Institute (SAI), Lyutyi and Cherepashchuk started narrow band ($\Delta\lambda \cong 100$ Å) photoelectric observations of three Seyfert galactic nuclei (NGC 4151, 3516, 1068) in the continuum adjacent to the emission line H_α + [NII] [77–81]. Observations were carried out using methods of variable star studies with relation to a comparison star, which enabled the absolute intensity of the emission line H_α + [NII] to be measured. A rapid (on a timescale of 5–15 days) variability of the H_α line intensity with the 15–35% amplitude was detected which was delayed relative to the variability in the continuum by $\Delta t = 15-30$ days [79] (Fig. 11; see also Fig. 2). Hydrogen emission lines in spectra of type I Seyfert galaxies consist of two components [73]: narrow (several hundred km s^{-1} in width) and broad (several thousand km s^{-1} in width) ones. The matter density in the formation region of the broad emission line component is larger [73] and rapid variability here is more probable. So, as noted in Ref. [79], the broad H_α emission line component is responsible for the rapid variability. The time delay Δt was interpreted in Refs [77–81] as the time it takes for the hard ionizing emission from the central source to travel to high-velocity gas clouds that emit the broad hydrogen emission line component. Then the estimate of the distance r from the central source to these clouds is simply $r \cong c\Delta t$ [79, 80]. The exact value of r can be found from the observed time delay Δt by studying the structure of the excitation and ionization region of high-velocity gas clouds illuminated by hard X-ray radiation from the central source [169, 170, 74–76]. Based on the solution of this problem, a wide-spread reverberation mapping method has been elaborated [75] allowing the determination of the value of r from the observed time delay Δt. The relation between the light curve $L(t)$ of the galactic nucleus and the emission line intensity $I(t)$ can be written in the form [75]

$$I(t) = \int_{-\infty}^{\infty} \psi(\tau)\, L(t-\tau)\, d\tau\,,$$

where $\psi(\tau)$ is the transmission function averaged over velocities which depends on the geometry of the broad emission line formation region, the line of sight, and the line emission coefficient. Cross-correlation between the light curve in the continuum and the emission line intensity variations is expressed as

$$\mathrm{CC}(\tau) = \int_{-\infty}^{\infty} \psi(\tau')\, \mathrm{AC}(\tau'-\tau)\, d\tau'\,,$$

where AC is the continuum autocorrelation function. As shown in Ref. [82], the cross-correlation function centroid $\tau_{\rm cent}$ yields the size $c\tau_{\rm cent}$ that reflects the average-weighted over the line intensity radius of the line formation region. The mass of the central object $M_{\rm rev}$ is determined as [88]

$$M_{\rm rev} \approx (1.45\times10^5 M_\odot)\left(\frac{c\tau_{\rm cent}}{\text{lt. day}}\right) v^2_{\rm rms,\,3}\,, \qquad (10)$$

where $v_{\rm rms,3} = v_{\rm FWHM}(\rm rms)\times10^{-3}$ km s^{-1}. Here $v_{\rm FWHM}(\rm rms)$ is the total width at half intensity of the emission line variable part.

The rapid variability of the emission line intensity and the retardation effect of emission lines relative to the continuum in nuclei of Seyfert galaxies were confirmed later by many authors (see, for example, Refs [84–86, 171, 172, 87, 82, 88, 83, 174, 173]) (Fig. 12). Moreover, the time delay Δt for higher ionization potential lines proved to be shorter than for lines with low ionization potentials [83, 86]. This indicates the stratification of radiation in lines and confirms the photoionization model of the nuclear region suggested in the pioneer papers by Zel'dovich and Novikov [41], Shklovskiĭ [71], and Bahcall and Kozlovsky [72]. So far, the reliability of the galactic nucleus mass estimation from the time delay Δt has been checked by two independent means [83, 88].

1. For one and the same galaxy NGC 5548 at a fixed moment (averaged over one year of observations), time delays Δt anti-correlate with the line widths v for lines with different ionization potentials (S IVλ1400+O IV]λ1402, C IVλ1546, C III]λ1909, HeIIλ1640, HeIIλ4686, $H_\beta\lambda$4861) in accordance with Kepler's law $v \sim r^{-1/2}$ (Fig. 13), so the mass of the nucleus as derived from different lines proves to be the same to within the measurement errors:

$$m_x^{(1)} = 6.8\times10^7 M_\odot\,.$$

And this is in spite of values of Δt varying from ~ 2 to ~ 30 days and values of v from ~ 4000 to ~ 13000 km s^{-1} (!).

2. For a given galaxy and one and the same line, the time delay Δt changes from year to year due to non-stationary

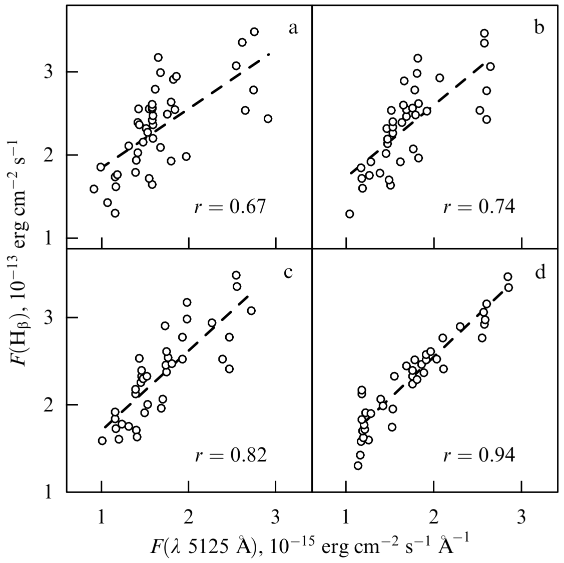

Figure 12. Correlations between the H_β emission line intensity and the continuum ($\lambda = 5125$ Å) in the spectrum of Seyfert galactic nucleus 3C 390.3 constructed for different time delays $\Delta t = 0$, 20, 40, and 100 days (figures a, b, c, and d, respectively). The corresponding values of the correlation coefficient r are given. The best correlation is obtained for $\Delta t = 100$ days (from Shapovalova et al. [174]).

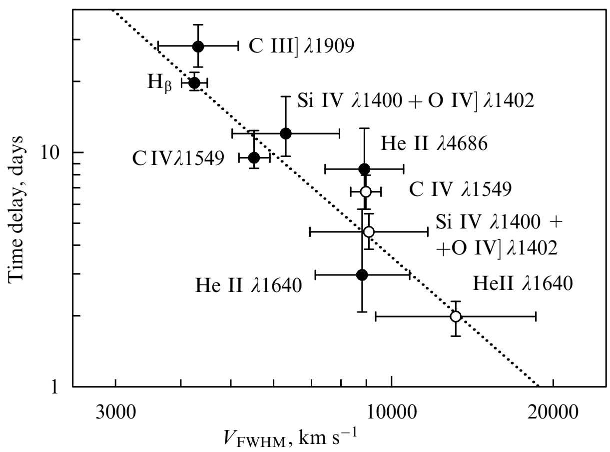

Figure 13. Anticorrelation of time delays between variability of different emission lines and the continuum and the line widths in accordance with the virial relation $v \sim r^{-1/2}$. Data are for galaxy NGC 5548. The dotted line corresponds to the virial mass of the galactic nucleus $m_x = 6.8 \times 10^7 M_\odot$ (from Peterson and Wandel [83]).

processes inside the nucleus. It turned out that, for example, for the H_β line in NGC 5548, in spite of Δt varying from ~ 11 to ~ 20 days over 6 years and the variable line width v varying from ~ 4300 to ~ 6900 km s^{-1} [83], the mean over year values Δt and v anti-correlate according to Kepler's law $v \sim r^{-1/2}$, and the corresponding masses of the nucleus agree to within the measurement errors [83, 88]:

$$m_x^{(2)} = (6.1 \pm 2) \times 10^7 M_\odot \,.$$

Remarkably, the values $m_x^{(1)}$ and $m_x^{(2)}$ are very consistent. Paper [89] shows that in the nucleus of an active galaxy, gravitational forces attracting gas emitting in lines are much larger than radiation pressure forces, which also justifies the applicability of the reverberation mapping method to evaluate BH masses in active galactic nuclei. All this makes a strong case for the method of the galactic nucleus mass estimation from the time delay between the line and continuum variability [79]. As was first noted by S Fabrika [169], studies of the broad emission line component profile variability in a Seyfert galactic nucleus with respect to the continuum variability provide the principal possibility to recover distribution and motion of gas clouds surrounding the central object (see also [75, 76] for detailed calculations). In galaxy 3C 390.3, the flux in the red and blue wings of the H_β line and in the core of this line was shown to vary simultaneously [174], which implies that gas clouds emitting in this line move mainly in circular orbits around the central BH, i.e., the emitting region there has a disk-like shape and is not a spherically symmetrical wind outflowing from the nucleus. According to Ref. [174], significant outbursts in the continuum of the nucleus of 3C 390.3 are accompanied by significant changes in the characteristic time delay of the line emission variability relative to the continuum, which evidences change in the illumination conditions and geometry of gas cloud distribution in the nucleus. As noted in Ref. [175], to reliably determine the central BH mass by the reverberation mapping method, the disk inclination angle to the line of sight should be known. According to Refs [176, 177], large changes in the continuum of Seyfert galaxy nuclei (for example, NGC 4151, 3C 390.3) can result in virtually total disappearance of the broad emission line component and transitions from Sy 1 type to Sy 2 and vice versa. The complex character of the broad emission line component variability relative to the continuum in the nucleus of NGC 4151 is described in a recent paper by Sergeev et al. [178].

Paper [179] reports on studies of X-ray and optical variability of the type I Seyfert galaxy NGC 4051. It is shown that rapid X-ray variability is not manifest in the optical continuum, however the variability of the X-ray flux averaged over time intervals of several weeks correlates with the continuum variability.

In recent years, a broad international campaign has been developed to monitor spectral variability of active galactic nuclei (see, for example, Refs [88, 180–183, 174] for descriptions of some projects). The time delay Δt is measured for 19 objects: 17 type I Seyfert galaxies and two quasars [50, 88]. Table 1, borrowed from paper [88], lists the results of the BH mass measurements in active galactic nuclei using the time delay Δt between the emission line and continuum variability. It is seen that the time delays Δt for the H_β line change for different galaxies from ~ 3 to ~ 100 days; the corresponding gas cloud velocities v, as derived from the variable part of the H_β emission, change from ~ 5000 to ~ 3000 km s^{-1}. The velocity range v for different galaxies spans from 1200 to 10000 km s^{-1}. The masses of active galactic nuclei determined by the time delay method lie within the range $\sim (0.1-40) \times 10^7 M_\odot$. The values of the virial masses for the nuclei found from the time delay effect are consistent with those derived from the photoionization model for the nuclei [88]. In the last case no long-term observations of the galactic nucleus are required and the value of r that characterizes the radius of the broad line emission region is determined from the photoionization model of the circumnuclear region by comparing the observed absolute spectral distribution with the calculated one [44, 65, 66, 88, 184]. The gauge relation between the photoionization masses of active galactic nuclei M_{ph} and masses of the nuclei M_{rev} derived from the

Table 1. Masses of supermassive BHs in active galactic nuclei determined by the reverberation mapping method† [88].

Object name	$V_{\rm FWHM}^{\rm H_\beta}$ (mean), km s^{-1}	$V_{\rm FWHM}^{\rm H_\beta}$ (rms), km s^{-1}	Time delay $\tau_{\rm cent}$, days	$M_{\rm BH}$, $10^7 M_\odot$
3C 120	1910	2210 ± 120	$43.8^{+27.7}_{-20.3}$	$3.1^{+2.0}_{-1.5}$
3C 390.3‡	10000	10500 ± 800	$24.2^{+6.7}_{-8.4}$	39.1^{+12}_{-15}
Akn 120	5800	5850 ± 480	$38.6^{+5.3}_{-6.5}$	$19.3^{+4.1}_{-4.6}$
F9	5780	5900 ± 650	$17.1^{+3.5}_{-8.0}$	$8.7^{+2.6}_{-4.5}$
IC 4329A	5050	5960 ± 2070	$1.4^{+3.4}_{-2.9}$	< 0.73
Mrk 79	4470	6280 ± 850	$18.1^{+4.9}_{-8.6}$	$10.5^{+4.0}_{-5.7}$
Mrk 110	1430	1670 ± 120	$19.5^{+6.5}_{-6.8}$	$0.80^{+0.29}_{-0.30}$
Mrk 335	1620	1260 ± 120	$16.8^{+5.2}_{-3.3}$	$0.39^{+0.14}_{-0.11}$
Mrk 509	2270	2860 ± 120	$79.3^{+6.5}_{-6.2}$	$9.5^{+1.1}_{-1.1}$
Mrk 590	2470	2170 ± 120	$20.5^{+4.5}_{-3.0}$	$1.4^{+0.3}_{-0.3}$
Mrk 817	4490	4010 ± 180	$15.5^{+4.3}_{-3.5}$	$3.7^{+1.1}_{-0.9}$
NGC 3227	4920	5530 ± 490	$10.9^{+5.6}_{-10.9}$	$4.9^{+2.7}_{-5.0}$
NGC 3783	3790	4100 ± 1160	$4.5^{+3.6}_{-3.1}$	$1.1^{+1.1}_{-1.0}$
NGC 4051	1170	1230 ± 60	$6.5^{+6.6}_{-4.1}$	$0.14^{+0.15}_{-0.09}$
NGC 4151	5910	5230 ± 920	$3.0^{+1.8}_{-1.4}$	$1.2^{+0.8}_{-0.7}$
NGC 5548	6300	5500 ± 400	$21.6^{+2.4}_{-0.7}$	$6.8^{+1.5}_{-1.0}$
NGC 7469	3000	3220 ± 1580	$5.0^{+0.6}_{-1.1}$	$0.76^{+0.75}_{-0.76}$
PG 0804 + 762	3090	3870 ± 110	$100^{+16.3}_{-19.8}$	$21.9^{+3.8}_{-4.5}$
PG 0953 + 414	2890	3140 ± 350	$107.1^{+71.2}_{-58.0}$	$15.5^{+10.8}_{-9.1}$

† Here $V_{\rm FWHM}^{\rm H_\beta}$ (mean) is the total width at half maximum of the mean intensity profile of the broad $\rm H_\beta$ hydrogen emission line component, $V_{\rm FWHM}^{\rm H_\beta}$ (rms) is the total width at half maximum of the variable part of the broad $\rm H_\beta$ hydrogen emission line component, $\tau_{\rm cent}$ is the characteristic time delay between the broad $\rm H_\beta$ hydrogen emission line variability and the continuum spectrum variability, and $M_{\rm BH}$ is the mass of the central BH.
‡ Based on the long-term optical monitoring of 3C 390.3 by Shapovalova et al. [174], new values $\tau_{\rm cent} = 100^d$, $M_{\rm BH} = 2.1 \times 10^9 M_\odot$ have been determined.

reverberation mapping Δt reads [88]

$$\lg \frac{M_{\rm rev}}{M_\odot} = (0.93 \pm 0.07)\, \lg \frac{M_{\rm ph}}{M_\odot} + (0.70 \pm 0.53)\,. \qquad (11)$$

Equation (11) enables the determination of the central masses for a great number of active galaxies, which is important to unveil the relationship between the central BH mass, the luminosity of the nucleus, and the mass of the galactic bulge [44, 88, 184, 163]. In paper [88], the comparison of the results obtained by two methods (photoionization and reverberation mapping) allowed one to evaluate the ionizing radiation luminosity in active galactic nuclei which is 10 times as large as their optical luminosity. The ratio of the ionization radiation luminosity to the Eddington value proved equal

$$\frac{L_{\rm ion}}{L_{\rm E}} \approx 0.01 - 0.3\,.$$

There is a statistically confident correlation between the nucleus mass in an active galaxy and its luminosity in visible light $L_{\rm v}$ ($\lambda = 5100$ Å) [88]:

$$\lg \frac{M}{M_\odot} = (0.77 \pm 0.07)\, \lg L_{44} + (7.92 \pm 0.04)\,, \qquad (12)$$

where $L_{44} = L_{\rm v}/(10^{44}$ erg s^{-1}). Statistical characteristics of masses of galactic nuclei evaluated by the dynamical method were found to be consistent with those obtained from the time delay effect [185 – 187]. In paper [163] most reliable masses of active galactic nuclei determined from the time delays Δt are compared with masses of the galactic bulges (the bulge is a spherical condensation of old generation stars in the central parts of a galaxy). A correlation between the BH mass and the galactic bulge mass is shown to exist: the BH mass on average increases with the bulge mass, with the BH to bulge mass ratio being $10^{-3.5}$. This is about 20 times smaller than for normal galaxies and bright quasars. The recent paper [188] argues that there is a unique relation between the BH mass and the galactic bulge mass both for normal galaxies and active galactic nuclei and quasars: $M_{\rm bh} = 0.0012 M_{\rm bulge}$.

5.2 Masses of supermassive black holes in nuclei of 'normal' galaxies

In the case of 'normal' galaxies (in which optical manifestations of the nucleus are small compared to the stellar component of the galaxy), it is possible to directly observe moving stars and gas near the nucleus. This provides the possibility to obtain more reliable BH mass estimates.

5.2.1 BH mass determination from the observed rotational velocities of the surrounding gas. In recent years, observations from the Hubble Space Telescope with a high angular resolution of several hundredths of an arcsecond revealed the presence of gas-dust disks around nuclei of many galaxies which rotate according to Kepler's law (see review [189] and references therein). Radii of these structures fall within the range from several ten to several hundred parsecs (Fig. 14).

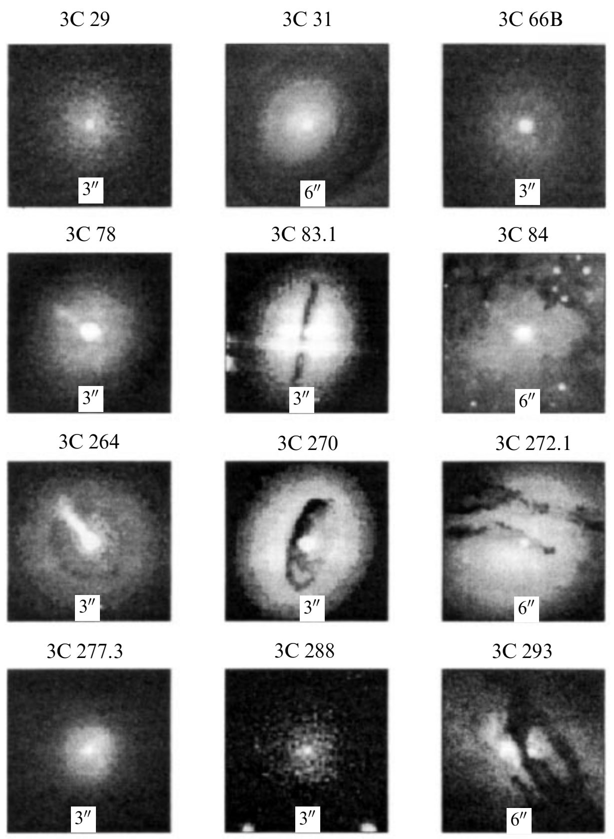

Figure 14. Images of circumnuclear dust-gaseous disks in some galaxies taken by the Hubble Space Telescope (from Maccheto [189]).

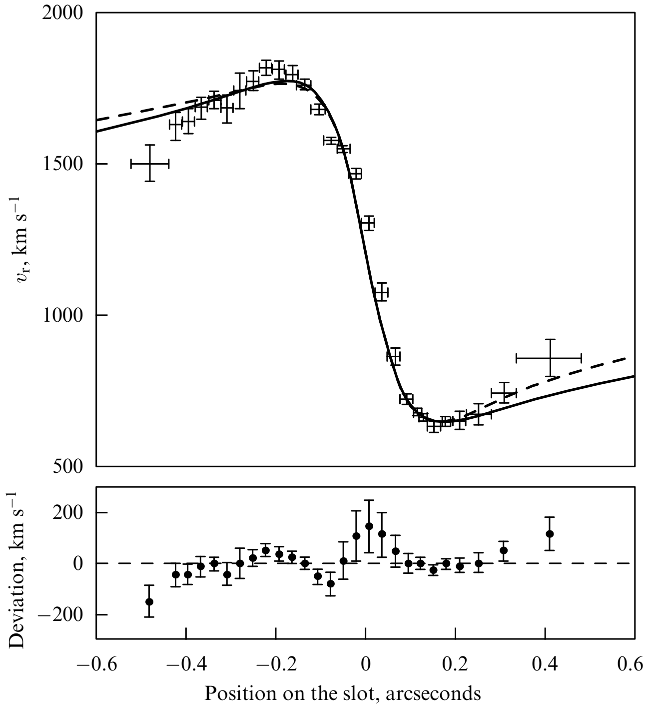

Figure 15. The rotation curve of the circumnuclear dust-gaseous disk in galaxy M87 obtained from optical emission lines. The solid and dashed lines correspond to the model of a thin Keplerian disk. At the bottom the residual deviations are shown for this model (from Maccheto et al. [192]).

Observations of the distribution of radial velocities v_r by studying emission line Doppler shifts in the projection on a sky plane confirm the Keplerian rotation of the disk matter and enables one to determine the disk inclination angle i to the line of sight (see, for example, Refs [190–192]). Then the mass $M(r)$ comprised inside the volume of radius r is uniquely determined from the formula similar to Eqn (1) at $\eta = 1$:

$$M(r) = \frac{r v_r^2}{G \sin^2 i} \,. \tag{13}$$

The possibility of the direct observation of the circumnuclear region enables also the estimation of the mass-luminosity ratio $M(r)/L(r)$ (M and L in solar units) and its comparison with the corresponding value for the outskirts of the galaxy ($M/L_v \cong 1-10$ [146]).

The first galaxy where the circumnuclear gas-dust disk was used to determine the nucleus mass was the M87 galaxy with a bright extended jet. Ford et al. [191] discovered a disk-like spiral gas-dust structure surrounding the M87 nucleus. The radius of this structure is $\sim 1''$ which corresponds to 73 pc at the 15 Mpc distance to M87. The mass of ionized gas in this disk is $\sim 4 \times 10^3 M_\odot$ and its axis makes an angle of $i \cong 42^\circ$ with the line of sight, with the disk plane being perpendicular to the jet axis. The spectra taken in different parts of the disk (Harms et al. [190]) showed its Keplerian rotation with radial velocities ± 500 km s^{-1} in two opposite disk points at a distance of $0''.25$ (18 pc) from the nucleus. These results are confirmed by more detailed spectral observations with a higher angular resolution of $0''.05$ or 3.5 pc (Maccheto et al. [192]) (Fig. 15). A detailed rotational curve of the disk was constructed, which is well fit by the Kepler's law in the inner parts. The disk inclination angle to the line of sight, as independently derived from spectral observations, is $i = 47^\circ - 65^\circ$. The mass of the nucleus for $i = 52^\circ$ is $(3.2 \pm 0.9) \times 10^9 M_\odot$ and the mass-luminosity ratio is $M/L_v > 110$, which suggests a significant excess of an invisible matter over the stellar component in the nucleus. The invisible matter density is estimated to be $\sim 10^7 M_\odot$ pc^{-3}. All these data make a strong case for the presence of a supermassive BH in the M87 nucleus, accretion onto which is responsible for various activities of the M87 nucleus, including the formation of the relativistic jet [190–192]. Studies of the circumnuclear gas-dust disk in galaxy NGC 4261 [193] suggested a nucleus mass of $(4.9 \pm 1) \times 10^8 M_\odot$ with a high mass-luminosity ratio of $M/L_v \cong 2 \times 10^3$. The nucleus mass in galaxy M84, whose luminosity is similar to M87, evaluated in the same way is $1.5 \times 10^9 M_\odot$ [194]; the mass of nucleus in galaxy NGC 7052 is $3 \times 10^8 M_\odot$ [195], and in galaxy NGC 3245 is $(2.1 \pm 0.5) \times 10^8 M_\odot$ [196]. The data on the BH masses in galactic nuclei measured from the kinematics of gas and stars in the circumnuclear region are collected in Table 2.

Outstanding results on BH mass measurements in galactic nuclei were recently obtained from megamaser studies by intercontinental radio astronomy (see review by Moran et al. [198] and references therein). In this case, by observing compact water vapor maser sources at the wavelength 1.35 cm, which are located in the inner parts of the circumnuclear molecular disk, an unprecedental angular resolution of 200 microseconds and a spectral resolution of better than 0.1 km s^{-1} have been achieved. Observations of the

Table 2. Masses of supermassive BHs inferred from kinematics of stars and gas [197].

Galaxy	Type	Distance, Mpc	M_B (bulge)	σ_1, km s^{-1}	M_{BH} (max; min), $M_\odot$	Determination method
Milky Way	SBbc	0.008	−17.65	103	1.8×10^6 (1.5; 2.2)	s, p
NGC 221 = M32	E2	0.81	−15.83	75	2.5×10^6 (2.0; 3.0)	s, 3I
NGC 224 = M31	Sb	0.76	−19.00	160	4.5×10^7 (2.0; 8.5)	s
NGC 821	E4	24.1	−20.41	209	3.7×10^7 (2.9; 6.1)	s, 3I
NGC 1023	SB0	11.4	−18.40	205	4.4×10^7 (3.9; 4.9)	s, 3I
NGC 1068	Sb	15.0	−18.82	151	1.5×10^7 (1.0; 3.0)	m
NGC 2778	E2	22.9	−18.59	175	1.4×10^7 (0.5; 2.2)	s, 3I
NGC 2787	SB0	7.5	−17.28	140	4.1×10^7 (3.6; 4.5)	g
NGC 3115	S0	9.7	−20.21	230	1.0×10^9 (0.4; 2.0)	s
NGC 3245	S0	20.9	−19.65	205	2.1×10^8 (1.6; 2.6)	g
NGC 3377	E5	11.2	−19.05	145	1.0×10^8 (0.9; 1.9)	s, 3I
NGC 3379	E1	10.6	−19.94	206	1.0×10^8 (0.5; 1.6)	s, 3I
NGC 3384	S0	11.6	−18.99	143	1.6×10^7 (1.4; 1.7)	s, 3I
NGC 3608	E2	22.9	−19.86	182	1.9×10^8 (1.3; 2.9)	s, 3I
NGC 4258	Sbc	7.2	−17.19	130	3.9×10^7 (3.8; 4.0)	m, a
NGC 4261	E2	31.6	−21.09	315	5.2×10^8 (4.1; 6.2)	g
NGC 4291	E2	26.2	−19.63	242	3.1×10^8 (0.8; 3.9)	s, 3I
NGC 4342	S0	15.3	−17.04	225	3.0×10^8 (2.0; 4.7)	s, 3I
NGC 4459	S0	16.1	−19.15	186	7.0×10^7 (5.7; 8.3)	g
NGC 4473	E5	15.7	−19.89	190	1.1×10^8 (0.31; 1.5)	s, 3I
NGC 4486 = M87	E0	16.1	−21.53	375	3.0×10^9 (2.0; 4.0)	g
NGC 4564	E3	15.0	−18.92	162	5.6×10^7 (4.8; 5.9)	s, 3I
NGC 4596	SB0	16.8	−19.48	152	7.8×10^7 (4.5; 12)	g
NGC 4649	E1	16.8	−21.30	385	2.0×10^9 (1.4; 2.4)	s, 3I
NGC 4697	E4	11.7	−20.24	177	1.7×10^8 (1.6; 1.9)	s, 3I
NGC 4742	E4	15.5	−18.94	90	1.4×10^7 (0.9; 1.8)	s, 3I
NGC 5845	E3	25.9	−18.72	234	2.4×10^8 (1.0; 2.8)	s, 3I
NGC 6251	E2	93.0	−21.81	290	5.3×10^8 (3.5; 7.0)	g
NGC 7052	E4	58.7	−21.31	266	3.3×10^8 (2.0; 5.6)	g
NGC 7457	S0	13.2	−17.69	67	3.5×10^6 (2.1; 4.6)	s, 3I
IC 1459	E3	29.2	−21.39	340	2.5×10^9 (2.1; 3.0)	s, 3I

Notes. Here M_B (bulge) is the stellar B-magnitude of the galactic bulge, σ_1 is the velocity dispersion of the bulge stars (see [197] for more detail on the velocity dispersion), M_{BH} is the central BH mass in solar units $M_\odot$ (maximal and minimal values of the BH mass corresponding to plus-minus the rms mass determination error are given in parentheses). The BH mass determination methods are: s — stellar radial velocities, p — proper motions of stars, m — radial velocities of gas clouds inferred from maser emission lines, a — accelerations of gas clouds from maser emission lines, g — observations of the rotating gas disk by emission lines, 3I — axisymmetric dynamical model including three integrals of motion.

NGC 4258 nucleus (Miyoshi et al. [193]) revealed 17 compact maser sources emitting extremely narrow water vapor lines which were located in a disk-like shell $\sim 10^{17}$ cm in radius seen nearly edge-on (Fig. 16). The maser sources in this circumnuclear molecular disk show a Keplerian velocity distribution: in the inner part of the disk (radius $r = 3.9$ milliarcseconds or 0.14 pc for the 7.2 Mpc distance to the galaxy) the rotational velocity is $v = 1100$ km s^{-1}, and in the outer parts ($r = 8.0$ milliarcseconds or 0.28 pc) $v = 770$ km s^{-1}. The inner orbital period is 800 years, while the outer is 2200 years. The disk inclination angle to the line of sight is $i = 89°$. The central BH mass calculated by formula (13) is $3.9\times10^7 M_\odot$. Although the inner part of the disk rotates with a period of 800 years, the high accuracy of the location of the maser sources enabled the measurement of their angular motion on the sky over several years of observations. This allowed the independent determination of the distance to the NGC 4258 nucleus to a 4% accuracy: $d = (7.2 \pm 0.3)$ Mpc [198]. So far, seven galactic nucleus masses have been measured by this method (Table 3).

5.2.2 BH mass determination from the surrounding star motions. The first efforts of searching for BHs in the nuclei of 'normal' galaxies were based on studying galactic central brightness distributions and looking for a sharp intensity peak centered on the nucleus (see, for example, Ref. [201]). This peak is due to a drastic increase in stellar density in the vicinity of a BH (in the adiabatic model following the law $\rho(r) \sim r^{-3/2}$ [202] or even steeper [203]). However, data on the BH searches based only on photometric investigations are unconvincing (see, for example, Refs [4, 204]). In particular, more bright and massive galaxies have on average more massive BHs in their nuclei, but they also have more diffusive cores of larger sizes [205, 206], so the matter in the outer parts is weakly affected by the BH gravity.

While the sharp brightness peak in the galactic center does not provide unambiguous evidence for the presence of a BH, the velocity dispersion σ increasing toward the center by the Kepler's law $\sigma(r) \sim r^{-1/2}$ can serve as a sufficiently reliable criterion of the existence of a supermassive BH [50, 207]. However, if there is some velocity anisotropy near the galactic nucleus, this method, too, can yield ambiguous results, especially for slowly rotating elliptical galaxies [69, 208–210]. The optimism in using Eqn (2) relating the central mass $M(r)$ with three components σ_r, σ_θ, and σ_φ of the velocity dispersion in the nuclear region of a galaxy comes from the fact (which is proved by direct observations in our Galaxy) that the distribution of stellar velocities in the nuclear region can be isotropic [68, 211–215].

In recent years the method based on Eqn (2) has been effectively applied to analyze circumnuclear galactic regions observed by the Hubble Space Telescope with the faint object spectrometer (FOS). Quite reliable mass estimates have been obtained for galaxies NGC 1115 [216], NGC 4594 [217], M32

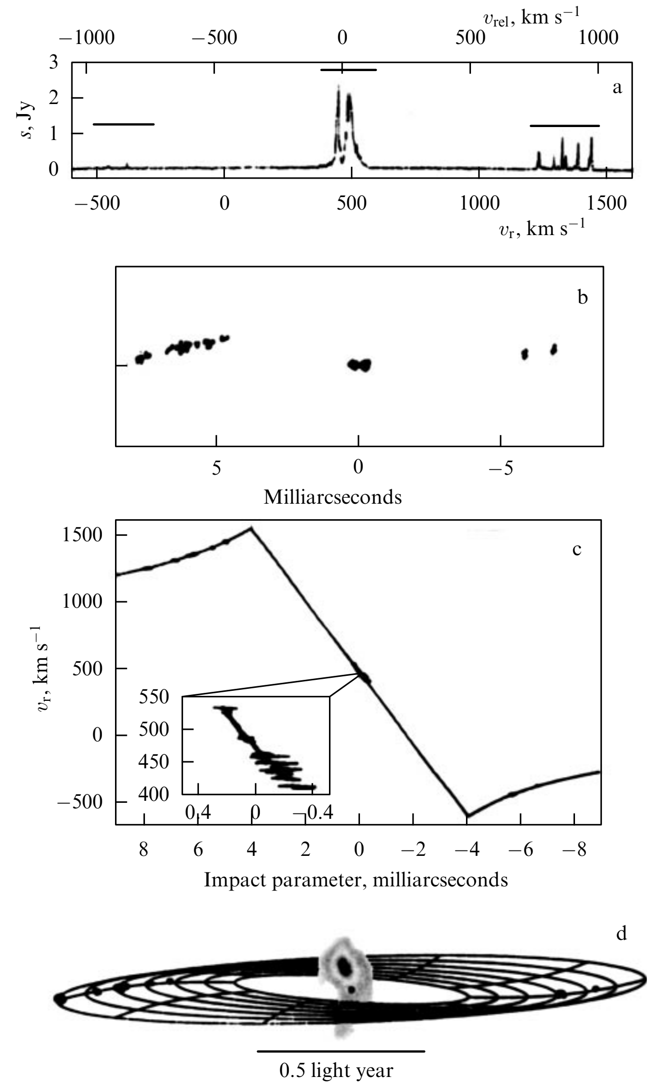

Figure 16. The results of intercontinental radio interferometry of water vapor line maser sources at the 1.35 cm wavelength in the NGC 4258 galaxy nucleus: (a) the spectrum; (b) spatial distribution of compact maser sources; (c) radial velocities of the maser sources; (d) kinematic model for the circumnuclear dust-gaseous disk with maser sources distributed inside (from Moran et al. [198]).

[218], and M31 [219]. Presently, systematic studies of stellar kinematics near galactic nuclei are carried out by the multi-slot high-resolution spectrograph STIS (Space Telescope Imaging Spectrograph) onboard the Hubble Space Telescope [220, 221].

When using gas kinematics near the galactic nucleus to determine the central BH mass, only inner parts of the gaseous disk with Keplerian rotation are useful. The outer parts of the disk can be distorted by perturbations from the nearby stars and frequently have significantly deformed shapes [50].

When utilizing stellar and gas kinematics in the galactic nucleus to estimate the BH mass, it is important to obtain at least a two-dimensional gas velocity field and to take into account stellar velocity dispersion anisotropy by using a multi-component stellar kinematic model [50, 220, 222]. For example, in the nucleus of galaxy NGC 3115, the central BH mass is estimated to be $10^9 M_\odot$ [216, 223] assuming isotropic stellar velocity dispersion, whereas in the model of anisotropic velocity dispersion it is found to be $2\times10^7 M_\odot$ [224].

The most convincing evidence for the existence of a supermassive BH in our Galaxy center has been obtained in recent years from studies of individual star motions in the immediate vicinity of the Sgr A source located in the Galaxy center [68, 211–215]. Studies of the mass distribution near the center of our Galaxy aimed at searching for a supermassive BH were initiated in papers by Oort [225] and Genzel and Townes [226].

In 1996–1998, Eckart and Genzel [211, 212] and Ghez et al. [68] reported on high-resolution ($\sim 0''.05 \cong 0.002$ pc) observations of the Galactic center in the infrared at $\lambda = 2.2$ μm (the nucleus of our Galaxy is hidden from the terrestrial observer by a thick layer of interstellar gas and dust so individual stars near the nucleus can be seen only in the infrared). In three years of observations the authors could directly spot and measure proper motions of stars in the sky plane near the nucleus, whose velocities were as high as many hundred kilometers per second (see Fig. 1). The velocity dispersion of proper motions of 90 stars was measured as a function of their distance to the Galactic nucleus, which perfectly agrees with their radial velocity dispersion inferred from spectral observations. This proves the isotropy of the velocity dispersion near the nucleus. Comparison of the observed velocity dispersion with theoretical distribution enables a reliable evaluation of the BH mass in the center of our Galaxy, which is $2.6\times10^6 M_\odot$ (Fig. 17). The estimated upper limit of the nucleus radius here is 0.006 pc, the mass-luminosity ratio is $M/L > 25-500$, and the mean density of matter inside the nucleus within the volume 0.006 pc in radius is $\rho \cong 2\times10^{12} M_\odot$ pc^{-3}, which is 13 orders of magnitude higher than the mean density in the non-nuclear regions of the

Table 3. Masses of supermassive BHs evaluated by intercontinental radio interferometry of megamasers (from review [198] and paper [200]).

Galaxy	Distance, Mpc	Rotational velocity $V_\varphi^{\rm i}$, km s^{-1}	$R_{\rm i}/R_{\rm o}$, pc	$M_{\rm BH}$, $M_\odot$	ρ, $M_\odot$ pc^{-3}	$L_{\rm x}$, erg s^{-1}	References
NGC 4258	7	1100	0.13/0.26	3.5×10^7	4×10^9 (5×10^{12})	4×10^{40}	[198, 199]
NGC 1068	15	330	0.6/1,2	1.7×10^7	3×10^7	4×10^{43}	[198]
Circinus	4	230	0.08/0.8	1.0×10^6	4×10^8	4×10^{43}	[198]
NGC 4945	4	150	0.2/0.4	1.0×10^6	2×10^7	1×10^{42}	[198]
NGC 1386	12	100	—/0.7	2.0×10^6	4×10^7	2×10^{40}	[198]
NGC 3079	16	150	—/1.0	1.0×10^6	2×10^6	2×10^{40}	[198]
IC 2560	26	418	0.07/0.26	2.8×10^6	2×10^9	1×10^{41}	[200]

Notes. Here $V_\varphi^{\rm i}$ is the Keplerian rotation velocity at the inner observed disk edge, $R_{\rm i}/R_{\rm o}$ is the inner/outer disk radius, $M_{\rm BH}$ is the central BH mass in units of $M_\odot$, ρ is the mean density of matter inside the minimal volume observed, and $L_{\rm x}$ is the 2–10 keV X-ray luminosity of the galaxy nucleus.

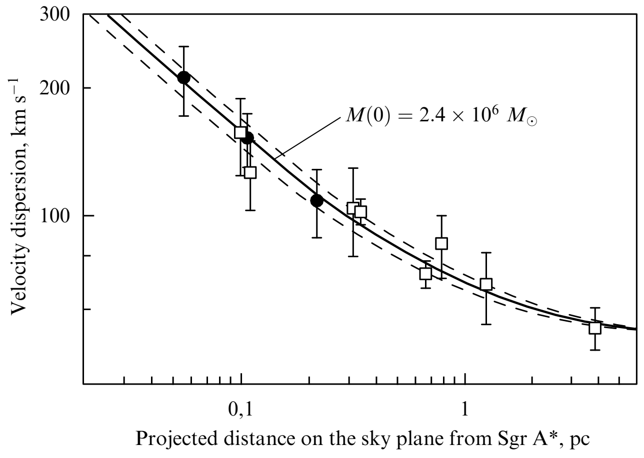

Figure 17. The dependence of the velocity dispersion of the proper motion of stars (filled circles) and their radial velocity dispersion (open squares) on the projected distance to the center of our Galaxy. The solid line shows the theoretical distribution of the velocity dispersion corresponding to a central BH mass of $2.4 \times 10^6 M_\odot$ (from Eckart and Genzel [211]).

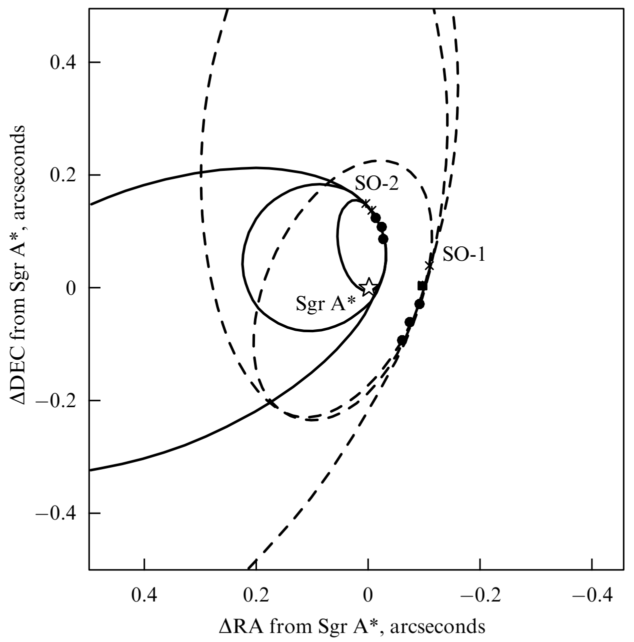

Figure 18. The observed curvilinear proper motions of stars SO-1 and SO-2 in the gravitational field of the nucleus of our Galaxy (points) and the recovered orbits of these stars in the projection on the sky plane (from Ghez et al. [215]).

Galaxy ($\rho \cong 0.1 M_\odot$ pc^{-3} in the Solar vicinity, $\rho \cong 10^5 M_\odot$ pc^{-3} for the most dense stellar clusters). Some stars which are closest to the nucleus (within 0.01 pc) move with velocities exceeding 1000 km s^{-1}. Even more convincing and beautiful results were recently published by Ghez et al. [215]. Observations by the 10-m Keck telescope, started in 1995, revealed the presence of accelerations in proper motions of three stars located within $\sim 0.005-0.01$ pc from the Galactic center (1 arcsecond at a distance of 8 kpc to the Galaxy center corresponds to 0.04 pc [227]). The proper motion trajectories of these stars are curvilinear (Fig. 18). The corresponding centripetal accelerations are comparable with that of the Earth in its motion around the Sun ($0.3-0.6$ cm s^{-2}), the velocities are $(570-1350)$ km s^{-1}, and the distances to the center of the Galaxy are $r_{1995} = (0.004-0.013)$ pc. The acceleration vectors of the stars intersect, at a point which to within $0''.05$ coincides with the dynamical Galactic center (Sgr A source), which proves that the supermassive BH is located exactly in the Galactic center. The BH mass determined by projections of radius-vectors and accelerations of the stars on the sky plane

$$M = \frac{a_{2\mathrm{D}} r_{2\mathrm{D}}^2}{G \cos^3 \theta} \tag{14}$$

is approximately $3 \times 10^6 M_\odot$, which is perfectly consistent with the BH mass found from the velocities of stars $(2.3-3.3) \times 10^6 M_\odot$. Here $a_{2\mathrm{D}}$ and $r_{2\mathrm{D}}$ are the acceleration and radius projections on the sky plane, respectively (for a central potential their directions coincide), and θ is the angle between the radius-vector and the sky plane. The mean density of dark matter comprised inside this volume in the center of the Galaxy is $8 \times 10^{12} M_\odot$ pc^{-3}. With the accelerations obtained, the authors [215] recovered individual orbits for two stars. The eccentricities of these orbits are $0-0.9$ and $0.5-0.9$, and the orbital periods fall within the range 35–1200 years and 15–550 years, respectively. If the orbital period of one of the stars (SO-2) is close to 15 years, the next 10 years of observations will enable the closing up of its orbit, which opens up good prospects to more precisely locate the supermassive BH and study its gravitational potential [228]. The results of new observations (Eckart et al. [229]) confirmed the conclusions of Ghez et al. [215]. Paper [230] proposed a new method of measurement of the angular momentum of the BH in our Galaxy center using observations of quasi-periodic ($p = 3-30$ min) variability at the millimeter and submillimeter wavelengths.

The results of the BH mass determinations from gas kinematics near the galactic nucleus are summarized in Table 2, which is borrowed from paper [197].

6. Arguments evidencing that supermassive compact bodies found in galactic nuclei are black holes

We use the term 'BH' with some caution since, as we already noted, thus far there have been no sufficient selection criteria for real BHs. Let us enumerate principal arguments that strengthen our belief that these are real BHs in the sense of GR. The direct information on the specific processes near the horizon of a supermassive BH (or at least at a distance of the last marginally stable orbit) can be obtained in the future with the help of space interferometers [115] (see above). Indirect information follows from the analysis of the broad fluorescent iron X-ray line profile at 6.4 keV [118, 119, 231–235, 120]. The full width of the broad component of this line attains 100 000 km s^{-1} in the velocity scale. The line profile and its redshift caused by relativistic effects, the disk inclination angle to the line of sight, and by the BH angular momentum evidence that the inner edge of the disk is located at a distance from 3 to 30–40 gravitational radii from the central BH. In galaxy MCG-6-30-15, there are indications of BH rotation since the inner disk edge stays at a distance less than $3r_g$ from the central BH. Unfortunately, these quantitative estimates depend on the specific accretion disk model [235]. Paper [120] notes that the extremely large width and huge redshift of the broad iron K_α line component in the X-ray spectrum of MCG-6-30-15 (Fig. 19) force us to apply

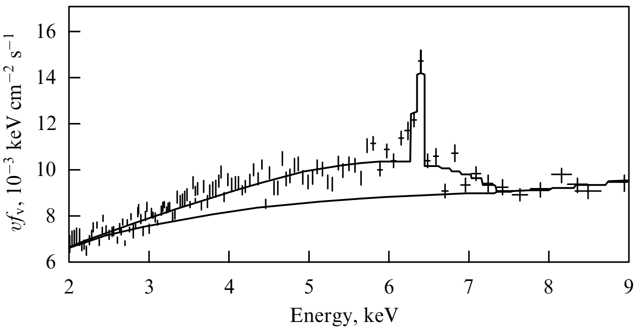

Figure 19. The iron K_α emission line profile in the nucleus of Seyfert galaxy MCG-6-30-15 in the low X-ray luminosity state obtained by the XMM X-ray observatory (from Wilms et al. [120]).

the model in which the rotational energy of the central BH is extracted by the magnetic field (the Blandford–Znajeck mechanism [157]).

The absence of the noticeable dependence of the stellar population in the nuclear region of a galaxy on the distance, which follows from the constant color distribution and the mean spectral class of stars along its diameter, enables us to consider that the huge (by ten times) increase in the mass-luminosity ratio M/L in approaching the galactic center can not be due to a simple concentration of ordinary stars in the nucleus. Apart from a supermassive BH, this could be a cluster of bodies with very small or zero luminosity: white dwarfs, neutron stars, stellar-mass BH, brown dwarfs, or planets. But the model of cluster of such objects fails at least for two galactic nuclei: our Galaxy and galaxy NGC 4258 [236], where the mean density of invisible matter inside the nucleus is $8 \times 10^{12} M_\odot$ pc^{-3} and $4.9 \times 10^{12} M_\odot$ pc^{-3}, respectively. As was shown by Maoz [236], the characteristic evaporation time of a cluster of individual gravitating bodies at a density exceeding $10^{12} M_\odot$ pc^{-3} is $\sim 10^8$ years, which is two orders of magnitude smaller than the age of the Universe. For nuclei of these galaxies, only two possibilities as alternatives to the BH hypothesis remain: a cluster consisting of a low-mass BH (with mass significantly smaller than $1 M_\odot$) or of elementary particles, for example, of degenerate heavy neutrinos [228]. In the last case, the degenerate neutrino pressure compensates gravitational attraction [228, 237, 238] and the equilibrium radius for the mass $\sim 2.6 \times 10^6 M_\odot$ is about 10^{16} cm, which is by 4 orders of magnitude larger than the gravitational radius of the corresponding BH. As shown in Ref. [228], this possibility can be tested in the forthcoming several years by studying in detail the orbit of the closest and most rapidly moving star SO-1 near Sgr A source in the center of our Galaxy [215]. In the general case, an alternative to the supermassive BH in the Galactic center can be the fermion ball model which can also be checked by studying the orbits of those closest to the Galactic nucleus stars SO-1 and SO-2 [239]. Accounting for the existence of dark matter in the Universe, such a model does not seem to be too unlikely.

Additional arguments for the supermassive BH in the galactic nucleus come from the existence of high-energy power-law 'tails' in the X-ray spectral energy distribution from an accreting BH [240, 241] and from the anomalously low luminosity of an accreting BH in most galactic nuclei (of the order of 10^{-4} – 10^{-9} of the Eddington value). The latter is connected with advection (mechanical motion) of a hot ion plasma with virial temperature and relatively cold electrons below the event horizon [36, 242, 243] (see, however, criticism of the advection-dominated disk theory that does not take into account the important role of the magnetic field and Ohmic plasma heating during accretion [143, 37, 244, 40]).

7. Demography (stellar astronomy) of supermassive black holes

Stellar astronomy studies statistic characteristics of stars and stellar systems. So far, 80 supermassive BH masses have been measured (Table 4). Presently, the STIS spectrograph onboard the Hubble Space Telescope is carrying out massive searches for supermassive BHs in galactic nuclei [220], which should sharply increase the number of supermassive BHs with measured masses. All this allows us to apply stellar astronomy (demographic) methods to study supermassive BHs. In recent years, a lot of papers have appeared on this subject (see, for example, reviews [50, 220]). Here we only briefly describe the most important results.

1. There is a correlation between the supermassive BH mass and the bulge mass (or the bulge luminosity) of a galaxy: the central BH mass $M_{\rm BH}$ increases with the bulge mass $M_{\rm bulge}$, $M_{\rm BH} \sim M_{\rm bulge}^{0.93}$ [220]. The correlation is almost linear and shows that the central BH mass is about 0.2% of the bulge mass [50, 189, 220, 246–249]. The same correlation is discovered for bright quasars [250] and active galactic nuclei [163]. This correlation has recently been confirmed in papers [188, 251] and, unlike the results in [163], has been shown to be the same for BHs both in nuclei of normal galaxies and type I Seyferts and quasars: $M_{\rm BH} \sim M_{\rm bulge}^{0.95\pm0.05}$ (Fig. 20). The normalization of this correlation relates the BH mass and the galactic bulge mass: $M_{\rm BH} = 0.0012 M_{\rm bulge}$ [188]. Thus, the non-linear dependence between the BH mass and galactic bulge mass proposed in Ref. [252] ($M_{\rm BH} \sim M_{\rm bulge}^{1.54\pm0.15}$) is not confirmed by new, more complete observational data [188, 251]. There also exists a good correlation between the central BH mass and the light concentration in the galactic bulge: more concentrated bulges hide more massive BHs [253].

The presence of such a correlation puts serious constraints on the formation mechanism of supermassive BHs [50, 247, 189, 220]. In particular, the model of growth of the supermassive BH mass due to accretion and coalescence in the

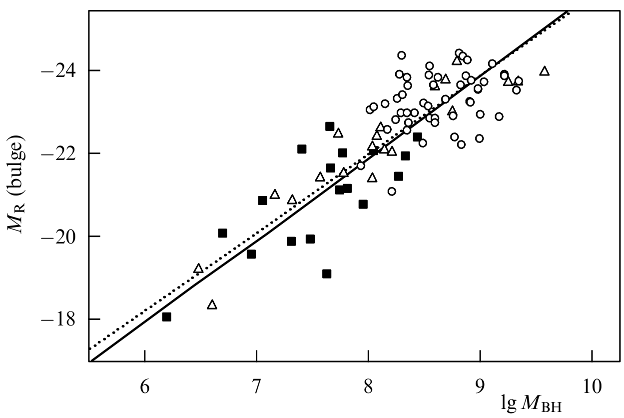

Figure 20. The absolute stellar R-magnitude of the bulge (the spherical condensation of old stars of a galaxy) proportional to its total mass, as a function of the central BH mass for a set of 90 galaxies of different types, including normal galaxies, type I Seyfert galaxies, and quasars (from McLure and Dunlop [183]): △ — normal galaxies, ■ — type I Seyfert galaxies, ○ — quasars. Here $M_{\rm BH}$ is in $M_\odot$ units.

Table 4. Overall list of supermassive BH with measured masses in galactic nuclei [245].

Galaxy	Hubble type	Spectral class	D, Mpc	$M_{\rm BH}$, $M_{\odot}$	Method
3C 120(Mrk 1506)	S0:	S1	137.8	2.3×10^7	R
3C 390.3(VII w 838)	E?	S1	241.2	3.4×10^8	R
Ark 120(Mrk 1095)	S0/a	S1	134.6	1.84×10^8	R
Arp 102B	E0	L1.8	99.7	2.2×10^8	G
Circinus	Sb:	S2	4.0	1.3×10^6	M
Fairall 9	S?	S1	199.8	8.0×10^7	R
IC 342	SABcd	H	1.8	$< 5.0 \times 10^5$	S
IC 1459	E3	L2	29.2	3.7×10^8	G
IC 4329A	S0+	S1	65.5	5.0×10^6	R
Milky Way	Sbc	—	0.008	2.95×10^6	S
Mrk 79(UGC 3973)	SBb	S1.5	91.3	5.2×10^7	R
Mrk 110	Pair?	S1	147.7	5.6×10^6	R
Mrk 279(UGC 8823)	S0	S1.5	126.6	4.2×10^7	R
Mrk 335	S0/a	S1.0	106.6	6.3×10^6	R
Mrk 509	comp	S1	143.8	5.78×10^7	R
Mrk 590(NGC 863)	Sa:	S1.2	109.2	1.78×10^7	R
Mrk 817(UGC 9412)	S?	S1.5	131.0	4.4×10^7	R
NGC 205(M110)	dE5	A	0.74	$< 9.3 \times 10^4$	S
NGC 221(M32)	E2	A	0.81	3.9×10^6	S
NGC 224(M31)	Sb	A	0.76	3.3×10^7	S
NGC 598(M33)	Scd	H	0.87	$< 1.5 \times 10^3$	S
NGC 821	E6?	A	24.1	5.0×10^7	S
NGC 1023	SB0−	A	11.4	3.9×10^7	S
NGC 1068(M77)	Sb	S1.9	14.4	1.6×10^7	M
NGC 2778	E	—	22.9	2.0×10^7	S
NGC 2787	SB0+	L1.9	7.5	3.9×10^7	G
NGC 3031(M81)	Sab	S1.5	3.9	6.3×10^7	S
NGC 3115	S0−	A	9.7	9.1×10^8	S
NGC 3227	SABa	S1.5	20.6	3.9×10^7	R
NGC 3245	S0?	T2	20.9	2.1×10^8	G
NGC 3377	E5+	A	11.2	1.0×10^8	S
NGC 3379(M105)	E1	L2/T2:	10.6	1.0×10^8	S
NGC 3384	SB0−:	A	11.6	1.8×10^7	S
NGC 3516	SB0:	S1.2	38.9	2.3×10^7	R
NGC 3608	E2	L2/S2:	22.9	1.1×10^8	S
NGC 3783	SBa	S1	38.5	9.4×10^6	R
NGC 3998	S0?	L1.9	14.1	5.6×10^8	S
NGC 4051	SABbc	S1.2	17.0	1.3×10^6	R
NGC 4151	SABab	S1.5	20.3	1.53×10^7	R
NGC 4203	SAB0	L1.9	14.1	$< 1.2 \times 10^7$	G
NGC 4258(M106)	SABbc	S1.9	7.3	4.1×10^7	M
NGC 4261(3C 270)	E2+	L2	31.6	5.2×10^8	G
NGC 4291	E	A	26.2	1.5×10^8	S
NGC 4342	S0−	—	16.8	3.4×10^8	S
NGC 4374(M84, 3C 272.1)	E1	L2	18.4	1.6×10^9	G
NGC 4395	Sm:	S1.5	3.6	$< 1.1 \times 10^5$	S
NGC 4459	S0+	T2:	16.1	6.5×10^7	G
NGC 4473	E5	A	15.7	1.0×10^8	S
NGC 4486(M87, 3C 274)	E0+	L2	16.1	3.4×10^9	G
NGC 4486B	E0	—	16.1	6.0×10^8	S
NGC 4564	E	A	15.0	5.7×10^7	S
NGC 4593	SBb	S1	39.5	8.1×10^6	R
NGC 4594(M104)	Sa	L2	9.8	1.1×10^9	S
NGC 4596	SB0	L2:	16.8	5.8×10^7	G
NGC 4649(M60)	E2	A	16.8	2.0×10^9	S
NGC 4697	E6	—	11.7	1.2×10^8	S
NGC 4945	SBcd	S2	4.2	1.1×10^6	M
NGC 5548	S0/a	S1.5	70.2	1.23×10^8	R
NGC 5845	E	—	25.9	3.2×10^8	S
NGC 6251	E0	S2	94.8	5.4×10^8	G
NGC 7052	E4	—	63.6	3.6×10^8	G
NGC 7457	S0−?	A	13.2	3.4×10^6	S
NGC 7469	SABa	S1.0	66.6	6.5×10^6	R
PG 0026 + 129	—	QSO	627.4	4.5×10^7	R
PG 0052 + 251	S	QSO	690.4	2.2×10^8	R
PG 0804 + 761	—	QSO	429.9	1.89×10^8	R

Table 4 (continued).

Galaxy	Hubble type	Spectral class	D, Mpc	$M_{\rm BH}$, $M_\odot$	Method
PG 0844 + 349	—	QSO	268.4	2.16×10^7	R
PG 0953 + 414	S	QSO	1118	1.84×10^8	R
PG 1211 + 143	—	QSO	361.7	4.05×10^7	R
PG 1226 + 023(3C 273)	E	QSO	705.1	5.5×10^8	R
PG 1229 + 204	S	QSO	268.4	7.5×10^7	R
PG 1307 + 085	E	QSO	690.4	2.8×10^8	R
PG 1351 + 640	—	QSO	370.7	4.6×10^7	R
PG 1411 + 442	—	QSO	379.8	8.0×10^7	R
PG 1426 + 015(Mrk 1383)	—	QSO	366.2	4.7×10^8	R
PG 1613 + 658(Mrk 876)	—	QSO	565.3	2.41×10^8	R
PG 1617 + 175(Mrk 877)	—	QSO	494.7	2.73×10^8	R
PG 1700 + 518	—	QSO	1406	6.0×10^7	R
PG 1704 + 608(3C 351)	E	QSO	1857	3.7×10^7	R
PG 2130 + 099	—	QSO	255.3	1.44×10^8	R

Notes. For references to the original papers and data see Ho [245]. The BH mass determination method: G — gas kinematics, M — maser sources' kinematics, R — reverberation mapping method, S — stellar kinematics.

hierarchical models of galactic formation appears quite probable [247].

2. The supermassive BH mass $M_{\rm BH}$ correlates with the average-weighted over the luminosity velocity dispersion of stars $\sigma_{\rm eff}$ populating the bulge inside its effective radius: the BH mass increases with $\sigma_{\rm eff}$ [220, 254, 197] (Fig. 21)

$$\lg \frac{M_{\rm BH}}{M\odot} = (8.13 \pm 0.06) + (4.02 \pm 0.32) \lg \frac{\sigma_{\rm eff}}{200 \text{ km s}^{-1}} .$$

A correlation between the supermassive BH mass and the galactic stellar population age appears as well [255]: the BH mass increases with age. This correlation is inconsistent with the model of a primordial supermassive BH and apparently evidences a hierarchical history of galactic evolution with the formation of the central BH due to accretion and coalescence of stars (see, for example, Ref. [256]).

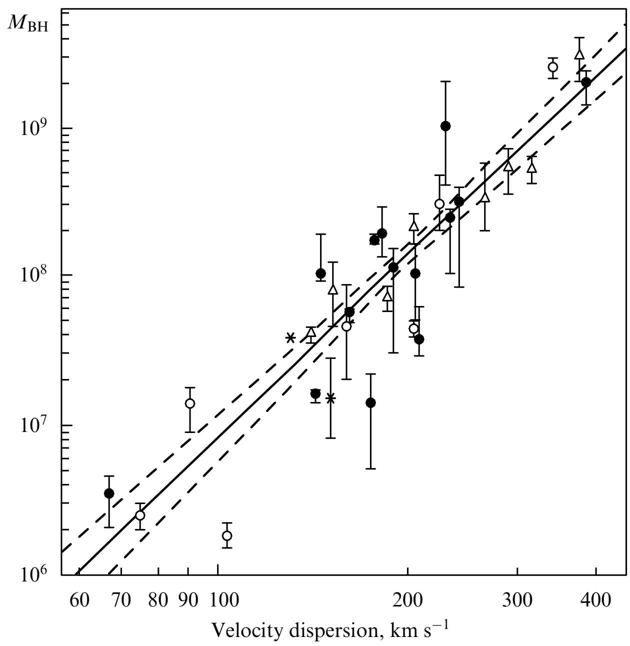

Figure 21. The BH mass in the nucleus of a galaxy as a function of the velocity dispersion of stars in its bulge. The solid line corresponds to the best fit with $\lg(M_{\rm BH}/M_\odot) = \alpha + \beta \lg(\sigma/\sigma_0)$, where $\alpha = 8.13 \pm 0.06$, $\beta = 4.02 \pm 0.32$, and $M_{\rm BH}$ is in solar units $M_\odot$ (from Tremaine et al. [197]).

3. The supermassive BH masses do not correlate with the galactic disk luminosities [220]. In those cases where a purely disk galaxy contains a central BH, its mass is much less than the standard value $\sim 0.2\%$ typical for the bulge [257, 258].

4. Paper [259] reports on anticorrelation between the rms amplitude of rapid (on timescales longer than 5 min) X-ray flux variability from Seyfert I nuclei, quasars, and low-luminosity active galactic nuclei, and the central BH mass: $\sigma^2_{\rm rms} \sim M^{-1}_{\rm BH}$. Thus, the amplitude of the rapid X-ray variability decreases with the central BH mass. Since the BH mass determines the size of the X-ray emitting accretion disk region, according to [259] this means that a single mechanism for the rapid variability operates in the galactic nuclei whose timescale is determined by the central BH size.

5. For active galactic nuclei, as already mentioned, there is a correlation between the central BH mass and the luminosity of the nucleus [88] [see Eqn (12)]. For normal galactic nuclei the correlation between the central BH mass and X-ray or infrared luminosity of the nucleus is rather weak [246], however there is a correlation between the supermassive BH mass and the radio luminosity of the nucleus and the entire galaxy (at cm wavelengths) [246]: $L_{\rm radio} \sim M^{2.5}_{\rm BH}$. Thus an appreciable total radio luminosity of a galaxy at the cm wavelengths serves as an indication of the presence of a supermassive BH in its center. Since the statistics of radio galaxies are very rich, this enables an indirect mass determination for a large number of galactic nuclei and the construction of the BH mass function (mass distribution) in the nearby part of the Universe [246]. In the recent paper by Ho [245], the correlation between the total radio luminosity of galaxies with supermassive BH masses in their centers was recently checked using an extensive observational data (80 galaxies with known central BH masses). The total radio luminosity of a galaxy turned out to only roughly correlate with the BH mass in its center (Fig. 22). The dependence $L_{\rm radio} \sim M^{2.0-2.5}_{\rm BH}$ is only the upper envelope on the corresponding plot. However, a good anticorrelation between the ratio of the radio luminosity of a galaxy to the optical luminosity of its nucleus and the ratio of the bolometric luminosity of the galactic nucleus to the Eddington luminosity (which determines the accretion rate) has been found.

6. Using rotation curves for about 1000 spiral galaxies ($r = 0.1-1$ kpc), central BH masses were estimated [260]. It was shown that in the late spirals (Sb-Im), the central BH

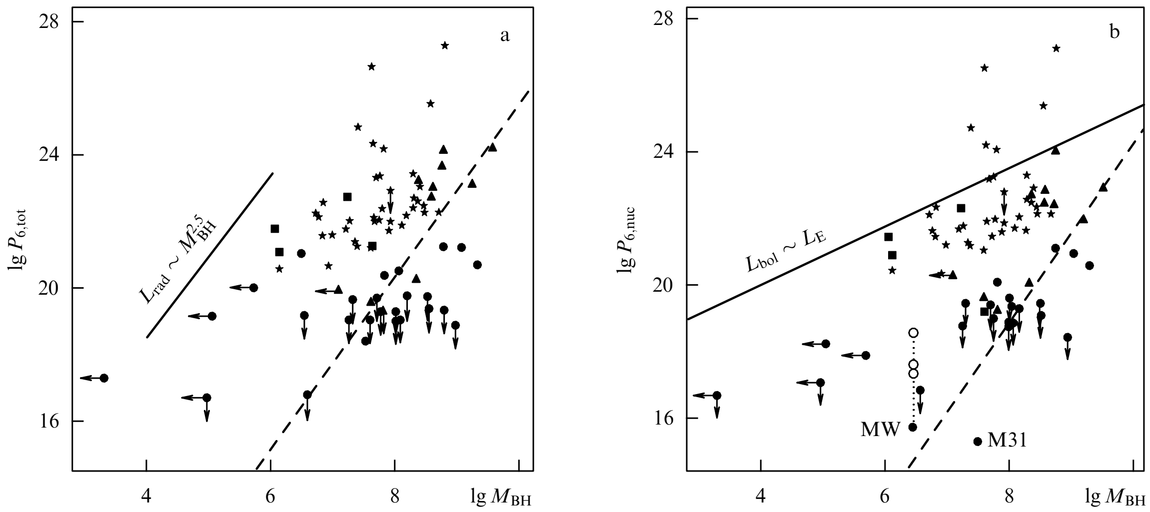

Figure 22. The dependence of the total specific radio luminosity (a) and the specific radio luminosity (b) from a galactic nucleus (in units W Hz^{-1}) on the mass of the central supermassive BH obtained by Ho [245]. BH masses were inferred from stellar kinematics (●), gas kinematics (▲), maser kinematics (■) and reverberation mapping (★). The dashed lines indicate the regression relationship suggested by Francenschini et al. [246]. The sign MW in Fig. (b) designates the nucleus of our Galaxy (four values of the radio luminosity are given corresponding, from top to bottom, to sources Sgr A*, Sgr A West, Sgr A West+East, and the central region $1 \times 1° = 150 \times 150$ pc in size).

masses are about 10 – 100 times smaller than in ellipticals, while in the early-type spirals (Sa) the central BH masses are of the same order of magnitude as in the ellipticals. Thus, the late spirals can not be 'sleeping' quasars, since BH masses in quasars, as follows from their huge luminosity, must be of the order of $(10^8 - 10^{10}) M_\odot$ [260, 189]. Estimates of the cosmological density of the supermassive BH in the Universe based on these studies yields [258]

$$\rho_{BH}(\text{Sb-Im}) < 4.5 \times 10^4 M_\odot \text{ Mpc}^{-3} ,$$

$$\rho_{BH}(\text{Sa}) < 1.6 \times 10^6 M_\odot \text{ Mpc}^{-3} ,$$

which may be used to test some cosmological predictions [189]. The total BH mass density in the local Universe evaluated from studies of normal galactic nuclei is $\sim 5 \times 10^5 M_\odot$ Mpc^{-3} [249], which is consistent with the total BH mass density derived from the analysis of active galactic nuclei at large redshifts $z \sim 2$ [246, 249].

For a more detailed discussion of the central BH relation to the morphology of galaxies see reviews [50, 189, 220].

To conclude, we note that it is becoming more and more recognized that practically all galaxies posses supermassive BHs with masses from 10^6 to $10^{10} M_\odot$ in their nuclei; less massive BHs may also be present in some galactic nuclei, but they are hard to measure so far [50, 189, 248].

8. Black holes in X-ray binary systems

There are two types of BH X-ray binary systems (see catalog [261]):

1. Persistent X-ray binaries with massive hot O – B stars (systems Cyg X-1, LMC X-1, LMC X-3).

2. Transient X-ray binaries (X-ray novae) with low-mass cold A – M stars (systems A0620–00, V404 Cyg, etc.). The typical X-ray nova exhibits X-ray outbursts when the X-ray luminosity L_x of the system rapidly (in several days) rises up from $L_x < (10^{30} - 10^{33})$ erg s^{-1} (the quiescent state) to $(10^{37} - 10^{39})$ erg s^{-1} at the maximum and then decreases (in most cases exponentially, in several months) down to the initial level where it stays for several years (Fig. 23). Occasionally, 2 – 3 months after the X-ray outburst, secondary outbursts occur both in the X-ray and optical bands. During the X-ray outburst, the optical outburst is also

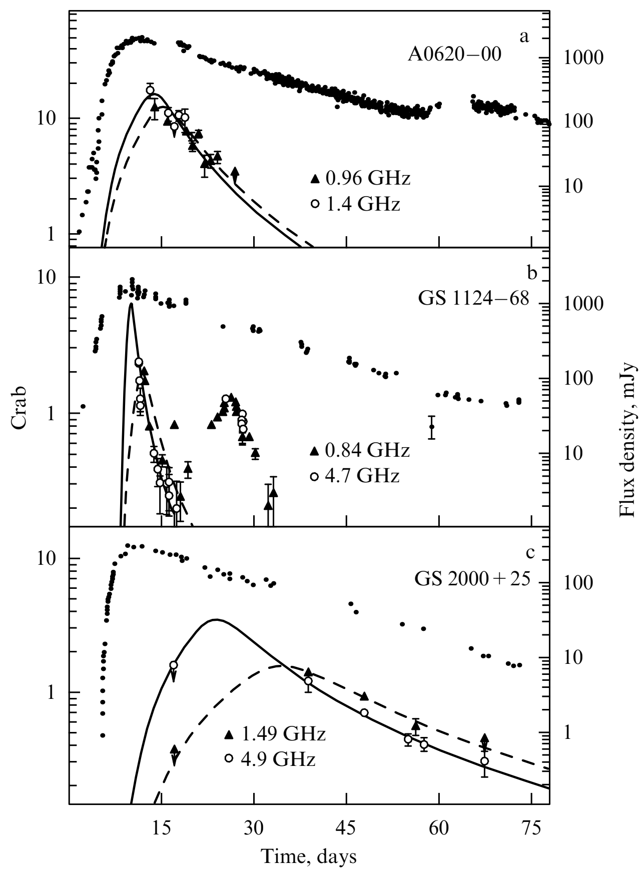

Figure 23. X-ray and radio light curves of X-ray novae with BHs during outbursts (obtained by Kuulkers et al. [262]).

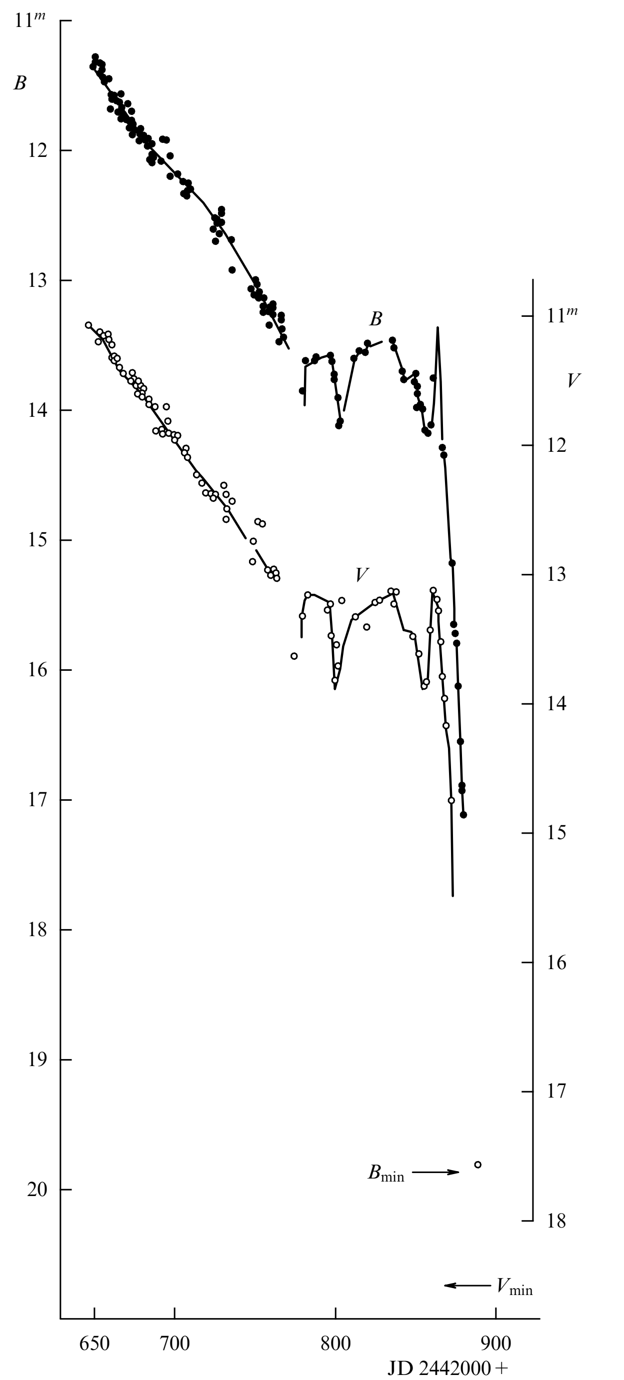

Figure 24. Optical B and V light curves of the BH X-ray binary A0620−00 (V616 Mon) during an outburst (from Goranskij et al. [263]).

observed due to the powerful X-ray illumination of the optical star and accretion disk around the relativistic object (Fig. 24). This enables reliable identification of the X-ray source with the optical star. In the quiescent state, the X-ray luminosity is low and absorption lines of the companion are visible in the optical spectrum. In addition, strong broad ($\sim 10^3$ km s^{-1}) and frequently two-humped emission lines of hydrogen and other elements characteristic of a rotating accretion disk are observed (see Fig. 3). In the quiescent state, the two-humped H_α emission from an accretion disk varies by a factor of two on timescales of several hours [264]. The presence of the accretion disk at practically zero X-ray luminosity in the quiescent state is the main mystery of X-ray novae. To explain this phenomenon, the advection-dominated accretion disk model is invoked [32–36] (see, however, [37–39]). X-ray nova outbursts are explained by non-stationary accretion at low accretion rates from the low-mass optical companion. Then the gravitational energy release in the disk is small and its mean temperature is low and close to the hydrogen ionization level ($\sim$ 8000 – 10000 K), corresponding to the opacity jump. Small changes in $\dot{M}$ due to, for example, the companion's activity, which is a late-type dwarf, could push the temperature below or above the critical value. So the disk material changes its state from neutral to ionized and back. Then the matter opacity strongly varies, which may lead to an instability and strong turbulence generation in the disk, to an increase in the disk viscosity, to an enhanced accretion rate, and, later on — to an outburst (see reviews [265–268, 53] for more detail). Strong X-ray radiation from the central source heats up the accretion disk above the critical 8000 K temperature, which additionally stabilizes accretion disk matter against convective instability [269]. In the quiescent state, Doppler shifts of absorption lines allow the optical star radial velocity curve to be constructed and its mass function to be found [see Eqn (4)].

In addition, in the quiescent state periodical optical and infrared variability of the X-ray nova is observed, which is primarily due to the optical star ellipticity [22, 23] (see Fig. 4). The orbital inclination of the binary system i is inferred from the light curve [see Eqn (6)]. All this allows the BH mass m_x to be calculated. For more information on X-ray novae see recent reviews [51, 53, 102].

The launch of the first American specialized X-ray satellite UHURU in 1971 led to the discovery of about 100 X-ray binary systems [18]. So far, new generation X-ray satellites (EINSTEIN, ROSAT, GINGA, ASCA, RXTE, CHANDRA, GRANAT, MIR-KVANT, etc.) have detected $\sim 10^3$ X-ray binaries in our and nearby galaxies. Soviet and Russian X-ray observatories MIR-KVANT and GRANAT headed by R A Sunyaev made important contributions to X-ray binary studies (see, for example, Refs [270–275]). The main spectral features of X-ray binaries with a BH presently known can be summarized as follows. Five different spectral states are known for these systems as derived from the X-ray spectral shape and the luminosity in the 1 – 10 keV range [276–281, 265].

1. *Quiescent state*. In recent years, new sensitive X-ray satellites (ASCA, CHANDRA, XMM) have made it possible to measure X-ray spectra of BH X-ray binaries in the 'turned-off', quiescent state ($L_x < 10^{33}$ erg s^{-1}). The quiescent X-ray spectra are non-thermal, with a photon index softer than in the low state and an X-ray luminosity L_x of several magnitudes smaller than in the other five states [282–286] (Fig. 25).

2. *Low/hard state*. In this state, the X-ray luminosity L_x is less than 10% of the Eddington value. The X-ray spectrum is a power-law with a photon index $\alpha_N \sim 1.5 - 1.9$ and has an exponential cutoff at about 100 keV [280, 288]. The power-law component is due to non-thermal processes, mainly due to Comptonization of soft quanta on hot electrons [289]. In this state, relativistic collimated matter outflows — jets — are observed in some BH systems [270, 290–292].

3. *High/soft state*. Systems with spectra in which a supersoft quasi-blackbody component with a characteristic temperature of $\sim$ 1 keV dominates [276, 265, 266] (caused by thermal emission from the classical optically thick accretion disk) and a total luminosity L_x above the value of L_x in the

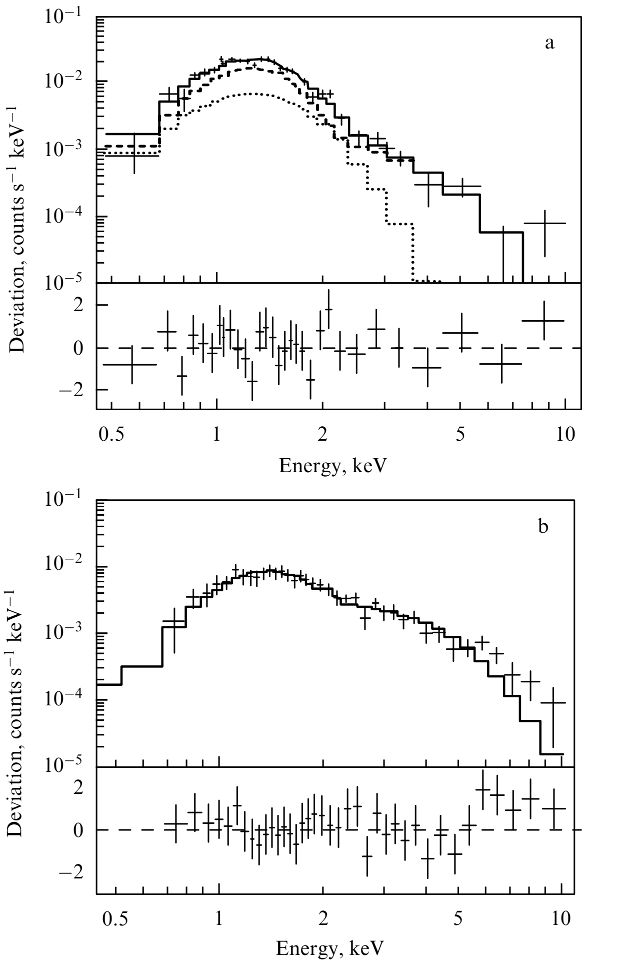

Figure 25. The observed and model spectra of X-ray novae with NS and BH in the quiescent state: (a) the binary with NS 4U 1908+005 (Aql X-1), (b) the binary with BH GS 2023+338 (V404 Cyg) (from Asai et al. [286]).

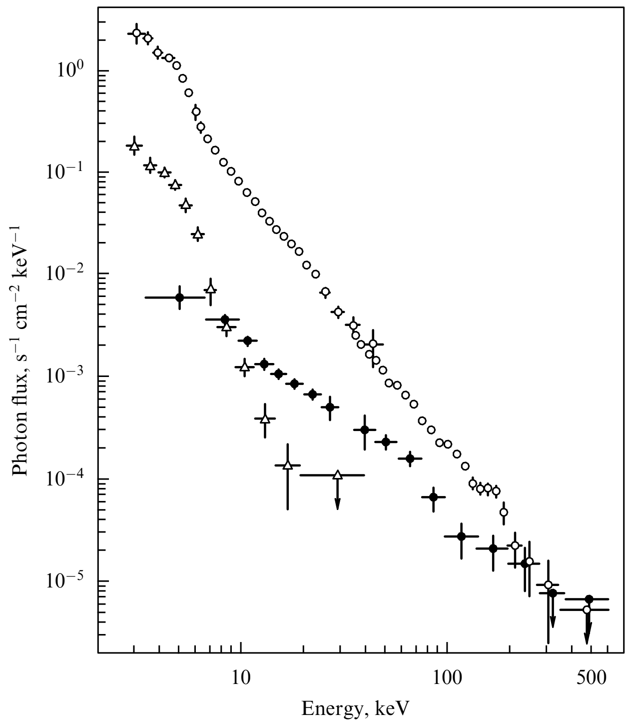

Figure 26. Broadband X-ray spectra of the X-ray nova binary system with BH GRS 1124–68 (GU Mus) in different spectral states. The spectra were obtained by Sunyaev's group [300] on the telescopes ART-P and SIGMA of the GRANAT X-ray observatory on January 16 (○), April 12 (△) and August 14 – 15 (●), 1991.

low state, are said to be in the 'high' or 'soft' state. In addition to the thermal component (which contributes $\sim 70-90\%$ to the total X-ray luminosity of the system), there is a power-law 'tail' in the spectrum, but the contribution of this hard component to the total luminosity $L_{\rm x}$ is much smaller than in the low state. The power-law component is highly variable, unlike the soft black-body component which is very stable. The photon index of the power-law component at this stage is about $\alpha_N \sim 2.5$ [265].

4. *Intermediate state*. In recent years, a new state has been identified in X-ray binaries [273, 277, 293, 294], which is named intermediate. The observed X-ray spectra in this state exhibit characteristics intermediate between the low and high spectral states.

5. *Very high state*. Occasionally, in some systems with a very high X-ray luminosity, the power-law spectrum and the soft component are comparable in luminosity. This state is called the very high state [295 – 297, 279]. The power-law component in the very high state has a photon index $\alpha_N \sim 2.5$, and the high energy cutoff is not observed up to many hundred keV.

Not all X-ray binary systems exhibit all these five states. Most systems mainly stay in only one of the states, making short-term transitions to other states. For example, Cyg X-1 is primarily observed in the low state with rare transitions to the high state. At the same time, system LMC X-3 almost always is in the high state [281]. X-ray novae GS 2023+338 and GRO J0422+32 demonstrate only power-law spectra for all range of luminosities $L_{\rm x}$ without any trace of the soft component [298]. Many X-ray novae pass through all five states. For example, XN Mus 1991 (GS 1124–683) passed very rapidly from the quiescent state to the very high state and then, having passed through the high state, returned back to the quiescent state [297, 273, 299, 293] (Fig. 26).

9. Masses of black holes in X-ray binary systems

Observational data and mass determination of BHs in X-ray binaries are described in recent reviews [49, 51, 53, 102]. To the present time (2002), BH masses have been measured in 15 X-ray binaries. Of these, three (SAX J1819.3–2525, XTE J1118+480, and GRS 1915+105) were measured very recently [301 – 303]. Let us briefly describe these data.

Orosz et al. [301] carried out optical spectroscopic observations and determined the component masses in the transient X-ray binary system SAX J1819.3–2525 (V4641 Sgr), in which visible superluminal motions of individual details of radio jets are observed during X-ray outbursts. The object SAX J1819.3–2525 was discovered as a transient X-ray source by Beppo SAX satellite in February 1999 and by RXTE X-ray observatory [304, 305]. The object was also detected as a bright radio source 16 hours after the X-ray outburst [306]. This radio source had non-zero size, appeared to expand, and glowed over three weeks after the outburst. It was identified with the optical variable star V4641 Sgr by Goranskij [307, 308]. Spectroscopic observations [301] revealed the orbital period $p = 2^d.81678$ close to one of the two photometric periods found by Goranskij. The optical light curve looks like a double wave over the orbital period with an amplitude of $\sim 0^m.5$ with two minima of unequal depth, which corresponds to the ellipticity of the optical star with traces of an eclipse by an accretion disk. No X-ray eclipses are observed in this binary system. These data yield a sufficiently reliable estimate of the orbital inclination: $60° < i < 70°.7$. The semi-amplitude of the optical star radial velocity curve is $K = (211{,}0 \pm 3{,}1)$ km s^{-1}, the corresponding mass function is $f_v(m) = (2.74 \pm 0.12) M_\odot$. The optical star atmosphere is fitted by a model with the effective temperature $T_{\rm eff} = (10500 \pm 200)$ K, the gravity force acceleration $\lg g = 3.5 \pm 0.1$, and the rotational equatorial velocity $V_{\rm rot} \sin i = (123 \pm 4)$ km s^{-1}. Hence assuming axial rotation of the star to be synchronous with orbital motion (which is quite reasonable for X-ray novae), the mass ratio of the components is found to be $q = m_x/m_v = 1.50 \pm 0.08$ [see Eqn (7)]. With these values of $f_v(m)$, q, and i, the BH mass is $8.73\, M_\odot \leqslant m_x \leqslant 11.70\, M_\odot$ [see Eqn (5)], and the optical star mass is $5.49\, M_\odot \leqslant m_v \leqslant 8.14\, M_\odot$. The spectral class of the optical companion is close to B9III, the color excess of the system is $E(B-V) = 0.32 \pm 0.1$, and the distance to the system at the visible stellar magnitude $V \cong 13^m.7$ is quite large $7.40 \leqslant d \leqslant 12.31$ kpc. The large distance and significant proper motions of details in the radio image suggest an apparent velocity of $9.5c$ (the corresponding Lorentz-factor is $\Gamma > 9.5$). The optical spectrum (as in the case of another X-ray nova GRO J1655−40 [309]) demonstrates an excess of the α-elements formed in α-processes in massive stellar cores: oxygen, calcium, magnesium, and titanium (an overabundance of 2 to 10 times compared to the solar abundance). This suggests that the formation of BHs in systems GRO J1655−40 and SAX J1819.3−2525 was associated with a supernova explosion which enriched the optical star atmosphere with the α-elements. It should be stressed that since there is marginal evidence of the optical star eclipse by an accretion disk, the orbital inclination estimate is quite reliable, so the BH mass value is obtained with a relatively small error: $m_x = 9.61(+2.08 - 0.88) M_\odot$. This value of m_x is close to the mean BH mass (see below).

Wagner et al. [302] carried out spectroscopic and photometric observations of X-ray nova XTE J1118+480 located high above the Galactic plane at $z \cong 1.7$ kpc and determined the masses of the BH and optical companion in this system.

The X-ray nova XTE J1118+480 was discovered by the RXTE satellite in 2000 and then identified with an optical star which reached a brightness of $V = 12^m.9$ in the maximum [310, 311] and was as dim as $V = 18^m.8$ in the quiescent state. The galactic latitude of the system is quite high, $b = +62°$. This strongly distinguishes this system from other BH X-ray novae [53, 268, 312] which are approximately homogeneously distributed near the galactic plane and are less concentrated toward the galactic bulge, as opposed to other low-mass X-ray binaries [313]. The optical spectrum of the object in the quiescent state shows two-humped emission hydrogen lines (FWHM $\cong 2400$ km s^{-1}) that arise in the accretion disk, as well as absorption lines corresponding to a late spectral class star K7V−M0V. The orbital period is $p = 0^d.169930$, the radial velocity semi-amplitude is $K_v = (701 \pm 10)$ km s^{-1}, the orbit is circular, and the optical star mass function is $f_v(m) = (6.1 \pm 0.3) M_\odot$. Thus, the relativistic object mass exceeds $6.1 M_\odot$ and is strongly above the maximum possible neutron star mass [4, 314], which suggests the presence of a BH in XTE J1118+480. The optical star luminosity, as follows from spectral data, is $(28 \pm 2)-(36 \pm 2)$% of the total luminosity of the system at (5800−6400) Å. The remaining fraction of the luminosity is contributed by the accretion disk in the quiescent state of the system. Photometric R-observations revealed the $0^m.2$ optical variability with the orbital period, which is caused by the optical star ellipticity and eclipses. From the optical light curve modeling the orbit inclination angle was found to be $i = (81 \pm 2)°$ and the mass ratio $q = m_x/m_v \cong 20$. The BH mass derived from these data is $m_x = (6.0-7.7) M_\odot$ (at a 90% confidence level), the optical star mass is $m_v = (0.09-0.5) M_\odot$. The distance to the system is estimated to be about (1.9 ± 0.4) kpc, the corresponding altitude of the system over the galactic plane is (1.7 ± 0.4) kpc. All these data suggest that XTE J1118+480 is the first reliable BH X-ray transient binary system located in the galactic halo. The system exhibits an appreciable proper motion (ΔRA $= -16.8 \pm 1.6$ mas yr^{-1}, ΔDEC $= -7.4 \pm 1.6$ mas yr^{-1}) [315]. If the system was expelled from the galactic plane by a momentum acquired in the supernova explosion, now we observe it at the galactic orbit point with a total peculiar velocity of 145 km s^{-1}. Then the total initial galactic velocity of the system was (217 ± 18) km s^{-1}, and the initial velocity component perpendicular to the galactic plane was (126 ± 18) km s^{-1} [315].

Greiner et al. [295] carried out infrared spectroscopic studies of the unique transient X-ray binary system, the microquasar GRS 1915+105. This system resides in the Galactic plane at a distance of $\sim 11-12$ kpc and suffers from a huge interstellar absorption of $A_v = 25^m - 30^m$. The spectroscopic observations of GRS 1915+105 in the H and K infrared bands revealed principal lines of the molecular absorption bands ^{12}CO and ^{13}CO, as well as lines of metals, which enabled the classification of the optical star as a red giant (K−M)III. From the Doppler shift of the absorption lines, the orbital period $p = 33^d.5 \pm 1^d.5$ is determined, the semi-amplitude of the radial velocities $K_v = (140 \pm 15)$ km s^{-1} is found, and the zero eccentricity orbit is established for this system. The corresponding optical mass function is

$$f_v(m) = \frac{m_x^3 \sin^3 i}{(m_x + m_v)^2} = (9.5 \pm 3.0) M_\odot \,.$$

It is the highest mass function of all known BH X-ray binaries. The radial velocity of the system's barycenter is $\gamma = (-3 \pm 10)$ km s^{-1}. The accretion disk or relativistic jets provide a significant contribution in the IR compared to the (K−M)III star, which gives only several per cent of the brightness in the K band. The orbital inclination $i = (70 \pm 2)°$ is inferred from the relativistic jet orientation, which is found from the analysis of jet clouds brightness approaching and receding from the observer. That the jets are perpendicular to the orbital plane comes from the absence of the jet precession on timescales of several years. Assuming in the first approximation the (K−M)III star mass to have the standard value $(1.2 \pm 0.2) M_\odot$, for $i = (70 \pm 2)°$ the BH mass in GRS 1915+105 is $m_x = (14 \pm 4) M_\odot$. This is one of the most massive stellar mass BHs in X-ray binaries. As the (K−M)III star intensively looses the mass (which follows from the high X-ray luminosity of GRS 1915+105), its mass may exceed the standard value for this spectral and luminosity class $1.2 M_\odot$. Then the value $m_x = 14 M_\odot$ in GRS 1915+105 can be considered as the lower limit on the BH mass. The mean radius of the Roche lobe for the (K−M)III star is $(21 \pm 4) R_\odot$. This value is close to the standard (K−M)III star radius, which suggests that the (K−M)III

Table 5. Parameters of binary systems with BHs.

System	Optical star spectrum	$P_{\rm orb}$, day	$f_{\rm v}(m)$, in $M_{\odot}$	$m_{\rm x}$, in $M_{\odot}$	$m_{\rm v}$, in $M_{\odot}$	$V_{\rm pec}$, km s^{-1}	Note
Cyg X-1 V 1357 Cyg	O 9.7 Iab	5.6	0.24 ± 0.01	16 ± 5	33 ± 9	2.4 ± 1.2	Persistent
LMC X-3	B3 Ve	1.7	2.3 ± 0.3	9 ± 2	6 ± 2	—	Persistent
LMC X-1	O (7–9) III	4.2	0.14 ± 0.05	7 ± 3	22 ± 4	—	Persistent
A0 620–00 (V616 Mon)	K5 V	0.3	2.91 ± 0.08	10 ± 5	0.6 ± 0.1	-15 ± 5	Transient
GS 2023+338 (V404 Cyg)	K0 IV	6.5	6.08 ± 0.06	12 ± 2	0.7 ± 0.1	8.5 ± 2.2	Transient
GRS 1124–68 (GU Mus)	K2 V	0.4	3.01 ± 0.15	$6(+5-2)$	0.8 ± 0.1	25 ± 5	Transient
GS 2000+25 (QZ Vul)	K5 V	0.3	4.97 ± 0.10	10 ± 4	0.5 ± 0.1	—	Transient
GRO J0422+32 (V518 Per)	M2 V	0.2	1.13 ± 0.09	10 ± 5	0.4 ± 0.1	—	Transient
GRO J1655–40 (XN Sco 1994)	F5 IV	2.6	2.73 ± 0.09	6.3 ± 0.5	2.4 ± 0.4	-114 ± 19	Transient
H 1705–250 (V2107 Oph)	K5 V	0.5	4.86 ± 0.13	6 ± 1	0.4 ± 0.1	38 ± 20	Transient
4U 1543–47 (HL Lup)	A2 V	1.1	0.22 ± 0.02	$4.0-6.7$	~ 2.5	—	Transient
GRS 1009–45 (MM Vel)	(K6–M0) V	0.3	3.17 ± 0.12	$3.6-4.7$	$0.5-0.7$	—	Transient
SAX J1819.3–2525 (V4641 Sgr)	B9 III	2.8	2.74 ± 0.12	$9.61(+208-0.88)$	$6.53(+1.6-1.03)$	—	Transient
XTE J1118+480	(K7–M0) V	0.17	6.1 ± 0.3	$6.0-7.7$	$0.09-0.5$	145†	Transient
GRS 1915+105	(K–M) III	33.5	9.5 ± 3.0	14 ± 4	1.2 ± 0.2		Transient

Notes. See reviews [53, 321] and references therein, as well as recent papers [301–303, 322, 323]. Here $P_{\rm orb}$ is the orbital period, $f_{\rm v}(m) = m_{\rm x}^3 \sin^3 i/(m_{\rm x} + m_{\rm v})^2$ is the optical star mass function, $m_{\rm x}$ and $m_{\rm v}$ are the masses of the relativistic object and the optical star, respectively, and $V_{\rm pec}$ is the peculiar radial velocity of the binary system's barycenter.
† The absolute value of the total peculiar velocity is given, according to Ref. [315].

giant fills its Roche lobe in this system. The rapid X-ray and radio variability and spectral characteristics of GRS 1915+105, as well as properties of the observed quasi-periodic oscillations, are described in papers [316, 317].

The large mass of the BH in GRS 1915+105 determines the physics of the microquasar observed in this system, and the large orbital period $p = 33^d.5$ and radius of the orbit $a = (108 \pm 4) R_{\odot}$ put constraints on the evolutionary scenario for this system [303].

System Cyg X-3 deserves special mentioning. In this system the optical component is a Wolf–Rayet (WR) star of WN 3–7 class. The high radial outflow velocities in the stellar wind of this star ($\sim 10^3$ km s^{-1}) and anisotropic ionization of the wind material by powerful X-ray radiation from the accreting relativistic object ($\sim 10^{38}$ erg s^{-1} in the 1–60 keV energy range) can induce a significant modulation of the observed emission line radial velocities, which correlates with the orbital period but is not related with the orbital motion of the WR barycenter. Nonetheless, analysis of the emission line radial velocities of Cyg X-3 made by Schmutz et al. [318] implies a large mass of the relativistic object of $m_{\rm x} = (7-40) M_{\odot}$, which can be a BH. The main arguments of the authors [318] that the emission lines in the Cyg X-3 spectra reflect the orbital motion of the WN 3–7 star are that the form of the lines does not change with the orbital phase and the lines shift as a whole. The following fact also suggests the presence of a BH in Cyg X-3: no steady X-ray pulsations have been found from this system, in spite of the dedicated searches [261]. Besides, as noted in Ref. [319], since the bolometric WR star luminosity in Cyg X-3 is large $L_{\rm bol} \sim 3 \times 10^{39}$ erg s^{-1} and a strong X-ray heating effect with an amplitude $\sim 15-30\%$ is observed in this system, the true X-ray luminosity of the accreting relativistic object in Cyg X-3 must be significantly greater than the observed $L_{\rm x} \cong 10^{38}$ erg s^{-1} in the hard 1–60 keV range (the dominating soft X-ray component is absorbed by the wind and in the interstellar medium). This last fact also makes a strong case for a massive BH in Cyg X-3. Recently, Hanson, Still, and Fender [320] carried out a detailed infrared spectroscopy of Cyg X-3. They confirmed the regular emission line radial velocity variability with the orbital period and the semi-amplitude $K = (480 \pm 50)$ km s^{-1} discovered by Schmutz et al. [318]. In addition, the authors found an absorption feature in the Cyg X-3 spectrum, for which the radial velocity curve is shifted by 1/4 of the orbital period with respect to the emission line radial velocity curve. The γ-velocity crossing for this radial velocity curve corresponds to the minimum of the X-ray and infrared light curves, which enabled the authors of Ref. [320] to conclude that this absorption feature originates in the WN stellar wind and better reflects the orbital motion than the emission line radial velocity curve does [318]. The absorption feature radial velocity semi-amplitude is $K = (109 \pm 13)$ km s^{-1}, and the corresponding WN star mass function is $f_{\rm v}(m) = 0.027 M_{\odot}$. Taking the orbital inclination angle $i > 60°$ and the accretor's mass $m_{\rm x} = 1.4 M_{\odot}$ (NS), the authors [320] evaluated a WN4 mass to be $5 M_{\odot} \leqslant m_{\rm WN} \leqslant 11 M_{\odot}$. On the other hand, assuming the WN star mass $m_{\rm WN} < 70 M_{\odot}$, the authors [320] obtained $m_{\rm x} < 10 M_{\odot}$. Thus, the new mass function $f_{\rm v}(m) = 0.027 M_{\odot}$ and the relativistic object mass estimate allows for the presence of both an NS and a BH in Cyg X-3. So at present we do not consider Cyg X-3 to be a reliable BH candidate.

Table 5 summarizes mass determinations for 15 BHs in X-ray binary systems. The dependence of the relativistic

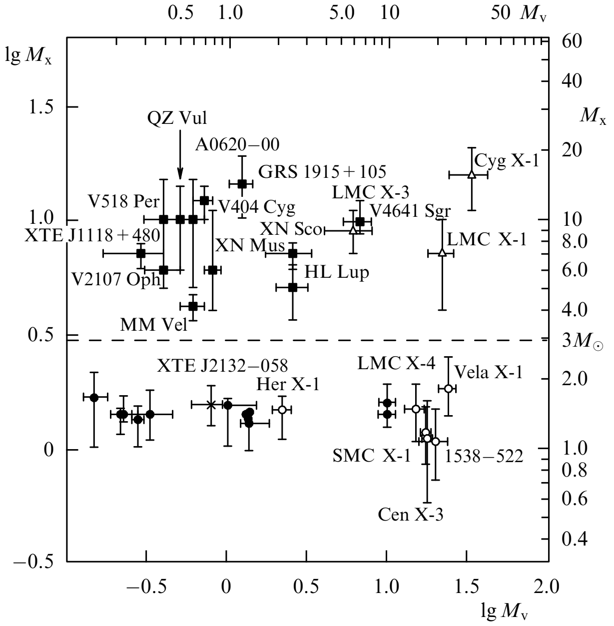

Figure 27. The dependence of masses M_x of NSs (circles and crosses) and BHs (triangles and squares) on the companion masses M_v in binary systems (masses are in solar units $M_\odot$). The filled circles correspond to radio pulsars, the open circles to X-ray pulsars, and the cross stands for the NS in X-ray nova XTE J2132−058 [324]. The filled squares correspond to BHs in X-ray novae and the open triangles to BHs in quasi-persistent X-ray binaries with massive O–B companions.

object masses on the companion masses in CBS is shown in Fig. 27. It is seen that optical companions to X-ray pulsars and BHs in close binary systems are O–M stars. The companions to radio pulsars are inactive neutron stars and white dwarfs, as well as massive stars of early spectral class $\sim$ B (we do not consider here radio pulsars with planets). Masses of radio pulsars can be measured with a high accuracy by relativistic effects in their orbital motion (see, for example, Refs [325–328]). It is clear from Fig. 27 that there is no dependence of the relativistic object masses on the satellite masses: both NSs and BHs occur in binary systems with companions of both high and low mass. In this sense CBS with relativistic components are similar to classical CBS where all possible combinations of components occur [329]. As we already noted, masses of all measured X-ray and radio pulsars do not exceed $3M_\odot$, the absolute upper limit of the NS mass in full accordance with GR. At the same time, none of the 15 massive ($m_x > 3M_\odot$) compact X-ray sources in CBS shows the X-ray-pulsar-like or type-I-X-ray-burster-like phenomenon, again with full consistency with GR predictions. Three X-ray novae with BHs (XN Sco 1994, SAX J1819.3−2525, XTE J1118+480) show signatures of the supernova explosion: in XN Sco 1994, high peculiar velocity of the system's barycenter $V_{\rm pec} = (-114 \pm 19)$ km s^{-1} is observed [330] and enhanced abundance of elements O, Si, and Mg originating in α-reactions is found in the optical star spectrum [309]. This evidences the supernova explosion which led to the optical star enrichment by the α-elements and the high system's barycenter velocity [309, 330]. Possibly, the formation of the BH in this case passed through two stages: first a NS resulted from the presupernova core collapse, and then a BH was produced by the fall-back accretion of matter on the NS [330].

Table 6. Microquasars in our Galaxy.

Source name	Compact object	$V_{\rm jet}$	References
GRS 1915+105	BH	$0.92c-0.98c$	[336]
GRO J1655−40	BH	$0.92c$	[336]
XTE J1748−288	BH	$0.93c-0.23c$	[336, 337]
SS 433	BH	$0.26c$	[336]
Cyg X-3	BH	$\sim 0.3c - \geqslant 0.8c$	[336, 338]
CI Cam	NS?	$\sim 0.15c$	[336]
Sco X-1	NS	$\sim 0.5c$	[336]
Cir X-1	NS	$\geqslant 0.1c$	[336]
1E 1740.7−2942	BH		[336]
GRS 1758−258	BH		[336]
SAX J1819.3−2525	BH	$\geqslant 0.95c$	[336, 301]
LS 5039	?	$\geqslant 0.15c$	[336]
Cyg X-1	BH	$> 0.6c$	[339]
XTE J1550−564	BH		[337, 291]

The optical star in SAX J1819.3−2525 also demonstrates an overabundance of α-elements evidencing the supernova explosion. XTE J1118+480 is located at a very high altitude over the Galactic plane $z = 1.7$ kpc [302] and has a large peculiar space velocity of the barycenter of 145 km s^{-1} [315], which also can indicate a supernova explosion occurred in the past that gave a high initial space velocity to the system ($V_{\rm init}^{\rm pec} = (217 \pm 18)$ km s^{-1}, according to [315]).

Spectra of optical stars in some X-ray novae with BHs exhibit an enhanced lithium line LiI λ6707.8 Å, which may indicate the optical star atmosphere enrichment by lithium due to its illumination by high-energy particles accelerated to relativistic velocities in the inner parts of the accretion disk around a BH (see reviews [49, 51, 53] for more detail).

In systems GRS 1915+105, SAX J1819.3−2525, GRO 1655−40 (XN Sco 1994), and 1E 1740.7−2942, relativistic collimated jets with velocities $V \geqslant 0.92c$ and apparent superluminal plasma cloud motions were discovered during X-ray outbursts [331–333]. X-ray binary systems with collimated relativistic jets are commonly called microquasars. Reviews on microquasars can be found in the proceedings of conferences [334, 335]. Table 6 displays the main characteristics of the known microquasars taken from the review by Rodriguez and Mirabel [336], in which the newest data on jets in BH X-ray binary system Cyg X-1 are also added [290, 339, 340].

10. Differences in observational appearances of accreting neutron stars and black holes

As we noted above, the measured masses of NSs in X-ray and radio pulsars does not exceed $3M_\odot$, in full agreement with GR, while the massive X-ray binaries with BHs do not show the phenomenon of X-ray pulsar or type I X-ray burster, again in consistency with GR. These facts strongly strengthen our certitude of the real existence of the stellar mass BH, but of course they are not the final proof of BH existence. Let us enumerate additional facts suggesting that NSs and BHs in binary systems differ not only by masses, but by observational appearances as well (see recent reviews by Sunyaev [341], Belloni [342], and Tanaka [343]).

According to [341–343], accreting NS and BHs demonstrate both similarities in observational appearances caused by the X-ray emission formation in the inner parts of the accretion disk, and differences in the X-ray emission characteristics due to NSs having solid surfaces, whereas BHs do not.

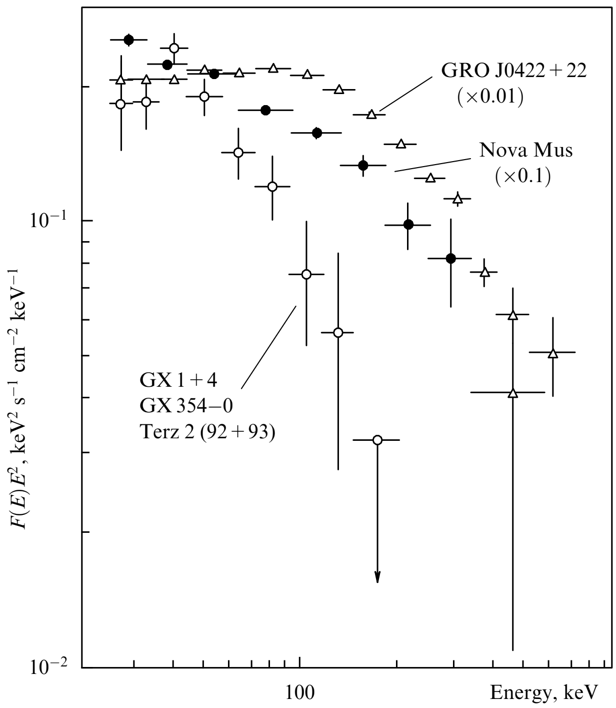

Figure 28. Spectra at energies above 35 keV of X-ray novae with NSs and BHs obtained by the SIGMA telescope on board the GRANAT X-ray observatory by Sunyaev's group [300]. The spectra are presented in the form $F(E)E^2$. GX 1+4, GX 354−0, and Terz 2 (92+93) are X-ray binaries with NS, while GRO J0422+22 and Nova Mus are X-ray novae with BHs.

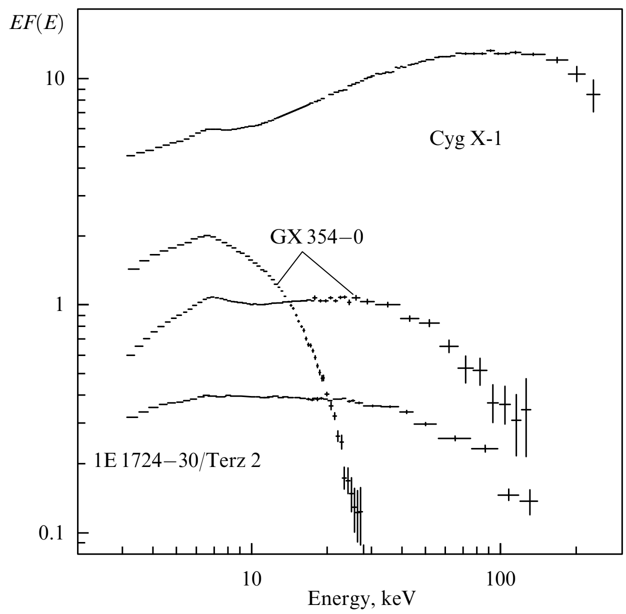

Figure 29. Energy spectra of three X-ray binary systems: with NS (GX 354−0/4U 1728−34 and 1E 1724−30/Terz 2) and BH (Cyg X-1). The NS binary system GX 354−0 is shown in two states: low/hard and high/soft. Even in the hard state the spectra of accreting NS are much softer than that of the accreting BH Cyg X-1 (from Sunyaev and Revnivtsev [344]).

1. X-ray spectra of accreting BHs show 'power-law tails' expanding up to $\sim$ 1 MeV energy [271, 272, 296, 297, 300]. At the same time, X-ray spectra of accreting NSs usually show a cutoff at 60 – 100 keV [300] (Figs 28 and 29). This difference bears only a statistic character, since X-ray spectra of some type I X-ray bursters, NSs with weak surface magnetic field (for example, KS 1731−260), also show power-law tails up to very high energies $\sim$ 150 keV [345]. According to [346, 347], the NS radius can be appreciably smaller than that of the marginally stable orbit. If the magnetic field is weak, particles from the inner edge of the accretion disk fall almost freely with a velocity close to the speed of light onto the neutron star surface and give off energy in collision with nuclei and through plasma instability effects. This mechanism can explain hard tails in the X-ray spectra of some bursters observed by the GRANAT, RXTE, and GRO observatories.

The formation of a non-thermal power-law spectrum can be related to thermal instabilities in the inner accretion disk [348, 349]. These instabilities are assumed to result in the accretion disk becoming optically thin [350], or in a hot corona forming above the disk [337, 338], or in hot, optically thick plasma clouds emerging, in which Compton scattering and heating of photons occur [274, 353, 389]. The difference in observational appearances of accreting NSs and BHs in X-ray novae during outbursts allowed the astronomers to elaborate some indirect criteria which make the BH model preferential even when the relativistic object mass is unknown. These criteria are based on the similarity of the observational appearance of a given object with the characteristic features of the BH X-ray binary Cyg X-1:

(a) bimodal spectral behavior with a supersoft very high state and a very hard low state;

(b) at least for the brightest sources, X-ray spectra exhibit an unsaturated Comptonized hard tail up to very high energies $\sim$ 1 MeV;

(c) rapid hard X-ray intensity fluctuations on timescales as short as 1 millisecond.

These criteria also have only a statistical, estimating character, because, for example, the type I X-ray bursts, a strong indicator of an accreting NS, were discovered from X-ray binary system Cir X-1, which, nonetheless, demonstrates rapid hard X-ray variability and bimodal spectral behavior. In addition, as noted above, even the presence of a hard component in the X-ray spectrum is not a unique indication of an accreting BH, because the hard tail expanding up to energy $\sim$ 150 keV was detected from soft X-ray transient, type I X-ray burster KS 1731−260, which is for sure an accreting NS.

Thus, none of the above X-ray signatures taken separately allows us to make a robust conclusion on the presence of a BH. However, combinations of some of these signatures could enable us to make more solid conclusions. In particular the hard X-ray power-law tail and bimodal X-ray spectral behavior have never been observed simultaneously from X-ray binaries containing reliably identified NSs. Table 7 presents spectral and temporal characteristics of some X-ray binaries with NSs and BHs (taken from papers [354, 270]).

As emphasized in Tanaka's review [343], when the X-ray luminosity L_x of an accreting relativistic object exceeds 10^{37} erg s^{-1}, there is a notable difference in form of the spectrum for NSs and BHs. At the same time, at luminosities below 10^{37} erg s^{-1} this difference disappears.

The X-ray spectrum of accreting NSs with luminosities above 10^{37} erg s^{-1} consists of two components: soft and hard. The soft component is the sum of local black-body radiations from an optically thick accretion disk (Shakura and Sunyaev [15]). This model is described by two parameters: r_{in} (the inner disk radius) and kT_{in} (the color temperature of X-ray

Table 7. X-ray emission characteristics of some X-ray binary systems with NSs and BHs (from [354, 270]).

Source name	Compact object type	Bimodal spectrum	Supersoft high state	Power-law tail	X-ray emission fluctuations on timescales $\leqslant 10$ ms	Binary system type
Cyg X-1	BH	x	x	x	x	HMXB
LMC X-3	BH		x	x		HMXB
LMC X-1	BH		x	x		HMXB
GS 2023 + 338	BH			x	x	X-ray nova
A0620 − 00	BH	x	x	x		X-ray nova
GS 2000 + 25	BH	x	x	x		X-ray nova
GX 339 − 4	BH	x	x	x	x	LMXB
Cir X-1	NS	x	x		x	X-ray burster
V0331 + 53	NS				x	X-ray pulsar

Note. HMXB — high-mass X-ray binary system, LMXM — low-mass X-ray binary system.

emission at the inner disk edge). The observed color temperature kT_{in} for an accreting NS is usually 1.4 – 1.5 keV at $L_{\text{x}} \sim 10^{38}$ erg s^{-1} and decreases with decreasing L_{x}. The hard component of an accreting NS spectra has a color temperature of $kT_{\text{c}} \sim 2.3-2.5$ keV and apparently corresponds to emission from the NS surface or an optically thick boundary layer on its surface (according to theory [341], this must be an extended boundary layer with two bright bands located at the same distance upward and downward from the NS equator, in which rapidly varying X-ray emission can be produced by different instabilities). The intensity of this black-body hard component varies irregularly by several times keeping the spectral form unchanged.

At $L_{\text{x}} > 10^{37}$ erg s^{-1}, accreting BHs exhibit, similar to NSs, a soft spectral component from the inner parts of an optically thick accretion disk (Shakura and Sunyaev [15]) with a color temperature of $kT_{\text{in}} \sim 1.2$ keV at $L_{\text{x}} \sim 10^{38}$ erg s^{-1} (much smaller than from an accreting NS with the same L_{x}). At the same time, the hard X-ray spectral component, which is characteristic for accreting NS surfaces at high $L_{\text{x}} > 10^{37}$ erg s^{-1}, is absent in the accreting BH spectra. Such a fundamental difference between spectra of most accreting NSs and BHs at high X-ray luminosities can be considered as a strong statistical indication of the absence of solid surfaces in BHs [343].

2. X-ray luminosities in X-ray novae in the quiescent state are on average $L_{\text{x}}^{\text{q}} \approx (10^{32} - 10^{33})$ erg s^{-1} for NS, and $L_{\text{x}}^{\text{q}} < (10^{31} - 10^{32})$ erg s^{-1} for BHs [286]. The relatively high 'quiescent' X-ray luminosity from BH binaries V404 Cyg (GS 2023+338) and GRO J1655−40 $L_{\text{x}}^{\text{q}} = (10^{32}–10^{33})$ erg s^{-1} [286, 266] seems to be due to the optical stars in these systems belonging not to the main sequence but being subgiants K0IV and F(3 – 6)IV, respectively, so the mass supply rate to the accretion disk here is higher.

Thus, the values of L_{x}^{q} for BHs are on average 1 – 2 orders of magnitude smaller than L_{x}^{q} for NS. Considering the X-ray emission contribution from coronas of X-ray nova companion stars [355, 356], the difference between L_{x}^{q} for NS and BHs becomes even larger. There is also a systematic difference in X-ray spectra of NSs and BHs in the X-ray nova quiescent state [266]: the spectra of some NSs in the quiescent state (Cen X-4, Aql X-1, etc.) in the 0.1 – 10 keV range show a very soft component ($kT \cong (0.13-0.30)$ keV) and a hard power-law tail with a photon index $\alpha = 1.9-2.3$, with the total luminosity of the hard X-ray component in the 0.5 – 10 keV range being comparable to that of the soft component. Some NS (for example, X 1608−522) have a very soft X-ray spectral component but insignificant hard tail (although the latter is not totally excluded). On the other hand, BHs in the quiescent state (for example, GS 2023+338 and GRO J1655−40) demonstrate a hard power-law tail ($\alpha = 0.7-1.7$) similar to systems with NSs (Cen X-4 and Aql X-1) but do not have the soft component.

The relatively low X-ray luminosity of accreting BHs in the quiescent state ($L_{\text{x}}^{\text{q}} < (10^{31} - 10^{32})$ erg s^{-1}) compared to NSs ($L_{\text{x}}^{\text{q}} = (10^{32} - 10^{33})$ erg s^{-1}) is in qualitative agreement with the advection-dominated accretion disk model [33 – 36], in which this difference in L_{x}^{q} for NSs and BHs is considered as the indication of the BH horizon. As was noted above, in the advection-dominated accretion disks the energy released in the disk by viscous dissipation is stored in hot ions which have no time to transfer energy to electrons and rapidly plunge under the event horizon. However, in this case there are significant quantitative inconsistencies which do not allow us to reliably judge the existence of the BH event horizon. The point is that the optical luminosity of the accretion disks of X-ray novae in the quiescent state is $L_{\text{opt}}^{\text{q}} = (10^{32} - 10^{33})$ erg s^{-1} [265], i.e., of the same order as the X-ray luminosity L_{x}^{q} of accreting NSs. Meantime, the optical luminosity is generated due to gravitational energy release at a distance of $r \cong 10^{10}$ cm from the central object while the X-rays come from the $r \cong 10^7$ cm radius (the light cylinder radius for a NS rotating with frequency ~ 500 Hz [357]). Since in the case of an accreting NS all the energy released by viscous dissipation is emitted from its surface or near the light cylinder (for a BH the thermal energy can rapidly disappear under the event horizon), the X-ray luminosity of an accreting NS in the quiescent state must be $L_{\text{x}}^{\text{q}} = (10^{35} - 10^{36})$ erg s^{-1}, which is not observed. Although magnetic fields of old accreting NSs in X-ray novae are relatively weak, at a high axial rotation frequency (~ 1 kHz) even with the field $\sim 10^8$ G, the magnetospheric propeller effect could be important [357].

So, although the observed differences in values L_{x}^{q} for an accreting NS and BH are in qualitative agreement with a BH having no observed solid surfaces, the above quantitative disagreement does not allow us to make robust conclusions on the BH event horizon. In particular, it may be possible that the low BH luminosity in the quiescent state is related to the presence of a storage gas disk with laminar motion, when the viscosity is small and no accretion occurs [358]. To explain accreting BH X-ray luminosities in the quiescent state, a hypothesis of internal magnetic moment in a rotating BH is involved [357]. In order to understand the reasons for the qualitative disagreements, detailed studies of both X-ray luminosities L_{x}^{q} and spectra, as well as of variability of X-ray novae in the quiescent state on different timescales are needed (see, for example, Refs [344, 359 – 361]).

For example, a broad spectrum of quasiperiodic oscillations (QPO) in X-ray variability is observed in BH binary system GRS 1915+105 [362, 316]. In particular, of special interest are QPO with a maximal relatively stable frequency of 67 Hz, which have been observed many times irrespective of the X-ray luminosity in this system [362]. There are grounds to believe that this maximal QPO frequency 67 Hz is a function of the fundamental accreting BH parameters, mainly its mass and angular momentum. This frequency may be related to the last marginally stable orbit of individual plasma blobs in the vicinity of the BH. The QPO frequency in GRO J1655−40 is 300 Hz [363]. Note that the orbital motion of hot spots near an accreting BH and the corresponding X-ray variability was first considered in a paper by Sunyaev in 1972 [144]. It was shown in this paper that the presence of hot spots on the inner disk surface could result in a specific quasi-periodic X-ray variability from the accretion disk. These hot spots could originate from the magnetic field line reconnection or turbulence. The lifetime of the spot and the characteristic time of its radial motion to the central BH can be significantly larger than the spot's orbital period. This leads to relative stability of the observed pulsations. As noted by Sunyaev [144], the minimal quasi-period of the X-ray pulsations from the inner parts of the accretion disk with hot spots in the case of a Kerr BH is 8 times smaller than for a non-rotating Schwarzschild BH of the same mass. The paper [144] stresses that observations of rapid quasi-periodic X-ray pulsations with periods $\sim 10^{-4} - 10^{-2}$ s would allow one to establish the nature of fluctuating X-ray sources, to find the BHs among them, and even to distinguish Kerr BHs from Schwarzschild ones.

The 67 Hz frequency can also be connected with seismic oscillations of an accretion disk in GR [364] or with a relativistic inertial frame dragging near the rapidly rotating BH [365].

In recent years, the problem of magnetic field existence near a rotating charged BH has been actively discussed (see, for example, Ruffini [366 – 368], and also [369 – 372] and Punsly's review [373]). In this setup, relativistic collimated jets can be formed that emit up to 80% of energy in the gamma-range (for a solitary BH). The synchrotron radiation in the relativistic jet gives rise to a weak radio and optical emission, and part of the synchrotron radiation is converted to gamma-rays by inverse Compton scattering on hot plasma. According to [373] (see also [157]), relativistic frame dragging near the event horizon of a rotating BH leading to the space-time rotation (inside the BH ergosphere, between the event horizon and the static limit) creates disbalanced, rotationally excited electromagnetic forces inducing charge separation. At the asymptotic infinity, the magnetic field is homogeneous and the BH electric field vanishes. However, near the rotating BH there are both the magnetic field and a significant non-zero electric field created by the space-time dragging effect. Since the Kerr – Newman electromagnetic field is always co-axial with the BH rotation, a rotating charged BH can not manifest itself as a pulsar. If such a single BH rapidly rotates, it constantly forms a relativistic jet along its rotational axis that emits (directionally) 80% of energy in γ-rays and less than 20% of energy at other wavelengths (radio, optical, etc.). If the BH angular momentum is small or the system of electric and magnetic fields of the rotating BH is destroyed by a strong accretion, the electric discharge of the BH occurs over a timescale of less than 1 second. According to [373], such a BH discharge could explain some γ-ray bursts. The application of the model of a rotating BH with an internal magnetic moment to low-mass X-ray binaries provides the explanation to the observed X-ray luminosity of the power-law component in the quiescent state [357]. This model assumes that the X-ray power-law component in the quiescent state is caused by energy losses by a rotating magnetized BH due to the interaction of the BH magnetic dipole (whose axis coincides with the BH spin) with the accretion disk inner edge. As shown in Ref. [291], in BH X-ray novae there is a good correlation between the maximal X-ray luminosity and the corresponding radio flux density. For X-ray novae with NS such a correlation is only marginally observed. The authors of Ref. [291] conclude that this is indicative of the relativistic jet formation during X-ray outburst. The jet luminosity is a function of the accretion rate onto the relativistic object, but its connection to the observed X-ray luminosity at maximum depends on the nature of the accreting relativistic star (NS or BH).

Observational facts on BH rotation in X-ray binaries based, in particular, on the analysis of the quasi-blackbody component of the accreting disk X-ray luminosity, are given in papers [374, 303]. Accretion disks corotating with a spinning BH penetrate much closer to the BH than for Schwarzschild BHs since the radius of the last marginally stable orbit for a rotating BH is smaller than for a non-rotating one. So the luminosity and temperature of the thermal X-ray component from rotating accreting BH must be higher. This is observed for two transient BH X-ray binaries — microquasars GRS 1915+105 and GRO J1655−40, which most probably contain a rapidly rotating BHs [303, 374]. At the same time, according to [374], most BHs in X-ray novae are non-rotating. Information on BH rotation and on space-time near the horizon can be obtained from analysis of high-frequency X-ray QPOs (see, for example, Refs [144, 375]). A review of the future space missions aimed at solving this important problem can be found in Ref. [376].

11. Mass distribution of relativistic objects, Wolf – Rayet (WR) stars and their CO-cores in binary systems

To date, 23 mass measurements have been made for WR stars in binary WR+O systems (see [377] and references therein). The WR masses lie within a wide range from $5M_\odot$ to $55.3M_\odot$. The WR mass distribution is continuous. At the same time, today masses of 34 relativistic objects are measured in binary systems, including 15 BHs and 19 NSs. Since the WR stars are deprived of their hydrogen envelopes, they are immediate precursors of relativistic objects. It appears interesting to compare the relativistic object mass distribution with that of WR stars and their CO-cores at final evolutionary stages [378].

11.1 Relativistic objects

As seen from Fig. 27, mass distribution of relativistic objects in binary systems is bimodal [379, 380]. Masses of 19 neutron stars lie within narrow limits $m_{\rm NS} = (1-2)M_\odot$ with the mean NS mass $\overline{m}_{\rm NS} = (1.35 \pm 0.15)M_\odot$, The mean mass of radio pulsars in binary systems is $(1.35 \pm 0.04)M_\odot$ [327] with no marked difference between radio pulsars formed from WR stars or from accretion-induced collapse of white dwarfs in binary systems. A relatively high NS mass value was recently confirmed in Ref. [381] by new observations of high-mass binary system Vela X-1, $m_x = (1.86 \pm 0.16)M_\odot$, which is of great importance to establish a NS equation of state. However, even this highest value of the NS mass lies below $2M_\odot$.

The measured masses of 15 BHs fall within the range $(\sim 4-16)M_\odot$. The mean BH mass derived from observations $\overline{m}_{BH} = 8.8M_\odot$. Then the mean BH mass should lie within $(8-10)M_\odot$. No NSs or BHs have been found within the mass range $m_x = (2-4)M_\odot$. This gap in the relativistic object mass distribution can not be due to observational selection effects [377–379].

Let us consider possible reasons for observational selection. First of all, let us consider the possibility of a binary system disruption during a supernova explosion and the relativistic object formation [377]. The smaller the relativistic object mass, the larger is the ejected envelope mass. Most BHs are discovered in X-ray novae with low-mass optical companions. During the formation of a low-mass relativistic object the presupernova envelope mass ejected during the explosion can exceed half a total binary system mass and hence lead to system disruption.

In this case the $m_x = (2-4)M_\odot$ gap in the relativistic mass distribution could be due to lack of close binary systems in this mass range because of their disruption, however the actual distribution of m_x is continuous, including the mass range $m_x = (2-4)M_\odot$ (we recall that all values of m_x in Table 5 were determined from the optical star motion in close binary systems). But then, since the probability of disruption increases as the relativistic object mass decreases, the minimal number of surviving binaries must be among systems with less massive relativistic objects, i.e., with NSs, which contradicts observations. There are a lot of low-mass X-ray binaries with NSs, with the fraction of NS binaries among X-ray binaries being as high as 30%. So the effect of observational selection due to binary system disruption is unimportant.

Another effect of observational selection in studying relativistic object mass distribution was noted by Charles [321]: for low m_x, the illumination of the accretion disk matter by X-ray emission from the central source prevents transient behavior from appearing, so the low-mass X-ray binary is in the permanent high state. This makes it impossible to observe the optical star absorption lines in its spectrum and measure the corresponding mass function. So it may turn out that the real m_x distribution is continuous, but in the mass range $m_x = (2-4)M_\odot$ all low-mass X-ray binaries are in the high state with bright accretion disks, which prevents the optical mass function from being measured. But in that case such an effect would be strongest for accreting NSs with small masses and solid surfaces and which hence could strongly illuminate the accretion disk. Meantime, as noted above, the fraction of low-mass X-ray binaries with NSs among X-ray novae is quite large, $\sim 30\%$, and in one case, V822 Cen, the optical mass function is measured: $f_v(m) = (0.20 \pm 0.05)M_\odot$. So observations indicate that the accretion disk heating even by an accreting NS can not always totally stabilize the disk and prevent the X-ray nova transient phenomenon from occurring. Therefore the observational selection effect noted by Charles [321] seems to be unimportant, too.

One more observational selection effect was considered by Wijers [382] in connection with the problem of the existence of low-mass BHs ($m_x \leqslant 2M_\odot$). If the collapsing iron core of a massive star has a somewhat smaller mass than the maximum NS mass, the bounce of the collapsing presupernova envelope and the shock wave formed result in a supernova explosion and NS formation. Once the NS matter cools down by neutrino cooling, the pressure decreases, the proto-NS mass becomes larger than the upper mass limit for a cold NS and it collapses to a BH [383, 384]. The fall-back of some matter from the envelope also stimulates the NS collapse and the formation of a relatively low-mass BH. In this connection, we note that Brandt et al. [330] explained the high peculiar velocity of the barycenter of X-ray nova GRO J1655−40 (-114 km s^{-1}) by the two-stage massive core collapse. Brown and Bethe [384] predicted that stars with initial masses $(18-30)M_\odot$ must create low-mass BHs with masses $m_x \leqslant 2M_\odot$. They assumed a soft equation of state of the NS matter where the maximal NS mass is $\sim 1.5M_\odot$. In that case $\sim 5 \times 10^8$ low-mass BHs should exist in the Galaxy, about as many as massive BHs. So why have low-mass BHs escaped detection in X-ray binary systems so far?

As was noted by Brown et al. [385], a very strong stellar wind mass loss from the naked helium core (WR star) of an initially massive star in a close binary system makes low-mass BH formation less likely than in the case of a single massive star with a thick hydrogen envelope. The WR star resulting from mass exchange in a close binary system loses most of its mass via intensive stellar wind before the iron core forms, and the final iron core mass becomes significantly smaller compared to a single star of the same initial mass [386, 387]. So in CBS, according to Wijers, only NSs with $m_x \leqslant 1.5M_\odot$ must form and BHs with $1.5 \leqslant m_x \leqslant 2M_\odot$ are not born.

However, considering new observational results on the patchy structure of WR winds (see below), we have to decrease WR stellar wind mass loss by at least 2–4 times [388–391]. So, as noted in Refs [380, 377, 53], for WR stars the stellar wind mass loss is not as effective as was thought earlier. Low-mass BHs, if they exist, must form with almost equal probability both from single stars and in close binary systems. The observational selection effect noted by Wijers and connected with the stellar wind mass loss of WR stars appears insignificant. But then the question arises: Why do we not observe low-mass BHs in X-ray binary systems? Wijers [382] proposed two X-ray binaries that could have low-mass BHs: 4U 1700−37 [a massive X-ray binary with a non-pulsating compact source of mass $(\sim 1.5-1.8)M_\odot$], and GRO J0422+32 (a low-mass X-ray binary with a transient X-ray source — a BH of presumably low mass $m_x \leqslant 2.5M_\odot$). The recent new orbit inclination i estimate for GRO J0422+32 derived from an IR ellipsoidal light curve suggested a large BH mass in this system $m_x > 9M_\odot$ [392]. On the other hand, the X-ray spectrum and spectral behavior in 4U 1700−37 do not significantly differ from the corresponding characteristics of typical X-ray pulsars in massive X-ray binaries [393, 394]. So we have no grounds to consider the non-pulsating source in 4U 1700−37 as a real low-mass BH. All these facts suggest that apparently low-mass BHs either do not exist, or their relative number is small, and the $m_x = (2-4)M_\odot$ gap in the mass distribution of NSs and BHs is real.

One more observational selection effect is connected with the additional accretion-induced relativistic object mass growth in a close binary system. This would lead to a systematic difference between NS and BH mass distribution in binary systems and single relativistic object masses. As noted in Refs [53, 395], accretion of matter in binary systems can not significantly change the relativistic object mass. It is well known that spin periods of millisecond pulsars in binary systems shorten systematically due to accumulation of angular momentum of accreting matter (see, for example, Ref. [396]). Accretion increases the millisecond pulsar masses, but insignificantly (by $\sim 0.2M_{\odot}$) compared to the initial NS mass at birth [397]. Observations demonstrate that there is no marked difference between the masses of millisecond radio pulsars and comparatively long-period X-ray pulsars, in accordance with theoretical predictions. Most optical companions to known BHs in X-ray binaries are dwarf stars of late spectral classes A – M close to the main sequence. These stars could have lost only a small fraction of their masses during mass transfer, so the BH masses in these systems are approximately the same as at birth. Three X-ray novae have subgiant and giant stars as the companions: V404 Cyg (K0IV), XN Sco 1994 (F5IV), and SAX J1819.3$-$2525 = V4641 Sgr (B9III). The BH masses in these systems might be expected to increase by accretion from the companions. However, considering induced stellar wind due to X-ray illumination from the accreting relativistic objects during X-ray outbursts, more than 90% of the companion's matter leaves the system and only $\leqslant 10\%$ is transferred onto the accreting BH [398 – 400]. So in these cases, too, we have to state an insignificant BH mass increase during the accretion.

In massive X-ray binaries (Cyg X-1, LMC X-1, LMC X-3) the timescale of mass exchange is very short ($\sim 10^4 - 10^5$ years), so the accretion-induced BH mass increase in these systems is also small. So we can conclude [395, 53] that large BH masses in close binary systems can not be explained by accretion-induced mass growth during mass exchange. In most cases, the BH masses must have been initially large (on average, $\sim (8-10)M_{\odot}$). So the gap in the BH and NS mass distribution at $(2-4)M_{\odot}$ can not be explained by effects connected with mass exchange and accretion in close binary systems.

Thus it proves difficult to invent some observational selection mechanism that would depend in such a non-monotonous way on the relativistic object mass m_{x} to provide the observed gap in the m_{x} distribution at $(2-4)M_{\odot}$. We have all grounds to consider this gap as real: for some reason, very massive ($m_{\mathrm{x}} > 2M_{\odot}$) NSs and low-massive BHs ($m_{\mathrm{x}} < 4M_{\odot}$) are not born in binary systems. Taking into account all of the above, the same conclusion can be related to single relativistic objects, too. In this connection, it appears intriguing to compare the observed bimodal relativistic object mass distribution with that of WR stars and their carbon-oxygen cores at the end of evolution $M_{\mathrm{CO}}^{\mathrm{f}}$, which are progenitors of NSs and BHs in binary systems.

11.2 Wolf – Rayet stars and their CO-cores at the end of evolution

According to modern concepts (see, for example, Ref. [377]), Wolf – Rayet stars (WR) of the stellar population I are naked helium cores of originally massive stars that lost most of their hydrogen envelopes either during mass exchange in binary systems [401], or by intensive stellar wind from solitary massive stars [402, 403]. WR stars are massive, hot, non-degenerate, mainly helium stars at late evolutionary stages and should explode as supernovae of type Ib or Ic. Relativistic objects should result from the collapse of their CO-cores.

Not only WR stars can be progenitors of relativistic objects, but other massive stars can be too, for example, red and blue supergiants with normal surface chemical composition. In particular, supernova SN 1987A in the Large Magellanic Cloud is related to the core collapse of a B3I supergiant star [404]. However, as we are interested in relativistic object masses only in binary systems, the comparison of the NS and BH masses is correct, since a massive star in a binary system always rapidly loses its hydrogen envelope and forms a WR star. In most evolutionary scenarios for close binary systems with a massive star, the latter always ultimately creates a WR star, which later explodes as a supernova and forms a NS or a BH (see, for example, Refs [405 – 407, 398, 399, 408 – 412, 396]). Only for radio pulsars in binary systems on circular orbits with massive white dwarf companions is the accretion-induced white dwarf collapse considered to be a possible mechanism of NS formation without the WR star stage [396].

Thus, modern data suggest that all NSs and BHs in X-ray binary systems (both massive and low-massive) and most radio pulsars in binary systems result from the collapse of the CO-cores of WR stars. The newest observational data (the enhanced abundance of heavy elements produced by α-capture found in the optical star spectra in X-ray binaries GRO J1655$-$40 (XN Sco 1994) and SAX J1819.3$-$2525, the large peculiar velocity in GRO J1655$-$40 and XTE J1118+480, as well as the high altitude over the Galactic plane for XTE J1118 + 480) make a strong case that at least for some WR stars in binary systems, the CO-core collapse is accompanied by supernova explosion (apparently of type Ib or Ic).

For comparison of relativistic object masses with WR star masses it is necessary to take into account intensive stellar wind mass losses from these stars (the mass loss estimate is $\dot{M} \cong 10^{-5} M_{\odot}\ \mathrm{yr}^{-1}$). Langer [413] was the first to consider stellar wind mass loss in WR stars depending on their masses. He derived the formula connecting $\dot{M}_{\mathrm{WR}}$ and M_{WR}:

$$\dot{M}_{\mathrm{WR}} = -(0.6-1.0) \times 10^{-7} \left(\frac{M_{\mathrm{WR}}}{M_{\odot}}\right)^{2.5},$$

where the coefficient 0.6 corresponds to WNE stars (WR stars of nitrogen sequence of early subclasses), and the coefficient 1.0 corresponds to WC and WO stars (WR stars of carbon and oxygen sequences). The use of this formula leads to the so-called convergence effect: virtually irrespective of the original mass of the WR star, the mass of the star and its carbon-oxygen core at the end of evolution does not exceed several solar masses [$\sim (2-4)M_{\odot}$]. But then how can one understand the existence of BHs with masses $(10-15)M_{\odot}$? Yet this is a reliable observational fact (see Table 5). Final masses of WR stars and their CO-cores were calculated in paper [377] accounting for the patchy structure of the WR stellar winds, which enables the value of $\dot{M}_{\mathrm{WR}}$ to be decreased several-fold. In that paper the empirical relation

$$\dot{M}_{\mathrm{WR}} = k M_{\mathrm{WR}}^{\alpha},$$

was utilized which was obtained from the analysis of polarization observations of about ten WR+O binary systems (papers by Moffat's group [414]). In the above formula, $\alpha = 1-2$, with $\alpha = 1$ being preferable [414].

The patchy structure of WR winds is established in papers [388, 415]. As noted in Refs [416, 389], the quadratic dependence of the intensity of thermal radio and infrared emission of WR stars on density implies that values of $\dot{M}$ derived from analysis of radio and infrared observations of WR stars (and this is the main source of data about $\dot{M}_{\mathrm{WR}}$) are

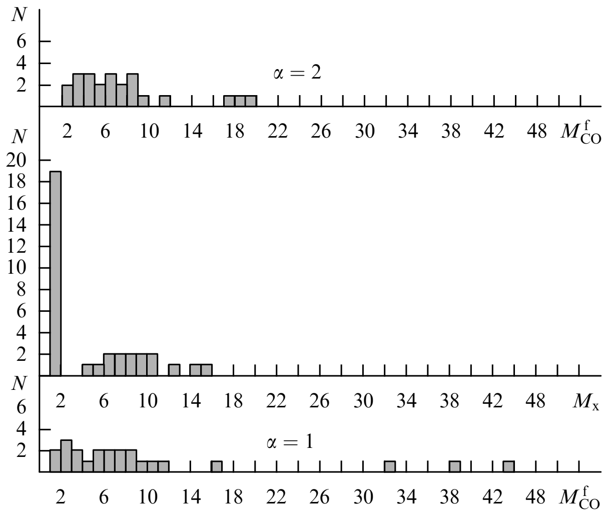

Figure 30. Histograms of distributions of the final masses of carbon-oxygen cores M_{CO}^f for 23 WR stars with known masses (the bottom plot corresponds to the case $\alpha = 1$ in $\dot{M}_{WR} = kM_{WR}^{\alpha}$, the upper plot to the case $\alpha = 2$). In the middle, the histogram of the M_x mass distribution for 34 relativistic objects in binary systems is shown. (Masses M_{CO}^f and M_x are in solar units $M_\odot$). The high peak at $(1-2)M_\odot$ corresponds to a NS. The distributions of M_{CO}^f are continuous, while the distribution for M_x is bimodal with a gap at $M_x = (2-4)M_\odot$ (from Refs [377, 378]).

overestimated by several times. The account for the patchy structure of the WR winds decreases $\dot{M}_{WR}$ by several times and thus allows us to avoid the known convergence effect in calculating final WR and their CO-core masses.

The results of calculations of the final CO-core masses of WR stars with known masses are summarized in Fig. 30, where mass distribution of 34 relativistic objects and of final CO-core masses for 23 WR stars are shown (for cases $\alpha = 1$ and $\alpha = 2$). It is seen that the patchy structure of the WR winds leads to a continuous distribution of the CO-core masses M_{CO}^f from $(1-2)$ to $(20-44)M_\odot$. The distribution of masses M_{CO}^f is continuous, unlike the relativistic object mass distribution. The mean mass is $\overline{M}_{CO}^f = 10.3M_\odot$ for $\alpha = 1$ and $\overline{M}_{CO}^f = 7.4M_\odot$ for $\alpha = 2$ and is close to the mean BH mass $\overline{M}_{BH} = (8-10)M_\odot$.

Thus (see Fig. 30), the relativistic object mass distribution is bimodal in spite of its progenitors' masses (CO-core of WR stars in the end of evolution) being continuous. Recently, observations suggested that type Ibc supernovae, which are associated with the collapses of CO-cores of WR stars, also show bimodal distribution of the luminosity at the maximum [417]. The difference in the mass distributions implies that the nature of the relativistic object formed (NS, BH) is determined not only by the progenitor's mass, but also by other parameters of the progenitor, such as magnetic field, rotation, statistical result of the collapse, etc. [411, 418–420]. Rotational effects for some WR stars were recently measured using depolarization of the radiation in emission lines (see, for example, Ref. [421]). The fraction of rapidly rotating WR stars is $\sim (15-20)\%$ [421]. Further theoretical studies of the difference discovered by us in the mass distribution of relativistic objects and their immediate progenitors, CO cores of WR stars, are of great interest for stellar evolution theory. For example, in Ref. [422] a qualitative conclusion is made that the gap in the mass distribution of BHs and NSs can be explained assuming a soft equation of state for NS matter and the magneto-rotational mechanism for a supernova explosion (like the scenario described in Ref. [420]), which under some conditions prevents the matter fall-back from the presupernova envelope onto a rapidly rotating strongly magnetized NS formed during the collapse. Another possibility to obtain the gap at $(2-4)M_\odot$ in the relativistic object mass distribution is by postulating a step function for the supernova explosion energy dependence on the progenitor's mass [423]: $E_{exp} = 2.5 \times 10^{51}$ erg for $M_{prog} < 23M_\odot$ and $E_{exp} = 0$ for $M_{prog} > 23M_\odot$. The formation routes of BHs in massive core collapses are described, for example, in Ref. [424].

Paper [425] puts forward the hypothesis that the core collapses of WR stars can be progenitors of γ-ray bursts, since, in particular, the large dispersion in the final CO-core masses of WR stars and the bimodal relativistic object mass distribution are consistent with the observed large energy difference of γ-ray bursts with known redshifts and their possible bimodal distribution. WR stars have no thick hydrogen envelopes, which facilitates the core collapse energy transformation to the observed γ-ray emission [426].

12. Conclusions

We described the modern state of the problem of searching for both supermassive BHs in galactic nuclei and stellar-mass BHs. We did not consider the problem of searching for primordial BHs and intermediate-mass BHs $[m_x = (10^2-10^4)M_\odot]$ because of the paucity of observational data and ambiguity in their interpretation. The interested reader can find more information on these problems in reviews [4, 56]. We also did not mention the very reassuring results on searches for single stellar-mass BHs $(m_x \cong 6M_\odot)$ using gravitational microlensing (see papers by Bennett et al. [63], Mao et al. [64]), as well as on searches for BHs in globular clusters [62, 427, 428], in the centers of which (for example, in M15) one may expect to find an intermediate-mass BH with $\sim 2500M_\odot$ [62]. It should be noted that for the first time the problem of systematic searching for a single BH accreting matter from the interstellar medium was set by Shwartzman [143, 429]. It is important that today the problem of BH searches stays on a solid observational basis, and now we have many (about 100) reliable BH candidates with measured masses and size constraints. We specially emphasize that observations suggest that all the necessary conditions for the observational appearance of BHs imposed by Einstein's GR are met. This strongly strengthens our certitude in the real existence of BHs in the Universe.

The main problem to solve in the next decade is to find sufficient conditions to prove the discovered BH candidates are real BHs. Let us briefly enumerate possible experiments that can solve this principal problem.

1. The use of space interferometers with an angular resolution up to 10^{-7} arcseconds (for example, an X-ray interferometer [115]) and direct observations of processes near the event horizon in the nucleus of our and nearby galaxies.

2. Searches for and studies of gravitational wave bursts produced by the coalescence of binary BHs using the new generation of laser gravitational wave interferometers (LIGO, LISA, etc.) — see the review by Grishchuk et al. [430] and the recent paper by Hages [431].

3. Detection of radio pulsars in binary systems with BH (about 1 such a pulsar paired with a BH is expected in

~ 1000 single radio pulsars; now about 1500 radio pulsars are known).

4. Detailed studies of spectra, intensity, polarization, and variability of X-ray and γ-ray emission from accreting BHs by new generation orbital observatories [432–434, 361].

5. Observations and interpretation of gravitational microlensing of galactic nuclei by stars of intervening galaxies — gravitational lenses. The angular resolution in this method can reach 10^{-6} arcseconds [435], which will enable studies of the nearby structure around BHs in galactic nuclei.

6. Routine accumulation of data on BH and NS masses, and statistical comparison of observational appearances of accreting BHs and NSs.

The author acknowledges B V Komberg and N G Bochkarev for attentively reading the manuscript and for their valuable notes, as well as Yu N Gnedin for discussions.

The work was supported by the Russian Fund for Basic Research under grant No. 00-15-96553.

Notes added in proof

In the paper by R Schödel et al. [436], the orbit of the S2 star around the supermassive BH in the center of our Galaxy is constructed. The orbital period of the S2 star is 15.2 years, the orbital eccentricity is 0.87, the major semi-axis of the orbit is 4.62×10^{-3} pc, and the mass of the BH is $(3.7 \pm 1) \times 10^6 M_\odot$. The density of dark matter inside the measured volume attains $10^{17} M_\odot$ pc^{-3}, and the characteristic dynamical decay time of a putative cluster of individual dark bodies in the Galactic center is $\sim 10^5$ years, which strengthens the conclusion that the massive compact object in the Galactic nucleus is a single body, most probably a black hole. These observations definitely refute the model of the degenerate fermion ball for the Galactic nucleus. C Tandhunter et al. [437] measured by the dynamical method the mass of the supermassive BH in the nucleus of active galaxy Cyg A: $m_x = (2.5 \pm 0.7) \times 10^9 M_\odot$. This value of the BH mass is consistent with general properties of the Cyg A galaxy in spite of its extremely strong radio luminosity.

R J McLure and M J Jarvis [438] proposed a method for estimation of supermassive BH masses in quasar nuclei based on using the quasar luminosity near 3000 Å in the comoving frame, which allows BH mass estimations in quasars with high redshifts $0.25 < z < 2.5$ using only optical observations. From rapid X-ray variability of two Seyfert I nuclei Ark 564 and Tons 180 ($\Delta t \approx 1000$ s, variability by two times), R Edelson et al. [439] derived the upper limit on the supermassive BH radii $r \leqslant 15 r_g$.

From the similarity of variability spectra of Cyg X-1 and the nucleus of dwarf galaxy NGC 4395, D C Shin et al. [440] estimated this dwarf galaxy nucleus mass to be $(10^4 - 10^5) M_\odot$, which falls within the intermediate BH mass range. A Fillipenko et al. [441] evaluated the BH mass in a bulgeless Seyfert I galaxy $(10^4 - 10^5) M_\odot$. A review on the intermediate mass BHs both in galaxies and globular clusters has been published by R P van der Marel [442].

G X Xie et al. [443] assumed that the photometric variability of quasar PKS 1510−089 has a period of 336 days and possibly the nucleus of this quasar contains a binary supermassive BH with masses of the components $10^8 M_\odot$ and $10^{6.2} M_\odot$ and the relative orbit radius in 378 gravitational radii of the primary BH; the lifetime of the system is about $\sim 10^6$ years. Using the dynamical method, E K Velorme et al. [444] obtained the mass of the nucleus of the M32 galaxy: $M_x = (2.5 \pm 0.5) \times 10^6 M_\odot$. Long-term X-ray observations by XMM of the Seyfert nucleus MCG-6-30-15 [445] confirmed the presence of the broad iron emission line component and the conclusion that the inner edge of the accretion disc is located near $2 r_g$ from the central BH. This indicates that the supermassive BH in this galaxy is rotating.

Q Yu and S Tremaine [446] considered models of supermassive BH growth and corresponding observational constraints. X-B Wu et al. [447] estimated masses of supermassive BHs in active galactic nuclei (63 BL Lac objects, 10 radio galaxies, 19 quasars) from galactic morphology; the masses were found to fall within the range $(10^{7.5} - 10^9) M_\odot$.

D G Gies et al. [448] discovered absorption lines of the optical star in the optical spectrum of SS 433 and measured its mass function. Masses of the optical A7 Ib star and the BH were found to be $m_v = (19 \pm 7) M_\odot$ and $m_x = (11 \pm 5) M_\odot$, respectively. J A Orosz et al. [449] obtained the following dynamical estimates of the component masses and parameters of the X-ray nova — microquasar XTE J1550−564: the orbital period $p = 1^d.552 \pm 0^d.010$, the mass function of the optical K3III star $f_v(m) = (6.86 \pm 0.71) M_\odot$, the mass ration $q = m_x / m_v = 6.6$ (+2.5; −1.6; 67% confidence level), and the BH mass $9.68 M_\odot \leqslant m_x \leqslant 11.58 M_\odot$. A V Fillipenko and R Chornock [450] determined the following parameters of X-ray nova XTE J1859+226: the orbital period $p = 0^d.382(3)$, $f_v(m) = (7.4 \pm 1.1) M_\odot$, and the BH mass $m_x = (7.6 - 12.0) M_\odot$.

M R Garcia et al. [451] noted that among 14 X-ray binary systems, X-ray novae with measured BH masses, four systems exhibit sufficiently elongated relativistic jets, and all four systems have long orbital periods. Apparently, there are some as yet unknown processes which favor the formation of elongated relativistic jets in long-period X-ray binaries. M B Bogdanov and A M Cherepashchuk [452] calculated observational effects of gravitational microlensing of stars by a space-time tunnel.

References

1. Wheeler J A *Am. Sci.* **56** 1 (1968)
2. Ginzburg V L *O Fizike i Astrofizike* (On Physics and Astrophysics) 3rd ed. (Moscow: Byuro Kvantum, 1995) p. 111 [Translated into English: *The Physics of a Lifetime*: *Reflections of the Problems and Personalities of 20th Century Physics* (Berlin: Springer-Verlag, 2001) p. 103]
3. Ginzburg V L *Usp. Fiz. Nauk* **169** 419 (1999) [*Phys. Usp.* **42** 353 (1999)]
4. Novikov I D, Frolov V P *Usp. Fiz. Nauk* **171** 307 (2001) [*Phys. Usp.* **44** 291 (2001)]
5. Novikov I D, Frolov V P *Fizika Chernykh Dyr* (Physics of Black Holes) (Moscow: Nauka, 1986) p. 88 [Translated into English (Dordrecht: Kluwer Acad., 1989)]
6. Shapiro S L, Teukolsky S A *Black Holes, White Dwarfs, and Neutron Stars*: *the Physics of Compact Objects* (New York: Wiley, 1983) [Translated into Russian: Vol. 2 (Moscow: Mir, 1985) p. 357]
7. Zel'dovich Ya B, Novikov I D *Relyativistskaya Astrofizika* (Relativistic Astrophysics) (Moscow: Nauka, 1967) p. 286 [Translated into English (Chicago: Univ. of Chicago Press, 1971)]
8. Thorne K S, Price R H, Macdonald D A (Eds) *Black Holes*: *The Membrane Paradigm* (New Haven: Yale Univ. Press, 1986)
9. Zel'dovich Ya B *Dokl. Akad. Nauk SSSR* **155** 67 (1964) [*Sov. Phys. Dokl.* **9** 195 (1964)]
10. Salpeter E E *Astrophys. J.* **140** 796 (1964)
11. Novikov I D, Zeldovich Ya B *Nuovo Cimento Suppl.* **4** 810 (1966)
12. Zeldovich Ya B, Guseynov O H *Astrophys. J.* **144** 840 (1966)
13. Trimble V L, Thorne K S *Astrophys. J.* **156** 1013 (1969)
14. Shakura N I *Astron. Zh.* **49** 921 (1972) [*Sov. Astron.* **16** 756 (1973)]
15. Shakura N I, Sunyaev R A *Astron. Astrophys.* **24** 337 (1973)
16. Pringle J E, Rees M J *Astron. Astrophys.* **21** 1 (1972)

17. Novikov I D, Thorne K S, in *Black Holes* (Eds C DeWitt, B S DeWitt) (New York: Gordon and Breach, 1973) p. 343
18. Forman W C et al. *Astrophys. J. Suppl.* **38** 357 (1978)
19. Webster N L, Murdin P *Nature* **235** 37 (1972)
20. Cherepashchuk A M et al. *Inform. Bull. Var. Stars* (720) 1 (1972)
21. Bahcall J N, Bahcall N A *Astrophys. J.* **178** L1 (1972)
22. Lyutyĭ V M, Syunyaev R A, Cherepashchuk A M *Astron. Zh.* **50** 3 (1973) [*Sov. Astron.* **17** 1 (1973)]
23. Lyutyĭ V M, Syunyaev R A, Cherepashchuk A M *Astron. Zh.* **51** 1150 (1974) [*Sov. Astron.* **18** 684 (1975)]
24. Goncharskiĭ A V, Romanov S Yu, Cherepashchuk A M *Konechno-parametricheskie Obratnye Zadachi Astrofiziki* (Finite-parametric Inverse Problems in Astrophysics) (Moscow: Izd. MGU, 1991) p. 99
25. Bisikalo D V et al. *Astron. Zh.* **74** 880 (1997) [*Astron. Rep.* **41** 786 (1997)]
26. Bisikalo D V et al. *Astron. Zh.* **74** 889 (1997) [*Astron. Rep.* **41** 794 (1997)]
27. Bisikalo D V et al. *Mon. Not. R. Astron. Soc.* **300** 39 (1998)
28. Bisikalo D V et al. *Astron. Zh.* **75** 40 (1998) [*Astron. Rep.* **42** 33 (1998)]
29. Khruzina T S et al. *Astron. Zh.* **78** 625 (2001) [*Astron. Rep.* **45** 538 (2001)]
30. Molteni D et al. *Mon. Not. R. Astron. Soc.* **327** 1103 (2001)
31. Rees M J, in *The Galactic Center* (AIP Conf. Proc., Vol. 83, Eds G R Riegler, R D Blandford) (New York: American Institute of Physics, 1982) p. 166
32. Begelman M C *Nature* **322** 614 (1986)
33. Abramowicz M A et al. *Astrophys. J.* **332** 646 (1988)
34. Narayan R, Yi I *Astrophys. J.* **452** 710 (1995)
35. Narayan R *Astrophys. J.* **462** 136 (1996)
36. Narayan R, McClintock J E, Yi I *Astrophys. J.* **457** 821 (1996)
37. Bisnovatyi-Kogan G S, Lovelace R V E *Astrophys. J.* **486** L43 (1997)
38. Blandford R D, Begelman M C *Mon. Not. R. Astron. Soc.* **303** L1 (1999)
39. Bisnovatyi-Kogan G S, Lovelace R V E *New Astron. Rev.* **45** 663 (2001)
40. Merloni A, Fabian A C *Mon. Not. R. Astron. Soc.* **332** 165 (2002)
41. Zel'dovich Ya B, Novikov I D *Dokl. Akad. Nauk SSSR* **158** 811 (1964)
42. Lynden-Bell D *Nature* **223** 690 (1969)
43. Rees M J *Annu. Rev. Astron. Astrophys.* **22** 471 (1984)
44. Dibaĭ E A *Astron. Zh.* **57** 677 (1980) [*Sov. Astron.* **24** 389 (1980)]
45. Blandford R D, Rees M J, in *Testing the AGN Paradigm*: *Proc. of the 2nd Annual Topical Astrophysics Conf., College Park, MD, Oct. 14–16, 1991* (AIP Conf. Proc., Vol. 254, Eds S S Holt, S G Neff, C M Urry) (New York: American Institute of Physics, 1992) p. 3
46. Chakrabarti S K (Ed.) *Observational Evidence for Black Holes in the Universe* (Astrophys. and Space Sci. Library, Vol. 234) (Dordrecht: Kluwer Acad. Publ., 1999)
47. Block D I et al. (Eds) *Toward a New Millennium in Galaxy Morphology*: *Proc. of an Intern. Conf., Midrand, South Africa, Sept. 13–18, 1999* (Dordrecht: Kluwer Acad. Publ., 2000)
48. Kaper L, van den Heuvel E P J, Woudt P A (Eds) *Black Holes in Binaries and Galactic Nuclei*: *Diagnostics, Demography, and Formation*: *Proc. of the ESO Workshop, Garching, Germany, 6–8 Sept. 1999, in Honour of Riccardo Giacconi* (ESO Astrophys. Symposia) (Berlin: Springer, 2001)
49. Cherepashchuk A M *Usp. Fiz. Nauk* **166** 809 (1996) [*Phys. Usp.* **39** 759 (1996)]
50. Ho L, in *Observational Evidence for the Black Holes in the Universe* (Astrophys. and Space Sci. Library, Vol. 234, Ed. S K Chakrabarti) (Dordrecht: Kluwer Acad. Publ., 1999) p. 157
51. Charles P, in *Theory of Black Hole Accretion Disks* (Eds M A Abramowicz, G Björnsson, J E Pringle) (Cambridge: Cambridge Univ. Press, 1998) p. 1
52. Novikov I D, in *Relativistic Astrophysics and Cosmology*: *Proc. of the Spanish Relativity Meeting, La Laguna, Tenerife, Spain, Sept. 4–7, 1995* (Eds J Buitrago, E Mediavilla, A Oscoz) (Singapore: World Scientific, 1997) p. 51
53. Cherepashchuk A M *Space Sci. Rev.* **93** 473 (2000)
54. Srinivasan G, in *Black Holes in Binaries and Galactic Nuclei*: *Diagnostics, Demography, and Formation* (ESO Astrophys. Symposia, Eds L Kaper, E P J van den Heuvel, P A Woudt) (Berlin: Springer, 2001) p. 45
55. Hawking S W *Nature* **248** 30 (1974)
56. Colbert E J M, Mushotzky R F *Astrophys. J.* **519** 89 (1999)
57. Taniguchi Y et al. *Publ. Astron. Soc. Jpn.* **52** 533 (2000)
58. Mouri H, Taniguchi Y *Astrophys. J. Lett.* **566** L17 (2002)
59. Larson R B *Mon. Not. R. Astron. Soc.* **332** 155 (2002)
60. Weisskopf M C *Chandra News* (8) 1 (2001)
61. Roberts T P et al. *Mon. Not. R. Astron. Soc.* **325** L7 (2001)
62. Gebhardt K et al. *Astron. J.* **119** 1268 (2000)
63. Bennett D P et al. *Astrophys. J.* **579** 639 (2002); astro-ph/0109467
64. Mao S et al. *Mon. Not. R. Astron. Soc.* **329** 349 (2002)
65. Dibaĭ E A *Astron. Zh.* **61** 417 (1984) [*Sov. Astron.* **28** 245 (1984)]
66. Dibaĭ E A *Astron. Zh.* **61** 209 (1984) [*Sov. Astron.* **28** 123 (1984)]
67. Woltjer L *Astrophys. J.* **130** 38 (1959)
68. Ghez A M et al. *Astrophys. J.* **509** 678 (1998)
69. Kormendy J, Richstone D *Annu. Rev. Astron. Astrophys.* **33** 581 (1995)
70. Fromerth M J, Melia F *Astrophys. J.* **549** 205 (2001)
71. Shklovskiĭ I S *Astron. Zh.* **42** 893 (1965) [*Sov. Astron.* **9** 683 (1966)]
72. Bahcall J N, Kozlovsky B-Z *Astrophys. J.* **155** 1077 (1969)
73. Dibaĭ E A, Pronik V I *Astron. Zh.* **44** 952 (1967) [*Sov. Astron.* **11** 767 (1968)]
74. Bahcall J N, Kozlovsky B-Z, Salpeter E E *Astrophys. J.* **171** 467 (1972)
75. Blandford R D, McKee C F *Astrophys. J.* **255** 419 (1982)
76. Antokhin I I, Bochkarev N G *Astron. Zh.* **60** 448 (1983) [*Sov. Astron.* **27** 261 (1983)]
77. Lyutyĭ V M, Cherepashchuk A M *Astron. Cirk.* (633) 3 (1971)
78. Lyutyĭ V M, Cherepashchuk A M *Astron. Cirk.* (688) 1 (1972)
79. Cherepashchuk A M, Lyutyi V M *Astrophys. Lett.* **13** 165 (1973)
80. Lyutyĭ V M, Cherepashchuk A M *Astron. Cirk.* (831) 1 (1974)
81. Lyutyĭ V M, Cherepashchuk A M *Astron. Zh.* **63** 897 (1986) [*Sov. Astron.* **30** 532 (1986)]
82. Koratkar A P, Gaskell C M *Astrophys. J. Suppl.* **75** 719 (1991)
83. Peterson B M, Wandel A *Astrophys. J.* **521** L95 (1999)
84. Tohline J E, Osterbrock D E *Astrophys. J.* **210** L117 (1976)
85. Phillips M M *Astrophys. J. Suppl.* **38** 187 (1978)
86. Ulrich M H et al. *Mon. Not. R. Astron. Soc.* **206** 221 (1984)
87. Peterson B M et al. *Astrophys. J.* **501** 82 (1998)
88. Wandel A, Peterson B M, Malkan M A *Astrophys. J.* **526** 579 (1999)
89. Peterson B M, Wandel A *Astrophys. J.* **540** L13 (2000)
90. Morales R, Fabian A C *Mon. Not. R. Astron. Soc.* **329** 209 (2002)
91. Filippenko A V et al. *Publ. Astron. Soc. Pacific* **109** 461 (1997)
92. Antokhina E A, Cherepashchuk A M *Astron. Zh.* **71** 420 (1994) [*Astron. Rep.* **38** 367 (1994)]
93. Cherepashchuk A M, in *Dvoĭnye Zvezdy* (Binary Stars) (Ed. A G Masevich) (Moscow: Kosmoinform, 1997) p. 45
94. Remillard R A, McClintock J E, Bailyn C D *Astrophys. J. Lett.* **399** L145 (1992)
95. Antokhina E A, Cherepashchuk A M *Pis'ma Astron. Zh.* **19** 500 (1993) [*Astron. Lett.* **19** 194 (1993)]
96. Avni Y, Bahcall J N *Astrophys. J.* **192** L139 (1974)
97. Avni Y, Bahcall J N *Astrophys. J.* **197** 675 (1975)
98. Bochkarev N G, Shakura N I *Astron. Cirk.* (853) 1 (1975)
99. Bochkarev N G, Karitskaya E A, Shakura N I *Pis'ma Astron. Zh.* **1** (12) 13 (1975) [*Sov. Astron. Lett.* **1** 237 (1975)]
100. Bochkarev N G, Karitskaya E A, Shakura N I *Astron. Zh.* **56** 16 (1979) [*Sov. Astron.* **23** 8 (1979)]
101. Bochkarev N G, Karitskaya E A *Astron. Zh.* **60** 727 (1983)
102. Shahbaz T *J. Astrophys. Astron.* **20** 197 (1999)
103. Casares J, Charles P A *Mon. Not. R. Astron. Soc.* **271** L5 (1994)
104. Wade R A, Horne K *Astrophys. J.* **324** 411 (1988)
105. Martin A C et al. *Mon. Not. R. Astron. Soc.* **274** L46 (1995)
106. Paczynsky B *Astron. Astrophys.* **34** 161 (1974)
107. Khruzina T S *Astron. Zh.* **62** 356 (1985) [*Sov. Astron.* **29** 205 (1985)]
108. Sokolov V V *Astron. Zh.* **64** 803 (1987) [*Sov. Astron.* **31** 419 (1987)]
109. Smith D A, Dhillon V S *Mon. Not. R. Astron. Soc.* **301** 767 (1998)
110. Bochkarev N G et al. *Pis'ma Astron. Zh.* **5** 185 (1979) [*Sov. Astron.* **5** 99 (1979)]
111. Antokhina E A, Cherepashchuk A M *Pis'ma Astron. Zh.* **23** 889 (1997) [*Astron. Lett.* **23** 773 (1997)]
112. Shahbaz T *Mon. Not. R. Astron. Soc.* **298** 153 (1998)

113. Antokhina E A, Cherepashchuk A M, Shimanskiĭ V V *Izv. Ross. Akad. Nauk Ser. Fiz.* (2003) (in press)
114. Titarchuk L, Osherovich V *Astrophys. J.* **542** L111 (2000)
115. White N *Nature* **407** 146 (2000)
116. Kardashev N S, Kreĭsman B B, Ponomarev Yu N *Tr. Fiz. Inst. Ross. Akad. Nauk* **228** 3 (2000)
117. Junor W, Biretta J A, Livio M *Nature* **401** 891 (1999)
118. Tanaka Y et al. *Nature* **375** 659 (1995)
119. Nandra K et al. *Astrophys. J.* **477** 602 (1997)
120. Wilms J et al. *Mon. Not. R. Astron. Soc.* **328** L27 (2001)
121. Terashima Y, Wilson A S *Astrophys. J.* **583** 145 (2003)
122. Krolik J H *Active Galactic Nuclei: from the Central Black Hole to the Galactic Environment* (Princeton, NJ: Princeton Univ. Press, 1999)
123. Mulchaey J S, Wilson A S, Tsvetanov Z *Astrophys. J.* **467** 197 (1996)
124. Malkan M A, Gorjian V, Tam R *Astrophys. J. Suppl.* **117** 25 (1998)
125. Yaqoob T et al. *Astrophys. J.* **546** 759 (2001)
126. Wang J-X, Wang T-G, Zhou Y-Y *Astrophys. J.* **549** 891 (2001)
127. Baganoff F K et al. *Nature* **413** 45 (2001)
128. Grupe D, Gliozzi M *Astron. Astrophys.* (2003) (in press)
129. Grupe D, Thomas H-C, Leighly K M *Astron. Astrophys.* **350** L31 (1999)
130. Brandt W N, Pounds K A, Fink H *Mon. Not. R. Astron. Soc.* **273** L47 (1995)
131. Grupe D et al. *Astron. Astrophys.* **299** L5 (1995)
132. Grupe D et al. *Astron. Astrophys.* **300** L21 (1995)
133. Komossa S, Fink H, in *Accretion Disks: New Aspects. Proc. of the EARA Workshop, Garching, Germany, 21 – 23 Oct. 1996* (Lecture Notes in Physics, Vol. 487, Eds E Meyer-Hofmeister, H Spruit) (Berlin: Springer, 1997) p. 250
134. Komossa S, in *JENAM-2001: Astronomy with Large Telescopes from Ground and Space* (Reviews in Modern Astronomy, Vol. 15, Ed. R E Schielicke) (Berlin: Wiley-VCH, 2002) p. 27
135. Komossa S, Bade N *Astron. Astrophys.* **343** 775 (1999)
136. Komossa S, Greiner J *Astron. Astrophys.* **349** L45 (1999)
137. Rees M J *Science* **247** 817 (1990)
138. Frank J, Rees M J *Mon. Not. R. Astron. Soc.* **176** 633 (1976)
139. Khokhlov A, Novikov I D, Pethick C J *Astrophys. J.* **418** 181 (1993)
140. Ivanov P B, Novikov I D *Astrophys. J.* **549** 467 (2001)
141. Alexander T, Livio M *Astrophys. J.* **560** L143 (2001)
142. Oda M *Space Sci. Rev.* **20** 757 (1977)
143. Shwartsman V F *Astron. Zh.* **48** 479 (1971) [*Sov. Astron.* **15** 377 (1971)]
144. Syunyaev R A *Astron. Zh.* **49** 1153 (1972) [*Sov. Astron.* **16** 941 (1973)]
145. Ebisawa K et al. *Astrophys. J.* **467** 419 (1996)
146. Vorontsov-Vel'yaminov B A *Vnegalakticheskaya Astronomiya* (Extragalactic Astronomy) 2nd ed. (Moscow: Nauka, 1978) p. 24, 160, 237 [Translated into English (Chur: Harwood Acad. Publ., 1987)]
147. Martynov D Ya (Ed.) *Aktivnye Yadra i Zvezdnaya Kosmogoniya* (Active Niclei and Stellar Cosmogony) (Moscow: Izd. MGU, 1987)
148. Ho L C et al. *Astrophys. J.* **549** L51 (2001)
149. Fitch W S, Pacholczyk A G, Weymann R J *Astrophys. J.* **150** L67 (1969)
150. Barnes T G *Astrophys. Lett.* **1** 171 (1968)
151. Zaĭtseva G V, Lyutyĭ V M *Astron. Cirk.* (470) 7 (1968)
152. Lyutyĭ V M *Astron. Zh.* **56** 918 (1979) [*Sov. Astron.* **23** 518 (1979)]
153. Lyutyi V M *Sov. Sci. Reviews Sect. E Astrophys. Space Phys. Rev.* (Ed. R A Sunyaev) **1** 61 (1981)
154. Dokuchaev V I *Usp. Fiz. Nauk* **161** (6) 1 (1991) [*Sov. Phys. Usp.* **34** 447 (1991)]
155. Ginzburg V L, Ozernoĭ L M *Zh. Eksp. Teor. Fiz.* **47** 1030 (1964) [*Sov. Phys. JETP* **20** 689 (1965)]
156. Zhuravlev V I, Komberg B V *Astron. Zh.* **76** 163 (1999) [*Astron. Rep.* **43** 135 (1999)]
157. Blandford R D, Znajek R L *Mon. Not. R. Astron. Soc.* **179** 433 (1977)
158. Kardashev N S *Mon. Not. R. Astron. Soc.* **326** 1122 (2001)
159. Jackson C A, Wall J V *Mon. Not. R. Astron. Soc.* **304** 160 (1999)
160. Beskin V S, Istomin Ya N, Pariev V I *Astron. Zh.* **69** 1258 (1992) [*Sov. Astron.* **36** 642 (1992)]
161. Istomin Ya N, Komberg B V *Astron. Zh.* **78** 871 (2001) [*Astron. Rep.* **45** 755 (2001)]
162. Nishikawa K-I et al., in *Particles and Fields in Radio Galaxies: Proc. of the Oxford Radio Galaxy Workshop, Oxford, UK, 3 – 5 Aug. 2000* (Astron. Soc. of the Pacific Conf. Ser., Vol. 250, Eds R A Laing, K M Blundell) (San Francisco, Calif.: Astronomical Society of the Pacific, 2002); astro-ph/0202396
163. Wandel A *Astrophys. J.* **519** L39 (1999)
164. Andrillat Y, Souffrin S *Astrophys. Lett.* **1** 111 (1968)
165. Dibaĭ E A, Esipov V F *Astron. Cirk.* (349) 1 (1965)
166. Burbidge E M, Burbidge G R *Astrophys. J.* **143** 271 (1966)
167. Sharov A S, Efremov Yu N *Astron. Zh.* **40** 950 (1963) [*Sov. Astron.* **7** 727 (1964)]
168. Smith H J, Hoffeit D *Nature* **198** 650 (1963)
169. Fabrika S N *Pis'ma Astron. Zh.* **6** 559 (1980) [*Sov. Astron. Lett.* **6** 293 (1980)]
170. Capriotti E R, Foltz C B, Peterson B M *Astrophys. J.* **261** 35 (1982)
171. Peterson B M et al. *Astrophys. J.* **368** 119 (1991)
172. Peterson B M et al. *Astrophys. J.* **510** 659 (1999)
173. Antonucci R R J, Cohen R D *Astrophys. J.* **271** 564 (1983)
174. Shapovalova A I et al. *Astron. Astrophys.* **376** 775 (2001)
175. Wu X-B, Han J L *Astrophys. J.* **561** L59 (2001)
176. Lyutyĭ V M, Oknyanskiĭ V L, Chuvaev K K *Pis'ma Astron. Zh.* **10** 803 (1984) [*Sov. Astron. Lett.* **10** 335 (1984)]
177. Penston M V, Perez E *Mon. Not. R. Astron. Soc.* **211** 33P (1984)
178. Sergeev S G, Pronik V I, Sergeeva E A *Astrophys. J.* **554** 245 (2001)
179. Peterson B M et al. *Astrophys. J.* **542** 161 (2000)
180. Bochkarev N G, in *Trudy Pervoĭ Vseross. Astronomicheskoĭ Konf., St. Petersburg, 6 – 12 Avgusta, 2001* (Proc. of the First All-Russian Astronomical Conference, St. Petersburg, 6 – 12 August, 2001) (Eds V N Obridko, V V Vityazev, V V Ivanov) (St. Petersburg: Izd. SPbGU, 2003) (in press)
181. Bochkarev M G *Pis'ma Astron. Zh.* **10** 574 (1984) [*Sov. Astron. Lett.* **10** 239 (1984)]
182. Shapovalova A I, Burenkov A N, Bochkarev N G *Bull. Special Astrophys. Obs.* **41** 28 (1996)
183. Bochkarev N G *ASP Conf. Ser.* (2003) (in press)
184. Wandel A, Yahil A *Astrophys. J. Lett.* **295** L1 (1985)
185. Gebhardt K et al. *Astrophys. J.* **543** L5 (2000)
186. Winge C et al. *Astrophys. J.* **519** 134 (1999)
187. Ferrarese L et al. *Astrophys. J.* **555** L79 (2001)
188. McLure R J, Dunlop J S *Mon. Not. R. Astron. Soc.* **331** 795 (2002)
189. Macchetto F D *Astrophys. Space Sci.* **269 – 270** 269 (1999)
190. Harms R J et al. *Astrophys. J. Lett.* **435** L35 (1994)
191. Ford H C et al. *Astrophys. J. Lett.* **435** L27 (1994)
192. Macchetto F et al. *Astrophys. J.* **489** 579 (1997)
193. Ferrarese L, Ford H C, Jaffe W *Astrophys. J.* **470** 444 (1996)
194. Bower G A et al. *Astrophys. J. Lett.* **492** L111 (1998)
195. van der Marel R P, van den Bosch F C *Astron. J.* **116** 2220 (1998)
196. Barth A J et al. *Astrophys. J.* **555** 685 (2001)
197. Tremaine S et al. *Astrophys. J.* **574** 740 (2002); astro-ph/0203468
198. Moran J M, Greenhill L J, Herrnstein J R *J. Astrophys. Astron.* **20** 165 (1999)
199. Miyoshi M et al. *Nature* **373** 127 (1995)
200. Ishihara Y et al. *Publ. Astron. Soc. Jpn.* **53** 215 (2001)
201. Young P J et al. *Astrophys. J.* **221** 721 (1978)
202. Young P *Astrophys. J.* **242** 1232 (1980)
203. Peebles P J E *Astrophys. J.* **178** 371 (1972)
204. Kormendy J, in *The Nearest Active Galaxies* (Eds J E Beckman, L Colina, H Netzer) (Madrid: CSIC Press, 1993) p. 197
205. Nieto J-L et al. *Astron. Astrophys.* **244** L25 (1991)
206. Lauer T R et al. *Astron. J.* **110** 2622 (1995)
207. Quinlan G D, Hernquist L, Sigurdsson S *Astrophys. J.* **440** 554 (1995)
208. Duncan M J, Wheeler J C *Astrophys. J. Lett.* **237** L27 (1980)
209. Binney J, Mamon G A *Mon. Not. R. Astron. Soc.* **200** 361 (1982)
210. van der Marel R P *Mon. Not. R. Astron. Soc.* **270** 271 (1994)
211. Eckart A, Genzel R, in *The Galactic Center: 4th ESO/CTIO Workshop, La Serena, Chile, 10 – 15 March 1996* (ASP Conf. Ser., Vol. 102, Ed. R Gredel) (San Francisco, Calif.: Astron. Soc. of the Pacific, 1996) p. 196
212. Eckart A, Genzel R *Nature* **383** 415 (1996)
213. Eckart A, Genzel R *Mon. Not. R. Astron. Soc.* **284** 576 (1997)
214. Genzel R et al. *Mon. Not. R. Astron. Soc.* **291** 219 (1997)
215. Ghez A M et al. *Nature* **407** 349 (2000)

216. Kormendy J et al. *Astrophys. J. Lett.* **459** L57 (1996)
217. Kormendy J et al. *Astrophys. J. Lett.* **473** L91 (1996)
218. van der Marel R P et al. *Nature* **385** 610 (1997)
219. Ford H C et al., in *The Central Regions of the Galaxy and Galaxies* (IAU Symp., No. 184, Ed. Y Sofue) (Boston, Mass.: Kluwer Acad., 1998) p. 377
220. Kormendy J, in *Galaxy Disks and Disk Galaxies: Proc. of a Conf., Rome, Italy, 12–16 June 2000* (ASP Conf. Ser., Vol. 230, Eds J G Funes, E M Corsini) (San Francisco, Calif.: Astron. Soc. of the Pacific, 2001) p. 247; astro-ph/0007401
221. Olling R P et al., in *Black Holes in Binaries and Galactic Nuclei: Diagnostics, Demography, and Formation* (ESO Astrophys. Symposia, Eds L Kaper, E P J van den Heuvel, P A Woudt) (Berlin: Springer, 2001) p. 91
222. Emsellem E, in *Black Holes in Binaries and Galactic Nuclei: Diagnostics, Demography, and Formation* (ESO Astrophys. Symposia, Eds L Kaper, E P J van den Heuvel, P A Woudt) (Berlin: Springer, 2001) p. 95
223. van der Marel R P et al. *Mon. Not. R. Astron. Soc.* **268** 521 (1994)
224. Anders S W, Thatte N, Genzel R, in *Black Holes in Binaries and Galactic Nuclei: Diagnostics, Demography, and Formation* (ESO Astrophys. Symposia, Eds L Kaper, E P J van den Heuvel, P A Woudt) (Berlin: Springer, 2001) p. 88
225. Oort J H *Annu. Rev. Astron. Astrophys.* **15** 295 (1977)
226. Genzel R, Townes C H *Annu. Rev. Astron. Astrophys.* **25** 377 (1987)
227. Reid M *Annu. Rev. Astron. Astrophys.* **31** 345 (1993)
228. Munyaneza F, Tsiklauri D, Viollier R D *Astrophys. J.* **526** 744 (1999)
229. Eckart A et al. *Mon. Not. R. Astron. Soc.* **331** 917 (2002)
230. Melia F et al. *Astrophys. J.* **554** L37 (2001)
231. Lubinski P, Zdziarski A A *Mon. Not. R. Astron. Soc.* **323** L37 (2001)
232. Pariev V I, Bromley B C *Astrophys. J.* **508** 590 (1998)
233. Mushotzky R F et al. *Mon. Not. R. Astron. Soc.* **272** L9 (1995)
234. Fabian A C, in *Theory of Black Hole Accretion Disks* (Eds M A Abramowicz, G Björnsson, J E Pringle) (Cambridge: Cambridge Univ. Press, 1998) p. 123
235. Usui F, Nishida S, Eriguchi Y *Mon. Not. R. Astron. Soc.* **301** 721 (1998)
236. Maoz E *Astrophys. J. Lett.* **494** L181 (1998)
237. Bilić N, Viollier R D *Phys. Lett. B* **408** 75 (1997)
238. Bilić N, Viollier R D *Gen. Relat. Gravit.* **31** 1105 (1999)
239. Munyaneza F, Viollier R D *Astrophys. J.* **564** 274 (2002)
240. Titarchuk L, Zannias T *Astrophys. J.* **493** 863 (1998)
241. Czerny B et al. *Mon. Not. R. Astron. Soc.* **325** 865 (2001)
242. Fabian A C, Rees M J *Mon. Not. R. Astron. Soc.* **277** L55 (1995)
243. Reynolds C S et al. *Mon. Not. R. Astron. Soc.* **283** L111 (1996)
244. Bisnovatyi-Kogan G S, in *Observational Evidence for the Black Holes in the Universe* (Astrophys. and Space Sci. Library, Vol. 234, Ed. S K Chakrabarti) (Dordrecht: Kluwer Acad. Publ., 1999) p. 1
245. Ho L C *Astrophys. J.* **564** 120 (2002)
246. Franceschini A, Vercellone S, Fabian A C *Mon. Not. R. Astron. Soc.* **297** 817 (1998)
247. Cattaneo A, Haehnelt M G, Rees M J *Mon. Not. R. Astron. Soc.* **308** 77 (1999)
248. Magorrian J et al. *Astron. J.* **115** 2285 (1998)
249. Merritt D, Ferrarese L *Mon. Not. R. Astron. Soc.* **320** L30 (2001)
250. McLeod K K, in *Quasar Hosts: Proc. of the ESO-IAC Conf., Tenerife, Spain, 24–27 Sept. 1996* (ESO Astrophys. Symposia, Eds D L Clements, I Pérez-Fournon) (Berlin: Springer, 1997) p. 45
251. Wandel A *Astrophys. J.* **565** 762 (2002)
252. Laor A *Astrophys. J.* **553** 677 (2001)
253. Graham A W et al. *Astrophys. J.* **563** L11 (2001)
254. Merritt D, Ferrarese L *Astrophys. J.* **547** 140 (2001)
255. Merrifield M R, Forbes D A, Terlevich A I *Mon. Not. R. Astron. Soc.* **313** L29 (2000)
256. Umemura M *Astrophys. J.* **560** L29 (2001)
257. Salucci P et al. *Mon. Not. R. Astron. Soc.* **307** 637 (1999)
258. Sarzi M et al. *Astrophys. J.* **550** 65 (2001)
259. Lu Y, Yu Q *Mon. Not. R. Astron. Soc.* **324** 653 (2001)
260. Salucci P et al. *Mon. Not. R. Astron. Soc.* **317** 488 (2000)
261. Cherepashchuk A M et al. *Highly Evolved Close Binary Stars* Vol. 1 *Catalog* (Adv. in Astron. and Astrophys., Vol. 1) (Amsterdam: Gordon and Breach, 1996)
262. Kuulkers E et al. *Mon. Not. R. Astron. Soc.* **306** 919 (1999)
263. Goranskiĭ V P et al. *Pis'ma Astron. Zh.* **22** 413 (1996) [*Astron. Lett.* **22** 371 (1996)]
264. Hynes R I et al. *Mon. Not. R. Astron. Soc.* **330** 1009 (2002)
265. Tanaka Y, Shibazaki N *Annu. Rev. Astron. Astrophys.* **34** 607 (1996)
266. Tanaka Y, in *Disk Instabilities in Close Binary Systems: 25 Years of the Disk-Instability Model* (Frontiers Sci. Ser., No. 26, Eds S Mineshige, J C Wheeler) (Tokyo: Universal Acad. Press, 1999) p. 21
267. Kato S, Fukue J, Mineshige S *Black-Hole Accretion Disks* (Kyoto: Kyoto Univ. Press, 1998)
268. Chen W, Shrader C R, Livio M *Astrophys. J.* **491** 312 (1997)
269. van Paradijs J *Astrophys. J. Lett.* **464** L139 (1996)
270. Sunyaev R A et al. *Pis'ma Astron. Zh.* **14** 771 (1988) [*Sov. Astron. Lett.* **14** 327 (1988)]
271. Sunyaev R et al. *Astron. Astrophys.* **247** L29 (1991)
272. Sunyaev R et al. *Astrophys. J. Lett.* **383** L49 (1991)
273. Sunyaev R et al. *Astrophys. J. Lett.* **389** L75 (1992)
274. Sunyaev R A et al. *Astron. Astrophys.* **280** L1 (1993)
275. Sunyaev R A et al. *Pis'ma Astron. Zh.* **20** 890 (1994) [*Astron. Lett.* **20** 777 (1994)]
276. Grebenev S A et al. *Pis'ma Astron. Zh.* **17** 985 (1991) [*Sov. Astron. Lett.* **17** 413 (1991)]
277. Grebenev S et al. *Astron. Astrophys. Suppl.* **97** 281 (1993)
278. Grebenev S A, Sunyaev R A, Pavlinsky M N *Adv. Space Res.* **19** 15 (1997)
279. van der Klis M *Astrophys. J. Suppl.* **92** 511 (1994)
280. Nowak M A *Publ. Astron. Soc. Pacific* **107** 1207 (1995)
281. Tanaka Y, Lewin W H G, in *X-Ray Binaries* (Cambridge Astrophys. Ser., Vol. 26, Eds W H G Lewin, J van Paradijs, E P J van den Heuvel) (Cambridge: Cambridge Univ. Press, 1995) p. 126
282. van Paradijs J et al. *Astron. Astrophys.* **182** 47 (1987)
283. McClintock J E, Horne K, Remillard R A *Astrophys. J.* **442** 358 (1995)
284. Narayan R, Barret D, McClintock J E *Astrophys. J.* **482** 448 (1977)
285. Narayan R, Garcia M R, McClintock J E *Astrophys. J. Lett.* **478** L79 (1997)
286. Asai K et al. *Publ. Astron. Soc. Jpn.* **50** 611 (1998)
287. Herrero A et al. *Astron. Astrophys.* **297** 556 (1995)
288. Esin A A, McClintock J E, Narayan R *Astrophys. J.* **489** 865 (1997)
289. Titarchuk L *Astrophys. J.* **434** 570 (1994)
290. Fender R P *Mon. Not. R. Astron. Soc.* **322** 301 (2001)
291. Fender R P, Kuulkers E *Mon. Not. R. Astron. Soc.* **324** 923 (2001)
292. Trushkin S A *Astron. Astrophys. Trans.* **19** 525 (2000)
293. Ebisawa K et al. *Publ. Astron. Soc. Jpn.* **46** 375 (1994)
294. Belloni T et al. *Astrophys. J. Lett.* **472** L107 (1996)
295. Miyamoto S et al. *Astrophys. J.* **383** 784 (1991)
296. Gilfanov M et al. *Astron. Astrophys. Suppl.* **97** 303 (1993)
297. Grebenev S A, Sunyaev R A, Pavlinsky M N, in *Proc. of the Workshop on Nova Muscae, Lyngby, Danemark, May 14–16, 1991* (Ed. S Brandt) (Lyngby: Danish Space Res. Inst., 1991) p. 19
298. Zycki P T, Done C, Smith D A *Mon. Not. R. Astron. Soc.* **309** 561 (1999)
299. Grebenev S A, Sunyaev R A, Pavlinskiĭ M N *Pis'ma Astron. Zh.* **18** 11 (1992) [*Sov. Astron. Lett.* **18** 5 (1992)]
300. Gil'fanov M R, Thesis for Doctorate of Physico-Mathematical Sciences (Moscow: Space Research Institute of Russian Academy of Sciences, 1995) p. 167
301. Orosz J A et al. *Astrophys. J.* **555** 489 (2001)
302. Wagner R M et al. *Astrophys. J.* **556** 42 (2001)
303. Greiner J, Cuby J G, McCaughrean M J *Nature* **414** 522 (2001)
304. In't Zand J J M et al. *Astron. Astrophys.* **357** 520 (2000)
305. Markwardt C B, Swank J H, Marshall F E *IAU Circular* (7120) 1 (1999)
306. Hjellming R M et al. *Astrophys. J.* **544** 977 (2000)
307. Goranskiĭ V P *Astron. Cirk.* (1024) 3 (1978)
308. Goranskij V P *Inform. Bull. Var. Stars* (3464) 1 (1990)
309. Israelian G et al. *Nature* **401** 142 (1999)
310. Uemura M et al. *Publ. Astron. Soc. Jpn.* **42** L15 (2000)
311. Garåia M et al. *IAU Circular* (7392) 2 (2000)
312. van Paradijs J, White N *Astrophys. J. Lett.* **447** L33 (1995)
313. Grimm H-J, Gilfanov M, Sunyaev R *Astron. Astrophys.* **391** 923 (2002); astro-ph/0109239
314. Rhoades C E (Jr), Ruffini R *Phys. Rev. Lett.* **32** 324 (1974)

315. Mirabel I F et al. *Nature* **413** 139 (2001)
316. Naik S et al. *Mon. Not. R. Astron. Soc.* **330** 487 (2002)
317. Fender R P et al. *Mon. Not. R. Astron. Soc.* **330** 212 (2002)
318. Schmutz W, Geballe T R, Schild H *Astron. Astrophys.* **111** L25 (1996)
319. Cherepashchuk A M, Moffat A F J *Astrophys. J. Lett.* **424** L53 (1994)
320. Hanson M M, Still M D, Fender R P *Astrophys. J.* **541** 308 (2000)
321. Charles P, in *Black Holes in Binaries and Galactic Nuclei*: *Diagnostics, Demography, and Formation* (ESO Astrophys. Symposia, Eds L Kaper, E P J van den Heuvel, P A Woudt) (Berlin: Springer, 2001) p. 27
322. Orosz J A et al., in *Black Holes in Binaries and Galactic Nuclei*: *Diagnostics, Demography, and Formation* (ESO Astrophys. Symposia, Eds L Kaper, E P J van den Heuvel, P A Woudt) (Berlin: Springer, 2001) p. 59
323. Greene J, Bailyn C D, Orosz J A *Astrophys. J.* **554** 1290 (2001)
324. Casares J et al. *Mon. Not. R. Astron. Soc.* **329** 29 (2002)
325. Taylor J H, Weisberg J M *Astrophys. J.* **253** 908 (1982)
326. Phinney E S *Astrophys. J. Lett.* **380** L17 (1991)
327. Thorsett S E, Chakrabarty D *Astrophys. J.* **512** 288 (1999)
328. van Kerkwijk M H, in *Black Holes in Binaries and Galactic Nuclei*: *Diagnostics, Demography, and Formation* (ESO Astrophys. Symposia, Eds L Kaper, E P J van den Heuvel, P A Woudt) (Berlin: Springer, 2001) p. 39
329. Martynov D Ya *Usp. Fiz. Nauk* **108** 701 (1972) [*Sov. Phys. Usp.* **15** 786 (1973)]
330. Brandt W N, Podsiadlowski Ph, Sigurdsson S *Mon. Not. R. Astron. Soc.* **277** L35 (1995)
331. Mirabel I F et al. *Nature* **358** 215 (1992)
332. Mirabel I F, Rodriguez L F *Nature* **371** 46 (1994)
333. Hjellming R M, Rupen M P *Nature* **375** 464 (1995)
334. Castro-Tirado A J, Greiner J, Paredes J M (Eds) *Microquasars*: *Proc. of the 3rd Microquasar Workshop*: *Granada Workshop on Galactic Relativistic Jet Sources, Granada, Spain, 11 – 13 Sept. 2000* (Astrophys. and Space Sci., Vol. 276) (Dordrecht: Kluwer Acad. Publ., 2001)
335. Carramiñana A, Reimer O, Thompson D J (Eds) *The Nature of Unidentified Galactic High-Energy Gamma-Ray Sources*: *Proc. of the Workshop, Tonantzintla, Puebla, México, 9 – 11 October 2000* (Astrophys. and Space Sci. Library, Vol. 267) (Dordrecht: Kluwer Acad. Publ., 2001)
336. Rodríguez L F, Mirabel I F, in *The Nature of Unidentified Galactic High-Energy Gamma-Ray Sources*: *Proc. of the Workshop, Tonantzintla, Puebla, México, 9 – 11 October 2000* (Astrophys. and Space Sci. Library, Vol. 267, Eds A Carramiñana, O Reimer, D J Thompson) (Dordrecht: Kluwer Acad. Publ., 2001) p. 245
337. Durouchoux Ph *Astrophys. Space Sci.* **276** (Suppl. 1) 91 (2001)
338. Mioduszewski A J et al. *Astrophys. J.* **553** 766 (2001); astro-ph/0102018
339. de la Force C et al. *Astrophys. Space Sci.* **276** (Suppl. 1) 121 (2001)
340. Stirling A M et al. *Mon. Not. R. Astron. Soc.* **327** 1273 (2001)
341. Sunyaev R, in *Black Holes in Binaries and Galactic Nuclei*: *Diagnostics, Demography, and Formation* (ESO Astrophys. Symposia, Eds L Kaper, E P J van den Heuvel, P A Woudt) (Berlin: Springer, 2001) p. 113
342. Belloni T, in *Black Holes in Binaries and Galactic Nuclei*: *Diagnostics, Demography, and Formation* (ESO Astrophys. Symposia, Eds L Kaper, E P J van den Heuvel, P A Woudt) (Berlin: Springer, 2001) p. 125
343. Tanaka Y, in *Black Holes in Binaries and Galactic Nuclei*: *Diagnostics, Demography, and Formation* (ESO Astrophys. Symposia, Eds L Kaper, E P J van den Heuvel, P A Woudt) (Berlin: Springer, 2001) p. 141
344. Sunyaev R, Revnivtsev M *Astron. Astrophys.* **358** 617 (2000)
345. Barret D et al. *Astrophys. J.* **394** 615 (1992)
346. Syunyaev R A, Shakura N I *Pis'ma Astron. Zh.* **12** 286 (1986) [*Sov. Astron. Lett.* **12** 117 (1986)]
347. Sibgatullin N R, Sunyaev R A *Pis'ma Astron. Zh.* **24** 894 (1998) [*Astron. Lett.* **24** 774 (1998)]
348. Lightman A P *Astrophys. J.* **194** 429 (1974)
349. Shakura N I, Suniaev R A *Mon. Not. R. Astron. Soc.* **175** 613 (1976)
350. Luo C, Liang E P *Mon. Not. R. Astron. Soc.* **266** 386 (1994)
351. Bisnovatyi-Kogan G S, Blinnikov S I *Astron. Astrophys.* **59** 111 (1977)
352. Done C et al. *Astrophys. J.* **395** 275 (1992)
353. Sunyaev R A et al. *Pis'ma Astron. Zh.* **17** 975 (1991) [*Sov. Astron. Lett.* **17** 409 (1991)]
354. McClintock J E, in *Texas/ESO-CERN Symp. on Relativistic Astrophysics, Cosmology, and Fundamental Physics* (Ann. of the New York Acad. of Sci., Vol. 647, Eds J D Barrow, L Mestel, P A Thomas) (New York: New York Acad. of Sci., 1991) p. 495
355. Katsova M M, Cherepashchuk A M *Astron. Zh.* **77** 909 (2000) [*Astron. Rep.* **44** 804 (2000)]
356. Bildsten L, Rutledge R E *Astrophys. J.* **541** 908 (2000)
357. Robertson S L, Leiter D J *Astrophys. J.* **565** 447 (2002); astro-ph/0102381
358. Bisnovatyĭ-Kogan G S et al. *Pis'ma Astron. Zh.* **4** 81 (1978) [*Sov. Astron. Lett.* **4** 43 (1978)]
359. Borozdin K N, Trudolyubov S P *Astrophys. J.* **533** L131 (2000)
360. Wijnands R et al. *Mon. Not. R. Astron. Soc.* **328** 451 (2001)
361. Kanbach G et al. *Nature* **414** 180 (2001)
362. Morgan E H, Remillard R A, Greiner J *Astrophys. J.* **482** 993 (1997)
363. Remillard R A et al. *Astrophys. J.* **522** 397 (1999)
364. Nowak M A et al. *Astrophys. J. Lett.* **477** L91 (1997)
365. Cui W, Zhang S N, Chen W *Astrophys. J. Lett.* **492** L53 (1998)
366. Ruffini R et al. *Astrophys. J.* **555** L113 (2001); astro-ph/0106532
367. Ruffini R et al. *Astrophys. J.* **555** L107 (2001); astro-ph/0106531
368. Ruffini R, in *Black Holes in Binaries and Galactic Nuclei*: *Diagnostics, Demography, and Formation* (ESO Astrophys. Symposia, Eds L Kaper, E P J van den Heuvel, P A Woudt) (Berlin: Springer, 2001) p. 334
369. Lee H K, Lee C H, van Putten M H P M, astro-ph/0009239
370. Weinberg E J, in *Advances in the Interplay between Quantum and Gravity Physics* (NATO Sci. Series. Ser II, Vol. 60, Eds P G Bergmann, V de Sabbata) (Dordrecht: Kluwer Acad. Publ., 2002) p. 523; gr-gc/0106030
371. Volkov M S, Gal'tsov D V *Phys. Rep.* **319** 1 (1999)
372. Beskin V S, Kuznetsova I V *Nuovo Cimento B* **115** 795 (2000)
373. Punsly B, in *The Nature of Unidentified Galactic High-Energy Gamma-Ray Sources*: *Proc. of the Workshop, Tonantzintla, Puebla, México, 9 – 11 October 2000* (Astrophys. and Space Sci. Library, Vol. 267, Eds A Carramiñana, O Reimer, D J Thompson) (Dordrecht: Kluwer Acad. Publ., 2001) p. 271
374. Zhang S N, Cui W, Chen W *Astrophys. J. Lett.* **482** L155 (1997)
375. McClintock J E *AIP Conf. Proc.* **431** 290 (1998)
376. Barret D et al. *Astrophys. Space Sci.* **276** (Suppl. 1) 305 (2001)
377. Cherepashchuk A M *Astron. Zh.* **78** 145 (2001) [*Astron. Rep.* **45** 120 (2001)]
378. Cherepashchuk A M *Usp. Fiz. Nauk* **172** 959 (2002) [*Phys. Usp.* **45** 896 (2002)]
379. Bailyn C D et al. *Astrophys. J.* **499** 367 (1998)
380. Cherepashchuk A, in *Modern Problems of Stellar Evolution*: *Proc. of the Intern. Conf. in Honour of Prof. A.G. Massevitch's 80th Birthday, Zvenigorod, Russia, 13 – 15 October 1998* (Ed. D S Wiebe) (Moscow: GEOS, 1998) p. 198
381. Barziv O et al. *Astron. Astrophys.* **377** 925 (2001)
382. Wijers R A M J, in *Evolutionary Processes in Binary Stars* (NATO ASI Series. Ser. C, Vol. 477, Eds R A M J Wijers, M B Davies, C A Tout) (Dordrecht: Kluwer Acad., 1996) p. 327
383. Bisnovatyi-Kogan G S, in *Proc. of the ESO Workshop on the SN 1987 A, Garching bei München, FRG, 6 – 8 July 1987* (ESO Conf. and Workshop Proc., Vol. 26, Ed. I J Danziger) (Garching bei München: European Southern Observatory, 1987) p. 347
384. Brown G E, Bethe H A *Astrophys. J.* **423** 659 (1994)
385. Brown G E, Weingartner J C, Wijers R A M J *Astrophys. J.* **463** 297 (1996)
386. Woosley S E, Langer N, Weaver T A *Astrophys. J.* **411** 823 (1993)
387. Woosley S E, Langer N, Weaver T A *Astrophys. J.* **448** 315 (1995)
388. Cherepashchuk A M, Khaliullin Kh F, Eaton J A *Astrophys. J.* **281** 774 (1984)
389. Cherepashchuk A M, in *Wolf – Rayet Stars and Interrelations with Other Massive Stars in Galaxies* (IAU Symp., No. 143, Eds K A van der Hucht, B Hidayat) (Dordrecht: Kluwer Acad., 1991) p. 280

390. Antokhin I I, Kholtygin A F, Cherepashchuk A M *Astron. Zh.* **65** 558 (1988) [*Sov. Astron.* **32** 285 (1988)]
391. Nugis T, Crowther P A, Willis A J *Astron. Astrophys.* **333** 956 (1998)
392. Beekman G et al. *Mon. Not. R. Astron. Soc.* **290** 303 (1997)
393. Reynolds A P et al. *Astron. Astrophys.* **349** 873 (1999)
394. Kaper L, Cherepashchuk A, in *Black Holes in Binaries and Galactic Nuclei: Diagnostics, Demography, and Formation* (ESO Astrophys. Symposia, Eds L Kaper, E P J van den Heuvel, P A Woudt) (Berlin: Springer, 2001) p. 289
395. Tagieva S O et al. *Astron. Astrophys. Trans.* **19** 123 (2000)
396. Shore S N, Livio M, van den Heuvel E P J *Interacting Binaries* (Saas-Free Adv. Course 22 Lecture Notes, 1992, Eds H Nussbaumer, A Orr) (Berlin: Springer-Verlag, 1994)
397. Alpar M A et al. *Nature* **300** 728 (1982)
398. Iben I (Jr), Tutukov A V, Yungelson L R *Astrophys. J. Suppl.* **100** 217 (1995)
399. Iben I (Jr), Tutukov A V, Yungelson L R *Astrophys. J. Suppl.* **100** 233 (1995)
400. Tavani M *Astrophys. J. Lett.* **366** L27 (1991)
401. Paczynski B, in *Wolf–Rayet and High-Temperature Stars* (IAU Symp., No. 49, Eds M K V Bappu, J Sahade) (Dordrecht: D. Reidel Publ. Co, 1973) p. 143
402. Conti P S *Mem. Soc. R. Sci. Liege* **9** (6) 193 (1976)
403. Bisnovatyi-Kogan G S, Nadyozhin D K *Astrophys. Space Sci.* **15** 353 (1972)
404. Chevalier R A *Space Sci. Rev.* **74** 289 (1995)
405. Tutukov A V, Yungel'son L R *Nauchnye Informatsii Astrosoveta Akad. Nauk SSSR* (27) 58 (1973)
406. van den Heuvel E P J, in *Structure and Evolution of Close Binary Systems* (IAU Symp., No. 73, Eds P Eggleton, S Mitton, J Whelan) (Dordrecht: D. Reidel Publ. Co., 1976) p. 35
407. van den Heuvel E P J, Habets G M H J *Nature* **309** 598 (1984)
408. Wellstein S, Langer N *Astron. Astrophys.* **350** 148 (1999)
409. Lipunov V M, Postnov K A, Prokhorov M E *The Scenario Machine: Binary Star Population Synthesis* (Astrophys. and Space Phys. Rev., Vol. 17, Ed. R A Sunyaev) (Amsterdam: Harwood Acad. Publ., 1996)
410. Portegies Zwart S F, Verbunt F, Ergma E *Astron. Astrophys.* **321** 207 (1997)
411. Ergma E, van den Heuvel E P J *Astron. Astrophys. Lett.* **331** L29 (1998)
412. Eggleton P P, Verbunt F *Mon. Not. R. Astron. Soc.* **220** 13P (1986)
413. Langer N *Astron. Astrophys.* **220** 135 (1989)
414. Moffat A F J, in *Wolf–Rayet Stars: Binaries, Colliding Winds, Evolution* (IAU Symp., No. 163, Eds K A van der Hucht, P M Williams) (Dordrecht: Kluwer Acad., 1995) p. 213
415. Moffat A F J et al. *Astrophys. J.* **334** 1038 (1988)
416. Cherepashchuk A M *Astron. Zh.* **67** 955 (1990) [*Sov. Astron.* **34** 481 (1990)]
417. Richardson D et al. *Astron. J.* **123** 745 (2002); astro-ph/0112051
418. Tutukov A V, Cherepashchuk A M *Astron. Zh.* **62** 1124 (1985) [*Sov. Astron.* **29** 654 (1985)]
419. Imshennik V S *Space Sci. Rev.* **74** 325 (1995)
420. Bisnovatyĭ-Kogan G S *Astron. Zh.* **47** 813 (1970) [*Sov. Astron.* **14** 652 (1971)]
421. Harries T J, Hillier D J, Howarth I D *Mon. Not. R. Astron. Soc.* **296** 1072 (1998)
422. Postnov K A, Prokhorov M E *Astron. Zh.* **78** 1025 (2001) [*Astron. Rep.* **45** 899 (2001)]
423. Fryer C L, Kalogera V *Astrophys. J.* **554** 548 (2001)
424. Balberg S, Zampieri L, Shapiro S L *Astrophys. J.* **541** 860 (2000)
425. Postnov K A, Cherepashchuk A M *Astron. Zh.* **78** 602 (2001) [*Astron. Rep.* **45** 517 (2001)]
426. Gershtein S S *Pis'ma Astron. Zh.* **26** 848 (2000) [*Astron. Lett.* **26** 730 (2000)]
427. Miller M C, Hamilton D P *Astrophys. J.* **576** 894 (2002); astro-ph/0202298
428. van der Marel R P, in *Black Holes in Binaries and Galactic Nuclei: Diagnostics, Demography, and Formation* (ESO Astrophys. Symposia, Eds L Kaper, E P J van den Heuvel, P A Woudt) (Berlin: Springer, 2001) p. 246
429. Shvartsman V F *Soobshcheniya SAO* (19) 5 (1977)
430. Grishchuk L P et al. *Usp. Fiz. Nauk* **171** 3 (2001) [*Phys. Usp.* **44** 3 (2001)]
431. Hughes S A *Mon. Not. R. Astron. Soc.* **331** 805 (2002)
432. Gnedin Iu N, Sunyaev R A *Astron. Astrophys.* **36** 379 (1974)
433. Bao G, Wiita P J, Hadrava P *Phys. Rev. Lett.* **77** 12 (1996)
434. Costa E et al. *Nature* **411** 662 (2001)
435. Bogdanov M B, Cherepashchuk A M *Astron. Zh.* **79** 693 (2002) [*Astron. Rep.* **46** 626 (2002)]
436. Schödel R et al. *Nature* **419** 694 (2002)
437. Tadhunter C et al., astro-ph/0302513
438. McLure R J, Jarvis M J *Mon. Not. R. Astron. Soc.* **337** 109 (2002)
439. Edelson R et al. *Astrophys. J.* **568** 610 (2002)
440. Shin D C, Iwasawa K, Fabian A C, astro-ph/0302108
441. Filippenko A V, Ho L C astro-ph/0303429
442. van der Marel R P, astro-ph/0302101
443. Xie G Z et al. *Mon. Not. R. Astron. Soc.* **334** 459 (2002)
444. Verolme E K et al. *Mon. Not. R. Astron. Soc.* **335** 517 (2002)
445. Fabian A C et al. *Mon. Not. R. Astron. Soc.* **335** L1 (2002)
446. Yu Q, Tremaine S *Mon. Not. R. Astron. Soc.* **335** 965 (2002)
447. Wu X-B, Liu F K, Zhang T Z *Astron. Astrophys.* **389** 742 (2002)
448. Gies D R, Huang W, McSwain M V *Astrophys. J.* **578** L67 (2002)
449. Orosz J A et al. *Astrophys. J.* **568** 845 (2002)
450. Filippenko A V, Chornock R *IAU Circ.* (7644) 2 (2001)
451. Garcia M R et al., astro-ph/0302230
452. Bogdanov M B, Cherepashchuk A M *Astron. Zh.* **79** 1109 (2002) [*Astron. Rep.* **79** 996 (2002)]